A multi-operational, combined PV/Thermal and solar air collector system: application, simulation and performance evaluation

Ben Cartmell

January 2004

Thesis submitted in partial fulfilment of the requirements of
De Montfort University for the degree of Doctor of Philosophy

The Institute of Energy and Sustainable Development
De Montfort University, Leicester

Abstract

In response to reported climate change, increased Governmental regulations and public awareness of environmental issues, more energy efficient buildings and renewable energy technologies are currently being developed and installed. Many of these renewable energy technologies may be considered as immature in market and technical terms, which has prompted significant levels of research in this field. If we are to meet our future energy needs and see wide-scale application of low energy buildings and renewable energy systems, further research is essential.

It is clear that within the built environment an integrated design approach provides the best method of limiting the overall environmental impact of a building. This approach looks to minimise the building energy load through appropriate environmental design practices and to meet this reduced load by efficient energy supply technologies and if possible, embedded renewable energy systems. The research described in this thesis considers the application of a new, immature, energy supply technology and its application to a low energy building in the UK. This technology is a hybrid solar collector which combines photovoltaic energy conversion with the collection of solar thermal energy and provides dual output for use within the building to which it is applied.

To further knowledge and understanding of this type of system, extensive modelling and simulation has been undertaken with results compared to measured data taken from an installed system at the Brockshill Environment Centre, Leicester. New simulation procedures are discussed in relation to previous research in this field and critically evaluated. Recommendations on further work are given both in terms of research and application.

Acknowledgements

Firstly, I would like to thank the late Professor Neil Bowman and Professor Kevin Lomas for providing the opportunity to be involved with the development of the Brockshill Environment Centre. Further thanks to Kevin for his research guidance and supervision.

In day to day research I would like to extend particularly thanks to Dr. Neil Shankland for his active support, good company and general joie de vivre. Thanks also to Dr. Dusan Fiala for help and friendship throughout my time at IESD and Professor Vic Hanby for later supervision and patience in thesis review.

External to IESD I would like to acknowledge the help of Dr. Nick Kelly at ESRU (University of Glasgow) on ESP-r code development and David Bradley (Solar Energy Laboratory, University of Wisconsin) for his guidance on TRNSYS component development and simulation.

In relation to the Brockshill Environment Centre, thank you to Margaret Smith, Annabel Kennedy and Jim Smith (Oadby & Wigston Borough Council) and the design team for their assistance.

Thank you to whitbybird engineers for giving me study leave to finish the writing of this thesis.

Finally, I would like to acknowledge the great support from family and friends. For daily life support and mental support, the credit goes to Lucy Harris. Cheers Lucy.

I declare that the content of this submission represents solely my own work. The contents of the work have not been submitted for any other academic or professional award. I acknowledge that the thesis as submitted complies with the conditions stated in De Montfort University regulations. I declare that the work carried out as part of the course of study for which I was registered and not previous or subsequent to it; and I draw attention to any relevant considerations of rights of third parties or of security which might merit a restriction on loan or access.

Contents

List of Figures

List of Tables

Nomenclature

α	Absorptance of collector plate
$\alpha'(E,W)$	Spectral absorbance (Nonabsorption losses)
β	Slope of collector
βr	Maximum power point efficiency temperature coefficient
ε_b	Emittance of back plate
ε_g	Emittance of glass
ε_p	Emittance of plate
ε_{pv}	Emittance of PV material
η	Cell efficiency at reference temperature
$\tilde{\eta}$	Florshuetz extension to cell efficiency
$\eta_{col}(E)$	Solar collection efficiency
η_e	Electrical efficiency
η_h	Heat removal efficiency
η_{mp}	Efficiency at maximum power
μ	Dynamic fluid viscosity
$\rho(E,W)$	Reflectance (Reflection losses)
σ	Stefan Boltzmann constant
$\tau(E,W)$	Transmittance (Transmission losses)
$\tau\alpha$	Transmittance absorptance product

A_C	Area of collector
A_{edge}	Area of collector edge
Af	Cross dimensional area of fluid flow
C_p	Specific heat of fluid
D_h	Hydraulic diameter
$D\dot{m}$	Dimensionless collector mass flow rate
E	Energy incident on the cell per unit area
E_G	Wavelength band gap
F'	PV/Thermal collector efficiency factor
F'_O	Solar Air collector efficiency factor
F''	Collector flow factor
FF	Fill factor
F_F	Fin efficiency of fin

F_P	Fin efficiency of plate
F_R	Collector heat removal factor
G_T	Incident radiation
h	Convective heat transfer coefficient
h_r	Radiative heat transfer coefficient
h_w	Wind heat transfer coefficient
I	Current
I_L	Photogenerated current
I_0	Dark saturation current
I_D	Dark current
I_M	Maximum current
I_{SC}	Short circuit current
k	Stefan Boltzmann constant
k_a	Thermal conductivity of air at specific temperature
k_i	Thermal conductivity of insulation
L_b	Thickness of back insulation
L_e	Thickness of edge insulation
m	Ideality factor
$\dot{m}$	mass flow rate
N	Number of glass covers
Nu	Nusselt number
P_m	Maximum power point
Pf	Cell packing factor
Q_e	Useful electrical gain
Q_u	Useful thermal gain
Re	Reynolds number
R_S	Series resistance
R_{SH}	Shunt resistance
S	Solar radiation per unit area
$\tilde{S}$	Florschuetz factor applied to solar radiation
S'	Number of photons
T	Absolute temperature
T_a	Ambient temperature
T_{cell}	Cell temperature
T_{fm}	Mean fluid temperatue
T_{in}	Inlet temperature
T_o	Outlet temperature

$\overline{T}_p$	Plate temperature on first iteration
T_{pm}	Mean plate temperature
T_{ref}	Reference cell temperature
U_b	Back loss coefficient
U_e	Edge loss coefficient
U_L	Collector overall heat loss coefficient
$\tilde{U}_L$	Florschuetz extension to collector overall heat loss coefficient
U_t	Top loss coefficient
V	Voltage
V_M	Maximum voltage
V_{OC}	Open circuit voltage
Y_f	Thickness of fin
Y_p	Thickness of plate

Chapter 1

Introduction

1.1 Introduction

"In this century, without action to reduce emissions, the earth's temperature is likely to rise at a faster rate than any time in the last 10,000 years or more. In the UK, the risks of droughts and flooding are likely to increase. Sea levels will rise, so that extreme high water levels could be 10 to 20 times more frequent on some parts of the east-coast by the end of the century. World-wide, the consequences could be devastating, especially in the developing world where many millions of people are likely to be exposed to the risk of disease, hunger and flooding. In addition, there is a risk of large scale changes such as the shut-down of the Gulf Stream or melting of the West Antarctic ice sheet, which although they may have a low probability of occurring, would have dramatic consequences" (Department of Trade & Industry, 2003).

When the UK Government use statements with this strength to justify direction on energy policy it is clear that climate change as an issue is now being taken very seriously and that our future energy use will have to adapt to account for environmental considerations alongside market forces.

The UK Government Energy White Paper sets out ambitions to cut emissions of greenhouse gases for the world's developed economies by 60% by around 2050. This

extends the previous target of providing 10% of energy from renewable sources by 2010 to give consideration to the total UK energy utilisation from demand reduction to future incorporation of technologies that may be termed immature in technical and market terms at present.

When considering energy consumption by end use in the UK, 26% is used for space heating, 8% for the provision of hot water and 6% for lighting and appliances (DTI, 2003). At 40%, buildings and their operation make up the largest single proportion of energy consumption in the UK at present. If we are to meet our long-term object of a 60% reduction by 2050, this demand will have to reduce significantly.

UK Government legislation is already active in this area, with ongoing revisions to the UK Building Regulations with regard to conservation of fuel and power. European legislation, in the form of the new EU Buildings Directive on the energy performance of buildings, will also enforce minimum energy performance on virtually all buildings by 2006. This Directive, which the UK Government is currently implementing, will also require publicly used buildings over 1000m^2 in floor area to certify and publicly display an energy certificate for the building. It is hoped that these initiatives will bring the energy used in buildings to a higher level of public awareness and hence develop an economic basis for deciding to operate buildings with a low environmental impact.

Good examples of low energy buildings in the UK, especially in the non-domestic sector, are currently few in number compared to the overall building stock. Many of these buildings have been developed for demonstration purposes or on an uneconomic basis as the owners or developers desired clear environmental credentials. Much has been learned from these buildings, however, if the Government's objectives are to be met, low energy buildings with integrated low impact energy systems and services will have to be applied as standard for new buildings and dramatic improvements made to the existing building stock.

To help realise this, design processes are currently being developed with regard to buildings of all types and the services, which they require. This process development is being approached with clear collaboration between the research community and the construction industry with ongoing transfer of knowledge on new design approaches and technologies from pure research through to demonstration and hopefully wide-scale application.

The research undertaken and described in this thesis is a good example of this transfer. The subject area of hybrid Photovoltaic (PV) and Solar Thermal collectors (termed PV/Thermal) has been studied over a number of years with clear indications that this is a viable technology. The next stage, of application, has seen a limited number of working systems installed, so little published knowledge has been gained on appropriate application, 'buildability' and system design development.

The concept of PV/Thermal technology is simple. Photovoltaic cells as a dark material subjected to solar radiation, rise in temperature. When this occurs, the efficiency of energy conversion reduces, so heat is usually vented at the rear of PV modules to maximise the potential electrical output from these expensive systems. PV/Thermal collectors take the thermal by-product and utilise this for either space or water heating while maintaining good electrical conversion efficiency within the PV cells.

To further knowledge and understanding of this type of technology and its applicability to the UK situation, the research presented in this thesis has been developed alongside the first UK installation of such a system at the Brockshill Environment Centre, near Leicester, UK. This development incorporates many environmental design features and integrated low energy systems. Within this broad ranging context the following research aims were set.

1.2 Research Aims

1. To develop an appropriate method of modelling combined PV/Thermal and Solar Air collectors when applied to low energy buildings.
2. To enhance existing knowledge on the simulation of these combined collectors and identify the relative importance of parametric settings and input variables.
3. To give guidance on the design of this type of system and develop an adaptable framework upon which future research may be undertaken.

1.3 Structure of Thesis

To present this research as an integral part of an holistic approach that provides low energy buildings with applied new and renewable technologies, the thesis is structured in two general parts.

Firstly, to provide context and introduce the design approach and systems applied at the Brockshill Environment Centre, Chapters 2 to 4 considers current UK practise in energy demand reduction and active solar technologies that are commonly applied to meet this reduced load. The Brockshill Environment Centre (Chapter 4) is then presented in detail to provide background to the modelling methodology that has been developed to provide performance predictions and assistance in systems design.

Chapters 5 to 8 then describes the underlying theory of PV/Thermal collectors, previous research in this field, new areas of investigation and simulation of these systems. Termed the Ventilated Photovoltaic and Solar Air System (VPVSAS) Method, new component subroutines are provided that can be used for modelling stand-alone collectors or as part of full building energy and plant simulation exercises. The output from both approaches are capable of providing general and detailed information that may be used for performance assessment, systems design or as a platform for further research. The thesis concludes with analysis of predicted results compared against measured data gathered

from the Brockshill Environment Centre and discusses the viability of this type of system with regard to the research aims stated above.

Chapter 2

Current Environmental Design Practices

2.1 Introduction

The Development of PV/Thermal systems and other energy saving systems and strategies has resulted from a recognised need to reduce the impact of further global warming. Within this overriding context, we must first consider the impact that the built environment exerts on this phenomenon, and the current environmental design practices, which aim to reduce this impact.

The combination of this environmental agenda and the need for functioning, comfortable and visually acceptable buildings, has led to the re-emergence of environmental design and bio-climatic architectural principles which have been used and developed since human beings first started building shelters. This new school of environmental design has significantly developed our understanding of the subject and has benefited from modern day computing capabilities, which enable the assessment of highly complex interactions between functioning buildings and the external environment. The development of such computer based design tools is central to the research presented in this thesis.

An environmental design approach generally attempts to minimise the building energy load using a combination of well-documented strategies. It then may be possible to apply renewable energy systems that further contribute to this load, while reducing the need for fossil fuel based energy supply. The complexity of a design will greatly depend on the function of the building and the environmental conditions, which it is subject to. This Chapter outlines the environmental design practices currently employed to create such buildings and provides context to the development of the Brockshill Environment Centre (Chapter 4) and the applied PV/Thermal system under investigation.

2.2 Low Energy Design Strategies

2.2.1 The Provision of Comfortable Spaces

The human body is thermally comfortable when the heat constantly produced by bodily processes balances heat losses and gains to and from the environment. The achievement of such a balance depends upon the combined effects of many factors. Personal variables such as activity and clothing must be considered along side the main physical variables: air temperature, radiant temperature, humidity and air movement (Smith *et al*, 1982). Under standard conditions, heat is lost from the body through evaporation (20%), convection (35%) and radiation (45%)(Baker, 2000). The proportion of these mechanisms will then change with regard to the level of activity and the amount of clothing worn, which can be inferred from the anticipated building function. Accepted design procedures, such as those documented in CIBSE Guide A – Environmental Design (CIBSE, 1999) can then be used to optimise comfortable internal conditions throughout the year.

When a building is designed under a low energy strategy, internal conditions are naturally more variable due to the increased use of solar gains, natural air movement and daylight. This variability must therefore be engineered to remain within acceptable boundaries in order to maintain thermal comfort. Standard methods involve the use of thermal indices

and charts to assess combined influences of air and radiant temperatures, humidity and air movement. Depending on the comfort issues in question, the calculation of a Dry Resultant Temperature will report on the combined effects of air temperature, mean radiant temperature and air velocity. If comfort issues relate to humidity and air temperature then a Psychrometric Chart would be used.

2.2.2 Passive Solar Design Concepts

The provision of comfortable conditions within a building are realised through the use of both active and passive means. Active systems can provide closely controlled internal conditions, however, building costs increase significantly due to initial capital expenditure on plant, fuel supplies and ongoing maintenance. These systems also contribute large quantities of CO_2 to the atmosphere along with other damaging emissions that can be related to the greenhouse effect and global warming.

The two main pre-requisites for a passive solar strategy are the provision of south facing glazed areas for solar collection (north facing in the southern hemisphere) and exposed thermal mass for heat absorption, storage and distribution. Further to this, the built form should be as compact as possible to reduce the exposed surface area to heated volume ratio. Unheated buffer spaces, such as conservatories or stores, can also assist in the protection of the main building envelope subject to heat loss.

It is recommended that one elevation should face within +/- 25° of due south (Yannas, 1994) to enable solar collection while the other, more exposed elevations, should be protected where possible with minimal glazing provided. Appropriate internal layout design can also assist in building energy performance. Open-plan arrangements along a north-south axis can help to optimise solar and daylight availability, while areas subject to high internal gains such as kitchens and areas of limited use (eg toilets) are usually located to the north side of the building.

The benefits of solar gain must also be considered against the potential for overheating during the summer months. In order to limit the extensive use of shading devices, which may have implications on daylight availability, the built form can be designed in such a way that low-level winter sun can penetrate while protection is provided under summer conditions. The concept is demonstrated in Figure 2.1.

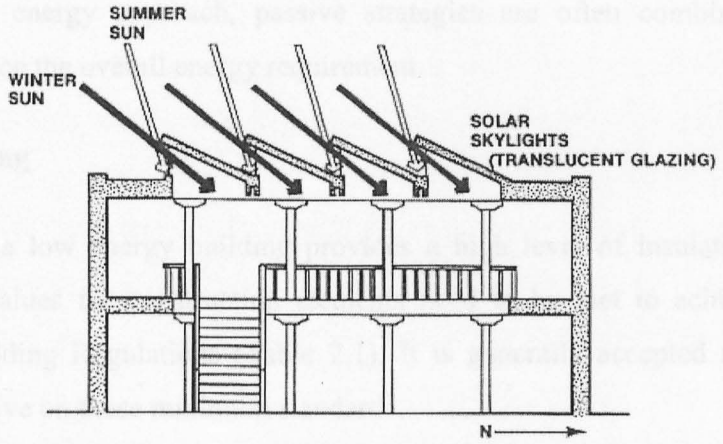

Figure 2.1 – Annual variation in solar penetration through passive design (Mazria, 1979)

The integrity of the building envelope is now recognised as having a major impact on the building's energy consumption. Air leakage can be defined as the movement of air into and out of the building, which is not for the specific and planned purpose of exhausting stale air or bringing in fresh air. The driving forces for this air movement are provided by external wind pressure variation, an internal pressure differential caused by buoyancy forces (generally positive at high level and negative at low levels), and mechanical systems which induce positive or negative pressures within the building. The significant energy penalty which uncontrolled air leakage imposes on buildings has been recognised by the UK Government through the introduction of maximum air leakage standards for all new non-domestic buildings over $1000m^2$ in floor area (DTLR, 2002). Testing procedures are published by The Chartered Institute of Building Services Engineers, which measure the rate of air leakage per square meter of external envelope per hour at an artificial differential across the envelope (measured in units of $m^3hr^{-1}m^{-2}$ @ 50 Pa). A typical air leakage target for a naturally ventilated office building is 10.0 $m^3hr^{-1}m^{-2}$, with

a typical low energy or air-conditioned building aiming for 5.0 $m^3hr^{-1}m^{-2}$ (CIBSE, 2000a).

The function of a building, development costs and site requirements often dictate that it cannot operate using passive measures alone. When a building is designed using an integrated low energy approach, passive strategies are often combined with active systems to reduce the overall energy requirement.

2.2.3 Heating

The design of a low energy building provides a high level of insulation as standard. Minimum U-Values for construction elements need to be met to achieve compliance under UK Building Regulations (Table 2.1). It is generally accepted that low energy buildings improve on these minimum standards.

Exposed element	U-Value (W/m^2K)
Pitched roof insulation between rafters	0.2
Pitched roof with integral insulation	0.25
Pitched roof with insulation between joists	0.16
Flat roof	0.25
Walls, including basement walls	0.35
Floors, including ground floors and basement floors	0.25
Windows doors and rooflights (area weighted average) glazing in metal frames	2.2
Windows doors and rooflights (area weighted average) glazing in PVC frames	2.0

Table 2.1 – Minimum U-Values for construction elements (DTLR, 2002)

The heated volume is further protected through detailing (BRE, 1994) to limit possible cold bridges across the insulated building envelope. This detailing can also help limit air leakage through the envelope.

Glazing systems need to be carefully considered due to the poor insulating properties compared with the positive benefits of solar gain. High performance glazing systems can assist overall energy performance. The provision of multi layer glazed units progressively reduced thermal transmittance due to the insulating properties of air gaps provided. This thermal performance can be further enhanced through the introduction of heavy gases, such as argon or krypton, which reduce buoyancy movement within the gaps and therefore convective heat transfer. Low emissivity films can be applied to internal surfaces within the glazed units to reduce radiative heat transfer between the panes.

Once the building envelope has been thermally optimised and available solar and internal gains utilised, the heating load for low energy buildings is generally small compared with conventional buildings with a dramatically reduced heating season. This means that conventional heating systems can downsized.

2.2.4 Passive Cooling

Passive cooling can broadly cover all the measures and processes that contribute to the control and reduction of cooling needs in the building. It includes all the preventative measures to avoid overheating in the interior of buildings and strategies for the rejection to the external environment of the internal heat, either generated in the interior or entering through the envelope of the building (Santamouris & Asimakopoulos, 1996).

Non-domestic buildings are usually subject to a higher potential for overheating, as they are occupied during the daytime when air temperatures are highest and solar gains are present. Cooling is therefore required to counter the affects of internal solar gains through windows, conductive gains through the building envelope, ventilation gains and internal gains from artificial lighting, occupants and equipment.

Conductive gains can be seen as a relatively minor contributor toward overheating, due to the higher levels of insulation required by current Building Regulations. However, the high levels of insulation associated with low energy buildings designed for the UK climate may increase summertime overheating if appropriate solar shading is not provided. An extensive range of shading devices is available, which cater for particular orientations, levels of shading, daylight penetration, glare reduction and aesthetic qualities (BRE, 2000).

After these gains have been minimised, a passively cooled building can make use of three complementary strategies, which can maintain a comfortable internal environment. These strategies are ventilation cooling, exposed thermal mass and night-time ventilation cooling. Ventilation cooling can only provide a useful heat loss when the ambient air temperature is lower than the maximum comfort temperature indoors. When further cooling is required exposed thermal mass can help attenuate internal temperatures by absorbing or releasing heat as appropriate. This phenomenon can be further assisted during hot periods by ventilating the building with cool night time air. This purges hot air from the building and cools the thermal mass to act as a heat sink during the following day.

2.2.5 Ventilation

Ventilation of buildings may be achieved by natural or mechanical means, in order to provide thermal comfort, humidity control and acceptable indoor air quality (Athienitis & Santamouris, 2002). Mechanical ventilation is commonly used when a constant or controlled airflow is necessary or when outdoor conditions are not favourable in the provision of a healthy and comfortable indoor environment for building occupants. The depth of the floor plan and the level of internal gains may also dictate the use of mechanical systems. Depending on whether the ventilation regime is designed for minimum requirements, space cooling or for general air movement, a mechanical system may be supply driven, extract driven or balanced between supply and extract. However

the system is designed, the requirements for energy supply, plant, ductwork and controls are extensive.

The application of a natural ventilation strategy can significantly reduce the electrical energy used within a building due to the reduced need for fans, pumps, and chillers, if an integrated cooling strategy is employed. Natural ventilation as a strategy for achieving acceptable indoor air quality is essentially based on the supply of fresh external air to a space and the dilution of the internal pollution concentrations (Allard *et al*, 1998). The driving forces for this flow are wind pressure and thermal buoyancy. Flows associated with wind pressure result from a change in momentum when air is deflected or reduced in speed when flowing against or around the building in question. Thermal buoyancy, or the stack effect, generates a vertical pressure difference between the column of warm air and the external temperature, and the height of the column of warm air (Baker, 2000). Appropriate design can assist in the optimisation of these forces, for example stacks, solar chimneys, and outlet terminals that induce negative pressures.

Depending on the building format, layout and function, general airflow paths can be established following general guidelines. Single-sided ventilation can be considered where the depth of the space is up to 2.5 times the floor to ceiling height, while cross and stack ventilation can service up to 5 times the floor to ceiling height (CIBSE, 1997). Once the principle driving forces and airflow paths have been identified, airflow rates need to be calculated, openings need to be sized and located, and a control system is specified.

When internal and / or external conditions dictate that a natural ventilation strategy is not capable of meeting requirements, a mixed mode approach may be used to reduce the need for full mechanical ventilation. A mixed-mode strategy involves maximising the use of the building fabric and envelope to achieve indoor environmental conditions, and then supplementing this with degrees of mechanical systems, in parts of the building (CIBSE, 2000b). These systems may be designed using a zonal or seasonal approach and are commonly applied to office developments.

A number of high profile naturally ventilated buildings have been constructed in the UK over the last decade. The Inland Revenue Headquarters, Nottingham (1995), provides 40000m^2 of office space that benefits from natural ventilation, a highly insulated envelope, exposed thermal mass, triple glazing with low-e coatings and optimised daylight penetration. Buildings use a narrow plan format to assist cross ventilation with towers provided at office block intersections and terminations to draw air through the offices. These towers make use of movable 'top hats', which help to regulate the flow of air. This strategy is represented in Figure 2.2.

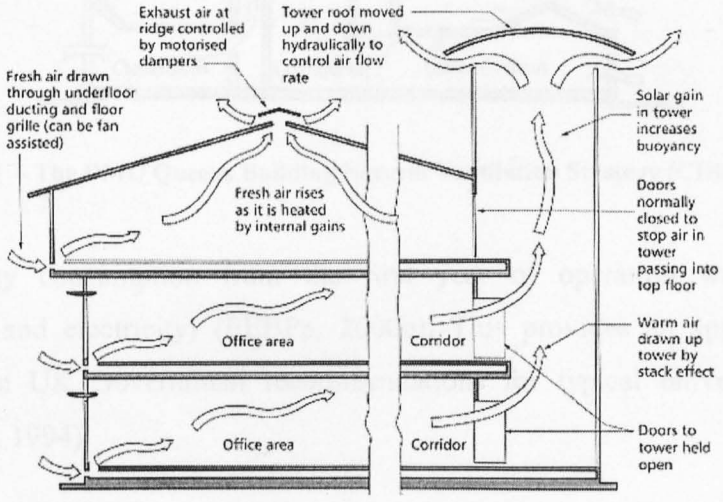

Figure 2.2 – The Inland Revenue Headquarters Natural Ventilation Strategy (CIBSE, 1997)

Compared to a good practice air conditioned building (DETR, 2000), the Inland Revenue Headquarters development uses 19% less energy in space heating and hot water provision (EEBPp, 2000a).

The De Montfort University Queens Building also demonstrates an integrated natural ventilation strategy that meets the varying airflow requirements of a multi-function engineering building throughout the year. This building uses a zonal approach that provides cross ventilation to shallow plan offices with large stacks and high level opening clerestorey windows are provided to assist buoyancy driven flows from the auditoria,

central concourse, workshops and a drawing studio. A simplified representation of this ventilation regime is shown in Figure 2.3.

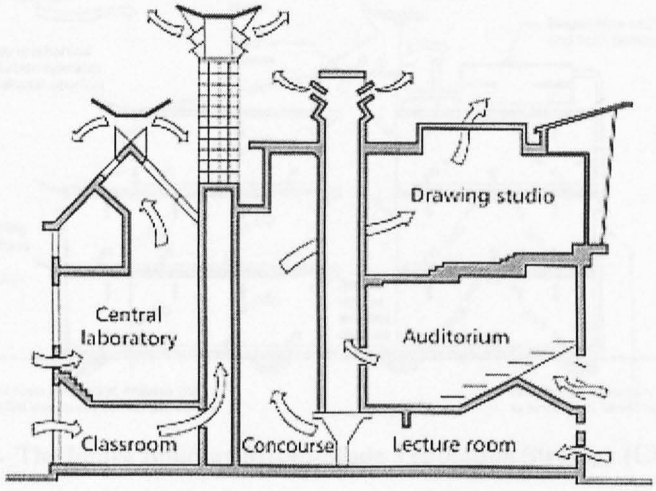

Figure 2.3 – The DMU Queens Building Natural Ventilation Strategy (CIBSE, 1997)

Reported energy consumption from the first year of operation was 157kWh/m^2 (combined gas and electricity) (EEBPp, 2000b). This provides an approximate 50% improvement on UK Government recommendations for typical university academic buildings (DOE, 1994).

The Ionica Building (Figure 2.4), Cambridge, utilises a mixed-mode ventilation strategy along with high levels of thermal mass to assist heating and cooling. Specialised wind towers help induce air out from the atrium and can mechanically adapt to optimise the draw of air when the prevailing wind changes direction. A zonal mixed-mode strategy is required because of the high internal gains from IT equipment in certain areas of the building.

Unfortunately, this building did not meet expectations with regard to energy performance. This was attributed to business practices within the building (EEBPp, 2000c).

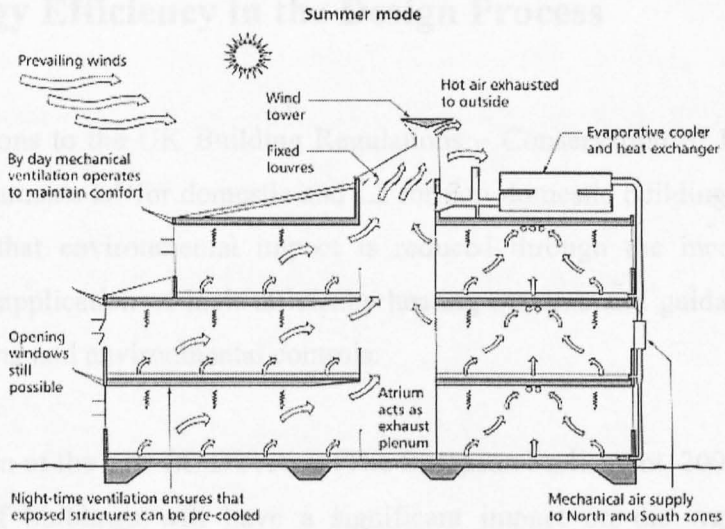

Figure 2.4 – The Ionica Building Mixed-Mode Ventilation Strategy (CIBSE, 1997)

2.2.6 Daylight Provision

When daylight is taken into a building the need for artificial lighting is reduced. Not only are there clear benefits on electrical load but also a major reduction in running costs can be realised when daylight provision is incorporated into the building design.

2.2.7 Control Strategies

The control strategy employed by low energy buildings needs to be carefully developed to maintain thermal comfort and desired operation. The level of occupant control also needs to considered at early design stage and depends on the complexity of the environmental control strategy and purpose of the building. With higher complexity comes increased potential of problems during operation, which means that more care needs to be taken in design and commissioning. Clear benefits can be realised through appropriate use of simulation under varying controls regimes during early design phases.

2.3 Energy Efficiency in the Design Process

Ongoing revisions to the UK Building Regulations – Conservation of Fuel and Power, Approved Documents L1 for domestic and L2 for non-domestic buildings (DTLR, 2002) have ensured that environmental impact is reduced through the increased levels of insulation, the application of high efficiency heating systems and guidance on building integrity, lighting and environmental controls.

The introduction of the new EC Directive (The European Parliament, 2002) on the energy performance of buildings will have a significant impact on the way buildings are constructed and operated in the UK by 2006. The overall objective of the Directive is to improve the energy performance of buildings within the European Community. To achieve this, five main requirements have been placed on member states:

1. The development of a new method which will calculate the integrated energy performance of buildings.
2. Minimum requirements on the energy performance of new buildings.
3. Minimum requirements on the energy performance of large existing buildings that are subject to renovation.
4. Energy certification of publicly used buildings.
5. Regular inspection of boilers and air conditioning systems in buildings.

Building categories affected by these requirements include: offices, educational buildings, hospitals, retail, sports facilities, apartment blocks, single-family houses of different types and 'other types of energy-consuming buildings'.

Those exempted include: officially protected / listed buildings and monuments, religious buildings, temporary buildings (planned use of less than 2 years) and residential buildings used for less than 4 months during the year.

The actual energy standards and calculation procedures will be developed over the next 2 years. These are expect these to be in-line with current Building Regulations with extended procedures to incorporate the following aspects of building energy performance:

- Thermal characteristics (envelope, internal partitions, insulation, air-tightness etc.).
- Heating installations and hot water supply.
- Air-conditioning installation.
- Ventilation.
- Natural ventilation.
- Lighting.
- Position and orientation of the building and outdoor climate.
- Passive solar systems and solar protection.
- Indoor climatic conditions, including the designed indoor climate

New developments over 1000m^2 in floor area will also have to consider low carbon technologies such as renewable energies, CHP, district heating and daylight provision.

It is hoped that the energy labelling scheme for buildings will eventually be as universally accepted as that used by white goods.

Certificates will be required for all buildings and will include reference values and benchmarks for easy comparison with recognised standards and best practice, and will have to be placed prominently in publicly used buildings over 1000m^2 in floor area. The building owner will have to provide this energy certificate (not exceeding 10 years old) to prospective buyers or tenants when a building is being constructed, sold or leased.

2.4 Conclusions

This Chapter has outlined current practices that are commonly used to reduce the energy load of buildings. When following a low energy approach to design, the interaction between the building, external environment, function, services and environmental control strategy may result in a high level of complexity compared to a standard building. This level of complexity creates a potential for the building not being operated as intended during design.

Chapter 3

Active solar systems for the built environment

3.1 Introduction

This Chapter focuses on the application of photovoltaic systems to the built environment. In relation to the concept of PV/Thermal co-generation collectors, photovoltaic performance will be described with particular emphasis on the effect of temperature on cell performance. This Chapter will also discuss issues associated with the design of Building Integrated Photovoltaic (BIPV) systems and will describe some UK installations that demonstrate current best practice. A brief introduction to solar hot water systems is also provided.

3.2 Photovoltaic Systems

As a technology, PV is highly applicable to the built environment as it can directly contribute to the energy requirements of a building and requires little maintenance. However, PV systems should be considered as an immature technology as the economics associated with their application can often not be justified against the provision of electricity from a grid. To assist the UK market and stimulate further demonstration and research, grant funding for PV installations is now available (Parkinson & Wilczek, 1999). This assistance, together with the energy saving potential (generated PV

electricity can off-set premium rates for grid supplied power), reduced need for construction materials and less well quantifiable factors such as publicity and planning issues has stimulated interest and new installations in the UK.

To put the UK PV provision in a world context, by 2000 approximately 2MWp capacity was installed. This represented 0.28% of that installed in countries covered by the International Energy Agency (IEA, 2001). The UK Government has recognised the potential for this market to grow. With the various incentives and market development it has been estimated that Building Integrated Photovoltaic (BIPV) systems will achieve wider economic viability between 2010 and 2020 in the UK (Thomas, 2001; Oliver & Jackson, 2001).

3.2.1 The Photovoltaic Cell

Photovoltaic cells use semiconducting materials to enable energy from incoming photons, within sunlight, to free valence electrons usually held fast in the material's lattice structure. Once a photon breaks a bond, the electron is free to move through the lattice along with the vacant position, or hole, that is left behind. These holes are considered to behave in a similar fashion to the free electrons, except that they carry a positive charge. As the free electrons and holes travel in an opposite direction within the semiconductor, an electric current is generated which may be carried through an external circuit to help meet a specific load, contribute to a network or be stored within a battery. To ensure that free electrons and holes do not recombine, an electrical field is provided which maintains the appropriate propelling forces and, therefore, the direction of the current.

This electric field is created at the junction (referred to as the *p-n junction*) between two semiconducting layers that provide contrasting levels of conductivity and enabling chemical properties. Most PV cells manufactured today use silicon as the basic semiconducting material. As a base material, silicon naturally provides four orbiting valence electrons. In the creation of a photovoltaic junction, impurities are added to the silicon in a process known as doping. One of the layers of silicon is doped with phosphorus (referred to as the *n-type layer*), which provides five valence electrons. The

second layer (*p-type layer*) is doped with boron, which provides three valence electrons. When these layers of doped silicon are brought together, the differing concentrations of electrons in the *n*-type layer and holes in the *p*-type cause an electric field to be directed from *n* to *p*. With this field in place, electrons and holes remain separate and can contribute current to an external circuit when incoming photons provide energy to break valence electrons from bonds in the *n*-type layer. This phenomena is demonstrated in Figure 3.1.

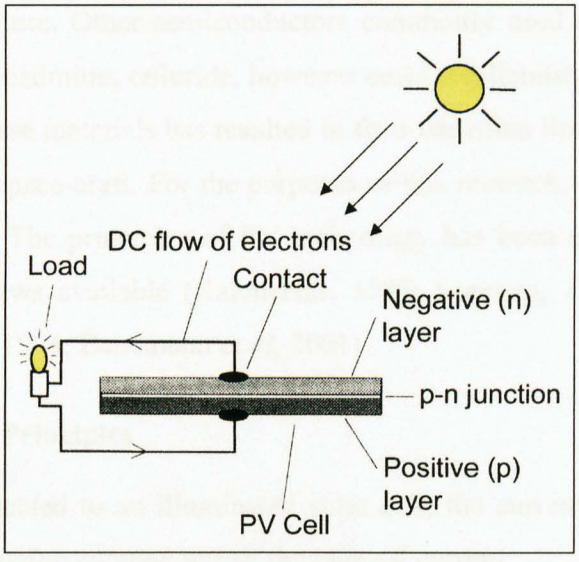

Figure 3.1 – The PV Effect (re-drawn [Thomas, 1999])

When the PV cell is connected to an external load and radiation provided, a potential difference will be created with current flowing from the positive upper terminal. Particular attention is required in the design of this upper electrical contact as most of the surface area needs to be uncovered to allow light to enter the cell, while electrical resistance resulting from limited contact must be minimised. Significant improvements in cell efficiencies have been made through laser grooving and buried contact fabrication techniques of positive terminals, developed by the Key Centre for Photovoltaic Engineering, University of New South Wales, Australia (Wenham *et al*, 1994). The current then returns via the rear negative contact, which being on the dark side, can cover the entire surface.

When the external load is removed, the PV cell must return to a state of equilibrium and the electron-hole pairs generated by incident radiation must disappear. This happens naturally when no external source of energy is available as electrons and holes move around the lattice until all recombinations have been made.

Silicon PV cells can be fabricated using monocrystalline, multicrystalline, polycrystalline and amorphous structure. Other semiconductors commonly used to make PV cells are gallium arsenide and cadmium telluride, however costs, availability of raw materials and the toxic nature of these materials has resulted in their use often limited to highly specific applications such as space-craft. For the purposes of this research, only silicon based PV cells are considered. The principles of PV technology has been extensively researched with detailed overviews available (Kazmerski, 1997; Lorenzo, 1994; Lasnier & Ang, 1990; Wenham et al, 1994; Benemann *et al*, 2001).

3.2.2 Photovoltaic Principles

When a load is connected to an illuminated solar cell, the current that flows is the net result of two counteracting components of the internal current:

1. The *Photogenerated Current* (I_L) due to the generation of carriers by incident radiation.
2. The *Dark Current* (I_D) due to the recombination of carriers driven by the external voltage. This voltage is needed to deliver power to the load.

It is often assumed that these two currents can be superimposed linearly. If I_L is taken as positive, then the current I can be considered as the differential of the two counteracting components:

$$I = I_L - I_D(V) \tag{3.1}$$

Calculation of Photogenerated Current

PV cells are selective in the wavelengths of light that contribute to the photovoltaic effect. Figure 3.2 shows the spectral distribution of solar radiation on the earth's surface. Cells respond to mainly visible light (~400nm – 700nm) with some activity in the UV and IR. Low-Iron content glass is used in the construction of PV cells as Iron traces found in normal glass absorb significant quantities of energy in the visible green range, otherwise available for conversion.

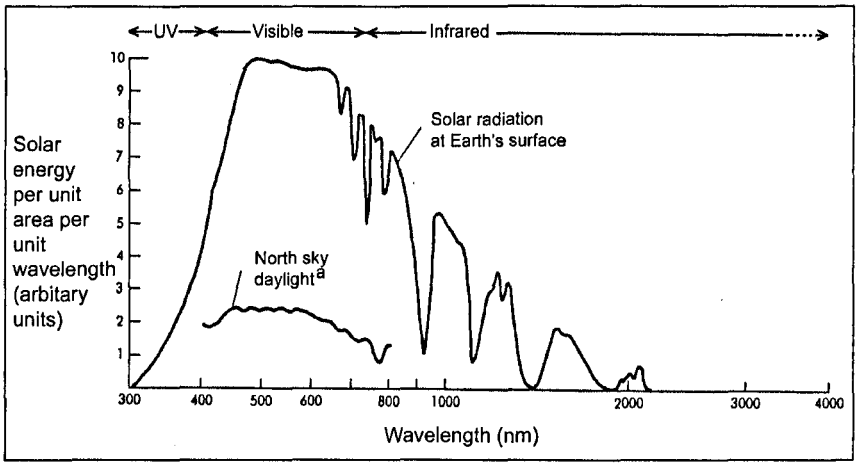

Figure 3.2 – Spectral composition of solar radiation

Carriers are generated when photons promote electrons from the valence band into the conduction band. However, not all photons incident on the cell will contribute towards photo absorption. *Nonabsorption Losses* occur when photons with energy below the band-gap of useful wavelength cross the semiconductor without being absorbed. A certain fraction of the suitable wavelength will also contribute towards *Transmission Losses* where cell thickness impacts on the absorption rate at higher wavelengths. *Reflection Losses* will also occur. These processes can be accounted for in the calculation of I_L, using the following integral:

$$I_L = eA_C \int_{E_G}^{\infty} S'(E)\alpha'(E,W)dE \equiv eA_C \int_{E_G}^{\infty} S'(E)\left[1-\rho(E,W)-\tau(E,W)\right]dE \qquad (3.2)$$

where A_C = Area of the illuminated cell

E = Energy incident on the cell per unit area

S' = Number of photons

E_G = Wavelength band-gap

$\alpha'(E,W)$ = Spectral absorbance (Nonabsorption losses)

$\tau(E,W)$ = Transmittance (Transmission losses)

$\rho(E,W)$ = Reflectance (Reflection losses)

The use of anti-reflective coatings and appropriate device design can help to reduce *Reflection* and *Transmission* losses respectively. Nonabsorption losses cannot be mitigated as they are intrinsic to the semiconductor properties. A theoretical maximum I_L can therefore be calculated at this stage with *Reflective* and *Transmission Losses* omitted:

$$I_L \leq eA_C \int_{E_G}^{\infty} S'(E)dE \tag{3.3}$$

Photogenerated current is also subject to losses associated with the carrier generation at locations too far from the main electric field. The *Collection Efficiency* $[\eta_{col}(E)]$ depends on optical and electrical characteristics of the semiconducting material. The inclusion of this factor completes the standard calculation for I_L:

$$I_L = eA_C \int_{E_G}^{\infty} S'(E)\alpha'(E)\eta_{col}(E)dE \tag{3.4}$$

Calculation of Dark Current

A bias current is created across the cell when an external voltage is present. This current, or *Dark Current* (I_D) will exist at all times including when there is no illumination present. The calculation of I_D therefore uses a variation to the Ideal Diode Law, which incorporates an *Ideality Factor* (m) that varies between 1 and 2. This factor generally increases as current decreases:

$$I_D(V) = I_0\left[\exp\frac{eV}{mkT} - 1\right] \tag{3.5}$$

where: I_0 = Dark saturation current

m = Ideality factor

k = Stefan Boltzmann's constant

T = Absolute temperature

The *I-V* Curve

Once the current associated with a specific PV cell is known, the performance of a PV module (made up of PV cells mounted in series and parallel) can be calculated under varying external resistive loads. These resistive loads vary between zero (to provide the Short Circuit Current, I_{SC}) and infinity (which will give the Open Circuit Voltage, V_{OC}). As a PV cell is essentially a diode with a forward bias, the conventional method of representing PV performance uses an inverse diode *IV Curve*. With reference to Figure 3.3, equation 3.6 can be used to plot the *IV Curve* for a specific PV module (This IV Curve is plotted in Figure 3.4). The *IV Curve* is presented here in order to highlight certain performance metrics that are used to assess the effect of temperature on PV efficiency.

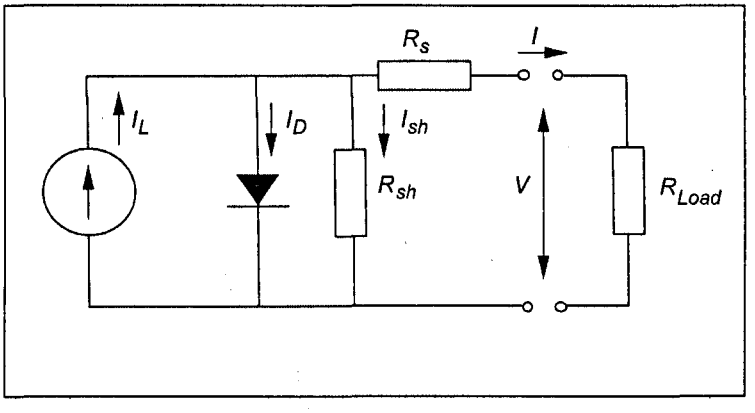

Figure 3.3 - Equivalent circuit for a PV generator

$$I = I_L - I_0\left[\exp\frac{e(V + IR_s)}{mkT} - 1\right] - \frac{V + IR_s}{R_{sh}} - \tag{3.6}$$

where: R_s = Series resistance

R_{sh} = Shunt resistance

The *Short Circuit Current* (I_{SC}) is the maximum current at zero voltage and is directly proportional to incident radiation. In relation to Equation 3.6, I_{SC} is given by:

$$I_{SC} = I(V = 0) = I_L \tag{3.7}$$

Similarly, the *Open Circuit Voltage* (V_{OC}) can be calculated using the following equation:

$$V_{OC} = m\frac{kT}{q}1n\left[\frac{I_L}{I_0}+1\right] \tag{3.8}$$

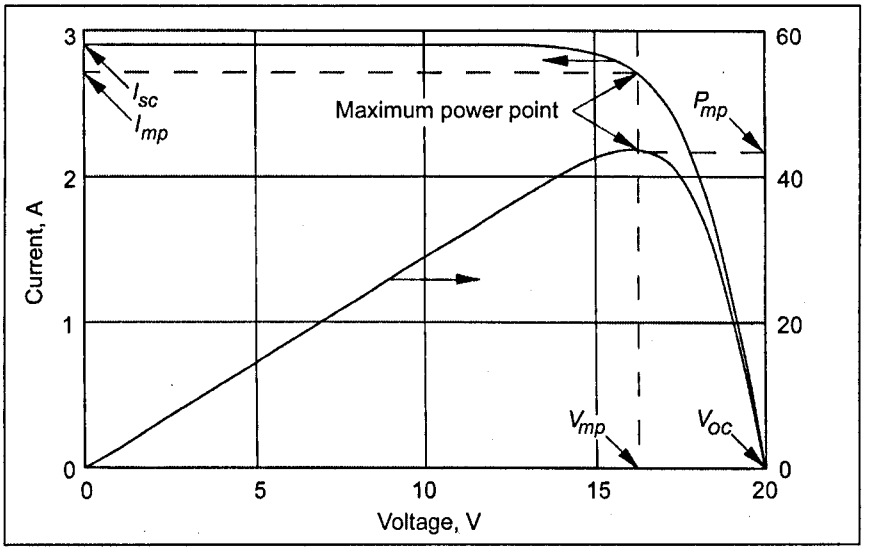

Figure 3.4 - Typical IV Curve and main performance metrics (re-drawn, Duffie & Beckman, 1991)

The power output of a PV cell is the product of *I* and *V*. This can be plotted on the *IV Curve* to give a *Maximum Power Point* (see Figure 3.4). At this point the power dissipated in the load is at a maximum and represented on the respective axes at points I_M and V_M. These metrics can be identified using:

$$\left[\frac{dI}{dV}\right]_M = -\frac{I_M}{V_M} \tag{3.9}$$

I_M and V_M can then be used to calculate the Fill Factor (FF). This is a measure of the junction quality and the series resistance of a cell, and provides a quantitative measure related to the form of the *I-V Curve.*

$$FF = \frac{I_M V_M}{I_{SC} V_{OC}} \tag{3.10}$$

This *Fill Factor* can then be used to calculate the Maximum Power Output (P_M) that can be expected from a cell, or module:

$$P_M = FF \cdot I_{SC} \cdot V_{OC} \tag{3.11}$$

This figure is often stated as the 'Rated Output' of a particular cell or module, however, it should be noted that all the above metrics are calculated under the following *Standard Test Conditions*:

- Incident Radiation (G_T) at 1000W/m^2
- Reference cell temperature (T_{ref}) at 25°C
- Spectral power distribution of air mass at AM 1.5

The Energy Conversion Efficiency at maximum power (η_{mp}) can finally be calculated as the ratio between the maximum electrical power delivered and the incident radiation on the cell:

$$\eta_{mp} \equiv \frac{I_M V_M}{A_C \cdot G_T} \equiv \frac{FF \cdot I_{SC} \cdot V_{OC}}{A_C \cdot G_T} \tag{3.12}$$

where G_T = Incident radiation (W/m^2)

Variation in efficiency due to cell temperature

This *Maximum Energy Conversion Efficiency* (η_{mp}) is temperature dependent. To assess the effect of temperature on cell efficiency for various semiconducting materials used in PV cells, experimentation has been carried out over a range of temperatures to ascertain *Maximum Power Point Efficiency Temperature Coefficients* (βr). For Silicon based cells a βr of 4 x 10^{-3}/°C is used (Twidell & Weir, 1986). Using this coefficient the following formula may be used to calculate the power available from a cell when temperature deviates from *Standard Test Conditions*:

$$P(T_{cell}) = P(T_{ref})\left[1 - \beta r(T_{cell} - T_{ref}\right] \quad (3.13)$$

where: T_{cell} = Cell temperature (°C)

Figure 3.5 shows results for a range of temperatures using this formula.

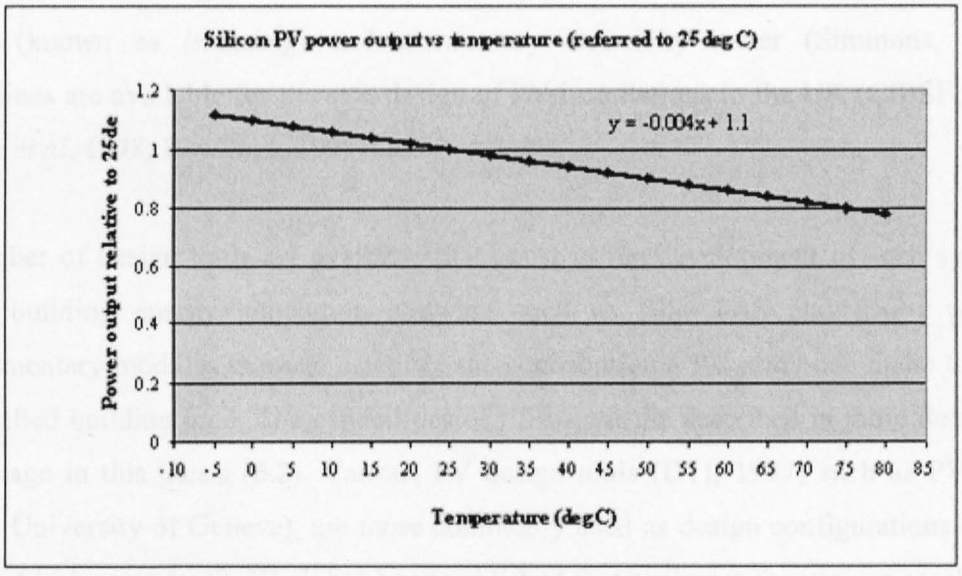

Figure 3.5 - Silicon based PV power output related to temperature

Under the research described in this thesis, this reduction of 0.4% / °C in efficiency above 25°C (Standard Test Conditions) is used as a set parameter within algorithms developed to assess PV/T collector performance.

The study of the thermal behaviour of PV cells, modules and installations has been extensively researched (Brinkworth *et al*, 1997; Gutschker *et al*, 1996; Wilshaw *et al*, 1997; Jones & Underwood, 2001).

3.3 Building Integrated Photovoltaic Systems

The initial design of a PV system will consider available area for collection, load requirements and costs to establish the appropriate PV technology to be used and the system configuration. Modules are then arranged in strings to provide the required voltage, which are then set up in parallel to increase current. The output from the array is then taken to a DC switch panel via junction boxes / terminals as required. This switch panel will contain protection devices such line and load switches, blocking diodes and fuses. The power can then be inverted to AC and provided to the building's loads by way of the main switchboard. If the building is to be grid connected an AC mains isolator is required to avoid dangers associated with the provision of power while the grid is not active (known as *islanding*) and a two-way electricity meter (Simmons, 1996). Guidelines are available for the safe design of PV installations in the UK (CIBSE, 2000; Munro *et al*, 1998; Rawlings, 1999)).

A number of design tools are available that assist in the development of such systems. Some building energy simulation software such as IES, TAS and ESP-r provide supplementary modules that can calculate the contribution a PV array can make towards a modelled building load. The capabilities of ESP-r will be described in more detail at a later stage in this thesis (6.2). Various PV design tools (DTI, 1997) such as PVSYST (GAP, University of Geneva), are more commonly used as design configurations can be assessed in greater detail. Work has been published that evaluates the various capabilities of available design tools (Jones *et al*, 1997).

3.4 UK PV Application

Compared to other countries, the UK possessed limited examples of BIPV until recent times. Domestic systems were installed in Oxford (Roaf *et al*, 2001) and Southwell, near Nottingham (Vale and Vale, 2000). The first large-scale application took place at The University of Northumbria in 1994, where a 40 kWp array was provided (case study - CIBSE, 2000). With the introduction of grant aid from UK Government and European programmes, a number of new and innovative systems have been installed with many more planned for development in the near future. A number of notable new BIPV installations should be mentioned here.

3.4.1 Doxford Solar Offices

This landmark development (see Figure 3.6), near Sunderland, has applied PV technology as part of an integrated energy strategy, that may adapt to the eventual needs of this speculatively constructed office building. Design team details and the overall PV system specification is provided in Table 3.1.

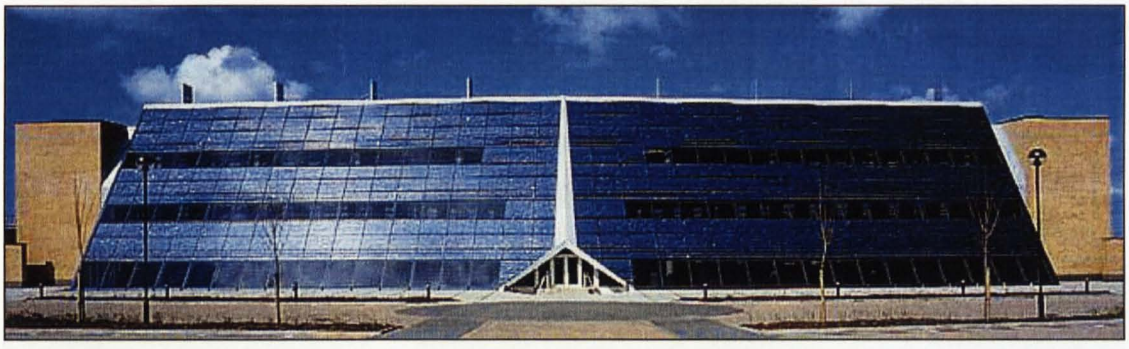

Figure 3.6 – The Doxford Solar Office (Thomas, 2000)

Architect	Studio E. Architects
Environmental Engineers	Rybka Battle
Array area (m^2)	950
Peak output (kWp)	73
Estimated annual output (kWh)	55100
Type of PV used	Polycrystalline

Table 3.1 – Doxford Solar Office PV design team and specifications (Jones *et al*, 2000)

3.4.2 Ladbroke Green Development

Figure 3.7 – The Ladbroke Green Development (courtesy of whitbybird)

Architect	CZWG Architects
Environmental Engineers	Whitby Bird & Partners
Array area (m^2)	2400
Peak output (kWp)	313
Estimated annual output (kWh)	223000
Type of PV used	Mixture specification to include Monocrystalline, Polycrystalline and Amorphous Thin Film

Table 3.2 – Ladbroke Green PV design team and specifications (Jones *et al*, 2000)

3.4.3 Beddington Zero Energy Development

Figure 3.8 – BEDZED (Bill Dunster Architects)

Architect	Bill Dunster Architects
Environmental Engineers	Ove Arup & Partners
Array area (m^2)	780
Peak output (kWp)	109
Estimated annual output (kWh)	97000
Type of PV used	Monocrystalline

Table 3.3 – BEDZED PV design team and specifications (Jones *et al*, 2000)

3.4.4 Nottingham Jubilee Campus

Figure 3.9 – Nottingham Jubilee Campus PV installation (Jones *et al*, 2000)

Architect	Michael Hopkins & Partners
Environmental Engineers	Ove Arup & Partners
Array area (m^2)	450
Peak output (kWp)	54
Estimated annual output (kWh)	51000
Type of PV used	Monocrystalline

Table 3.4 – Nottingham Jubilee Campus PV design team and specifications (Jones *et al*, 2000)

3.5 Solar hot water systems

Solar hot water systems are provided in many different designs and system configurations to meet various building hot water loads and respond to different climatic conditions. The storage tank is central to most solar hot water installations and can also be configured in numerous ways to integrate with other heat inputs and system designs. Figure 3.10 shows a solar hot water system similar to that which has been installed at the Brockshill Environment Centre. This shows a stratified storage tank that can take heat inputs at various temperature without diluting the water at highest temperature. A secondary tank, is then fed which supplies the hot water requirements of the building.

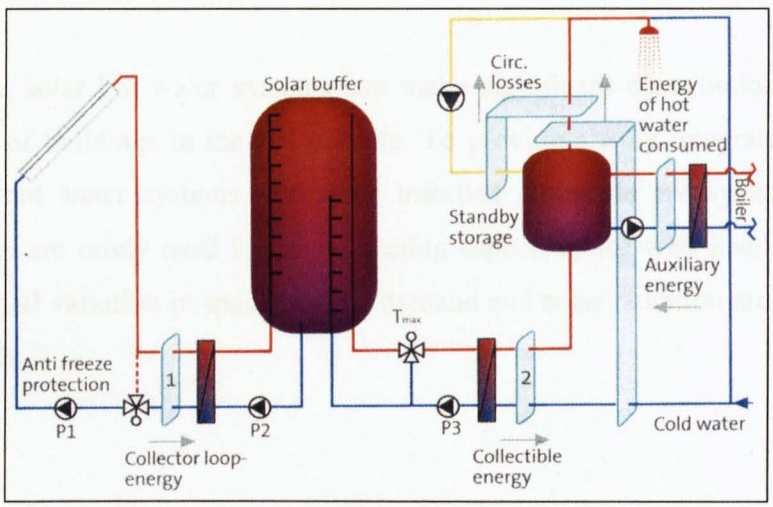

Figure 3.10 – A typical solar hot water system with a stratified storage tank (Peuser *et al*, 2002)

Hybrid PV/Thermal systems that incorporate solar hot water collection have been researched with a small number of demonstration schemes in place. There are clear technical problems with mixing a DC electrical network and water so it is expected that this area of application will remain limited.

3.6 Conclusions

In this Chapter, the concept of integrating PV technology into the built environment has been introduced and the principles behind photovoltaic cells presented, with particular emphasis on the effect of temperature. Issues associated with building integration have also been discussed and case studies presented.

It is clear that cell temperature has a significant impact on operational performance and therefore, a deleterious effect on operational costs and the economic viability of PV systems. This may be considered as part justification for the validity of the research described within this thesis.

It is clear that solar hot water systems can make significant contribution to the water heating loads of buildings in the UK climate. To provide a truly integrated low energy system solar hot water systems should be installed alongside PV systems. Solar hot waters systems are rarely used for space heating especially for well insulated buildings where the annual variation in space heating demand and solar radiation are mainly out of synchronisation.

Chapter 4

The Brockshill Environment Centre

4.1 Introduction

This Chapter describes the development of the Brockshill Environment Centre (BHEC) in Oadby and Wigston, Leicestershire. After introducing the main concepts of environmental design and building integrated solar thermal and photovoltaic technologies in preceding Chapters, this section of the thesis describes their application and integration within the development of a Local Authority owned visitors centre. This building is now in operation and widely recognised as an excellent working example of how these design strategies and low energy technologies can be implemented.

The author became involved in the development of the Brockshill Environment Centre in November 1998. At this time the project was at scheme design stage and the author undertook studies into building thermal performance and solar shading strategies. Assistance was then provided to the design team through design and construction. The author then assisted Dr Neil Shankland in the design, installation and commissioning of the monitoring systems prior to the building being opened to the public. From this stage data was collected from the systems relevant to the research described in this thesis.

In relation to the main research aims stated in Chapter 1, the installed ventilated photovoltaic and associated systems are described in detail and form a basis for the modelling activities presented in later chapters.

The Brockshill Environment Centre is the centre-piece of the Brockshill Millennium Park which has been developed by Oadby & Wigston Borough Council on the southern boundary of the city of Leicester. The total cost of this project was £1.88 million, with The Millennium Commission providing 50% and matched by contributions from Oadby & Wigston Borough Council, Leicestershire County Council, Circa Leisure, SITA Environmental Trust Limited, De Montfort University, Powergen and the Ministry of Agriculture, Fisheries and Food.

The original concept of the Brockshill Millennium Park project (originally outlined by the council in 1996) was to provide a park that emphasises the concepts of sustainable development to the local population, while providing a focus for the town's millennium celebrations. The Parkland covers an area of 36 hectares and is sectioned into a number of themed zones and woodland areas (Figure 4.1), with the focal point being the wind turbine that will in the future feed electricity to the visitors centre. Benefiting from an elevated location to the south of the park, this turbine will be clearly visible to local communities while maintaining a maximum possible distance from local housing to reduce noise impacts.

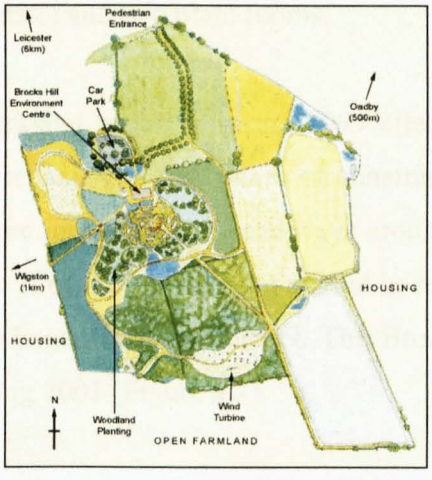

Figure 4.1 – Brockshill Millennium Park Map

The design concept for Environment Centre was to provide a public utility building incorporating an exhibition space, teaching facilities and a small restaurant, with the original intention that the building be self-sufficient in energy and water supply. The entire building could then be seen as an exhibit of current environmental design and technological capabilities to help promote sustainability issues and practice to the local population. During the design phase it was estimated that 20 000 people would visit the centre annually with a staff of five.

Six main functional zones are provided within the building. The exhibition hall provides the largest space and houses permanent exhibits describing the building and its systems, temporary exhibitions and may also be used for functions and events. The small café/restaurant is situated on the south side of the building and provides hot and cold drinks, snacks and light lunches. The classroom is also situated on the south side of the building with access from the conservatory and the exhibition hall, and is the base for visiting school parties. The educational activities based in the centre cater to all age groups and levels of expertise, with the building and its systems extensively monitored by the IESD to facilitate ongoing research and building systems' optimisation. This monitoring system was funded under an EPSRC Partnership for Public Understanding award, with the intention of providing usable data on the building and systems performance to the widest possible audience. A residential flat has also been provided (to be fully fitted out at a later date) and two plant rooms.

The development of the parkland began in spring 1999 after the land became available from the previous farming tenant. The first phase of construction was completed by the end of summer 1999 with the introduction of pathways around the park and the planting of thousands of trees. Phase II of the landscaping started in spring 2000 and construction of the Environment Centre began in August 1999. The Brockshill Environment Centre opened to the public in Spring 2001 (Figure 4.2).

Figure 4.2 – The Brockshill Millennium Environment Centre

The internal layout of the BHEC has been dictated by energy considerations and the functionality of the building. It is generally considered appropriate to locate living spaces and areas of high occupancy on the south side of the building where they may benefit from the higher levels of solar radiation. As kitchens are usually subject to overheating from appliances, they are often given a northern orientation along with bathrooms, utility rooms and areas of access, which do not need high levels of heating due to the intermittent use. For the layout of the BHEC, the zones assigned the valuable southern aspect are the restaurant and the classroom due to the high levels of occupancy expected during the daytime. The large exhibition hall is located at the rear of the building due to an expected intermittent occupancy and possible high levels of heat gain from lighting and computer driven exhibits, along with the toilets, kitchen and office. It is also natural to have the main entrance on the north side of the building as this services the car park and main routes of pedestrian access into the park.

Figure 4.3 – View from South-East

Figure 4.4 – View from North-West

4.2 The Built Form

The original design criteria for the MPVC maintained that the building should be of high architectural merit, however, the need to improve the building's energy performance and the active solar collectors also affects the style of the built form.

Daylight infiltration has been optimised in the public areas of the building to off-set the need for artificial lighting. This has been provided by large windows in the classroom and restaurant, the clerestory for the exhibition hall and the conservatory which will provide good daylight penetration, especially through to the foyer at the rear of the building. These areas of glazing provide the valuable solar gain, which is required to reduce the length of the heating season and contribute towards wintertime space heating.

The south-facing roof of the building has been designed to maximize the collection of solar radiation throughout the year, and therefore, may improve the active solar systems which this roof supports. The roof is provided with two angled surfaces, at 65^{o} to collect the low level winter sun and a 35^{o} surface that optimises the collection of the year round daylight. The upper section provides the inclined clerestory window to the exhibition hall along with an array of evacuated tube solar hot water collectors. The lower section of the roof is the platform for the photovoltaic (PV) array which is angled to give optimal year round performance. A solar air system is also supported on this section of the roof.

Other main functions of the roof include the need for access to the upper windows and solar systems for maintenance purposes and rainwater collection for use within the centre.

Zone	Floor Area (m^2)	Volume (m^3)
Exhibition	217.9	1510.7
Classroom	74.0	277.6
Restaurant	178.6	670.0
Conservatory	51.3	291.2
Plantroom	74.0	142.3
Flat	135.5	320.6
Roofspace	n/a	267.6
Total	**731.3**	**3337.7**

Table 4.1 – Zonal Floor Areas and Volumes

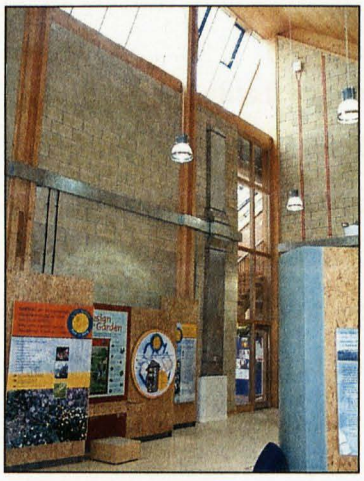

Figure 4.5 – The Exhibition Hall

Figure 4.6 – The Conservatory

4.2.1 Building Fabric

The building has been designed to be thermally massive to help regulate the internal temperatures throughout the year. The building fabric may therefore store heat when it is available, for later release during the night time. Conversely, during the warmer periods of the year, the building structure may be cooled during the night time to help regulate the internal temperature during the following day. This capability has been achieved by providing large areas of exposed, heavy weight masonry walls, partitions and ceramic floor tiles in the south facing rooms. An earth berm is provided around the northern edges of the building which has a dual function of reducing infiltration while acting as an insulating buffer on this more exposed surface of the building.

The insulation of the MPVC is one of the most important components of the building fabric as it limits the amount of energy that is lost to the environment. The benefits of insulation are most noticeable during the winter months when heat energy supplied from solar radiation, building occupants, appliances and also energy supplied by the active heating system, can be retained for a longer period inside the building. Consequently, less fuel is required and less pollution released to the environment.

The MPVC benefits from very high levels of insulation at all boundaries with the outside environment. The roof of the building has been provided with 500mm of dry-blown Warmcel cellulose insulation (see Table 4.2 for U-values of composite structures of the MPVC compared to current building regulations). The external cavity walls have been specified with 300mm of rockwool insulation batts and the ground space of the building with 200mm of expanded polystyrene plus a layer of glass fibre quilting.

Construction Composite	Material	Material thickness (mm)	U-Value (W/m^2K)	U-value - Building Regulations 1995 (W/m^2K)
External Walls	Brick Mineral Fibre Block	100 300 150	0.12	0.45
Internal walls	Brick Mineral fibre Brick	100 60 100	0.47	n/a
Roof	Clay tile Air Cellulose fibre Ply/Pine ceiling	15 20 500 15	0.09	0.25
Balcony Roof	Asphalt Plywood Mineral fibre Plasterboard	5 18 400 24	0.09	0.25
Floor	Earth Polystyrene Glass fibre quilt Concrete Screed	 200 50 150 75	0.18	0.25

Table 4.2 – Construction Composite Data

Figure 4.7 – Ground Floor Insulation

Figure 4.8 – Glu-Lam Timber Structure

4.2.2 Glazing Systems

The glazing of the building has been carefully specified to enhance the thermal and daylighting concepts of the building. The windows of any building result in a complex

energy balance where radiation passes through the glazing to off-set the need for artificial lighting and also heats the internal spaces by warming surfaces. However, these useful gains have to be considered against the heat which is lost during night time and periods of low sunlight, as the poor thermal properties of glazing provide a low resistance path to heat losses. To reduce these thermal losses, triple glazed windows have been specified for all windows in the building except the clerestory and conservatory roof where double glazed units are used (see Table 4.1 for U-values). All of the windows benefit from argon filled cavities and a low emissivity (low-e) coating which reduces radiative exchange. The glazing of the building has also been designed to aid the ventilation system, with the clerestory windows used during the natural ventilation and night venting modes of operation and the ground floor windows accessible for control by the building occupants.

This large area of glazing, combined with the high levels of insulation results in a great potential for over heating during the summer months. For this reason, seasonal shading louvres have been considered for application to ground floor windows between April and September. These louvres would protect the internal space from direct sunlight, while providing an adequate amount of daylight penetration and visual access to the park outside. Shading devices have also been considered for the clerestory windows where translucent roller blinds would reduce the solar gain and glare within the exhibition hall. To date, no internal or external shading devices have been installed.

Figure 4.9 – Triple Glazed Unit with Ventilation Opening

Figure 4.10 – Solaglaz Double Glazing

Glazing System	Material	Material Thickness (mm)	U-Value (W/m^2K)	U-value - Building Regulations 1995 (W/m^2K)
Solaglas (Saint Gobain)	clear float low-e air clear float low-e	7 12 7	1.3	3.3
Triple glazing (Allan Brothers)	clear float low-e air clear float air clear float	4 8 4 8 4	1.2	3.3

Table 4.3 – Glazing System Data

Zone	Area of Glazing (m^2)	Proportion Facing	Glazing to Floor
Exhibition	78.78	84.5	36.1
Restaurant	15.09	61.7	8.4
Classroom	13.90	81.9	18.8
Flat	22.90	72.5	16.9
Conservatory	72.49	-	143.3
Total	203.18	79.8	27.8

Table 4.4 – Glazing Statistics

Zone	Exposed Surface area	Heated Volume (m^3)
Exhibition	489.9	1510.7
Restaurant	151.9	670.0
Classroom	67.7	277.6
Flat	109.3	320.6
Total	818.9	2778.9
Building	**Exposed surface area to volume ratio (%)**	
BHEC	29.5	
Cubic Building	51.5	

Table 4.5 – Exposed Surface Area to Heated Volume Ratios for BHEC and a Cubic Building

4.2.3 Building Integrity

The quality of construction of the building envelope affects the infiltration rate through the envelope and hence the demand for heating. Airtightness testing has been undertaken (by Stuart Borland of Building Sciences Ltd.) at the Brockshill Environment Centre to ascertain the quality of construction and the likely impact of cold air infiltration. Figure 4.11 shows the testing equipment in place between the restaurant and the conservatory (considered to be outside the main building envelope). The air leakage rate is tested using a fan to raise the internal air pressure above atmospheric levels and the flow rate measured to maintain a given internal pressure. This procedure is repeated for a range of internal / external pressure differences and the results used to determine the air leakage rate at a standard reference pressure difference of 50 Pascals. The target air leakage rate at 50 Pa was $5m^3/h$ per m^2 of exposed envelope area, which is stringent compared with 2002 Building Regulations recommended target of 10 m^3/h per m^2 for commercial buildings. Test results indicated that the actual air leakage rate was $6m^3/h$ per m^2. This infiltration rate has been used for thermal modelling described later in this thesis.

Figure 4.11 – Air Tightness Testing

Particular attention has also been given to provision of draft stripping of all opening doors and windows and a draft lobby provided at the main entrance to limit cold air ingress as people enter and leave the building.

4.2.4 Sustainable Building Practices

It is estimated that 50% of material resources taken from the environment are building related, over 50% of national waste production comes from the building sector, and 40% of the energy consumption in Europe is used within the built environment (Anink *et al*, 1996). Along with energy and water, construction materials can be identified as the third main 'flow' within the building that has an impact on the environment and with a mandate to provide a building that promotes all areas of sustainable design to the wider community, a commitment to the specification of suitable materials was given at the project outset.

Specification was based on the need to select materials with the least environmental impact arising from emissions (CO_2, SO_2, VOC, NOx), embodied energy (from extraction, production and transport), generated wastes and eventual disposal. The use of renewable and recycled products was encouraged and the efficient use of materials promoted. Identification and comparison between materials was undertaken using the BRE Environmental Profiling System methodology (Howard *et al*, 1998) and the Environmental Preference methodology (Anink *et al*, 1996). Once suitable materials were identified, products and sources were established using the Association of Environment Conscious Building Greener Building Directory (Hall & Warm, 1995) to provide the architect and structural engineer appropriate information for consideration.

The design team then specified with the maximum use of low impact materials whilst maintaining the structural and thermal integrity of the building. Subsequently, four main features of the Environment Centre can be noted under sustainable building practices:

- The main structure of the building uses laminated timber instead of steelwork due to its high embodied energy and environmental impact during fabrication. The timber was sources from sustainably managed Scandinavian forests.

- Roof insulation consists of Warmcel ™ cellulose (recycled newspaper), rockwool (natural volcanic material) within cavity walls and expanded polystyrene underfloor.
- Recycled rooftiles.
- Low toxicity paints and finishes.

Where possible materials were sourced locally.

4.3 Building Services

4.3.1 Thermal Systems

In line with the low energy concept of the building, the thermal systems have been designed to interact closely with the dynamic nature of the building fabric and external conditions to provide thermally comfortable internal conditions throughout the year.

Due to the passive solar design, the high levels of insulation and good air-tight construction, heating requirement and the length of the heating season are considerable lower than standard buildings of this nature. When space heating is required, the load is delivered using the minimum volume of air needed for ventilation. To enable this, the system has been designed to integrate or isolate various components depending on energy availability and load at any particular time. This requires a central heat store as the main component of the system that can regulate the available heat energy between periods of high energy supply and demand.

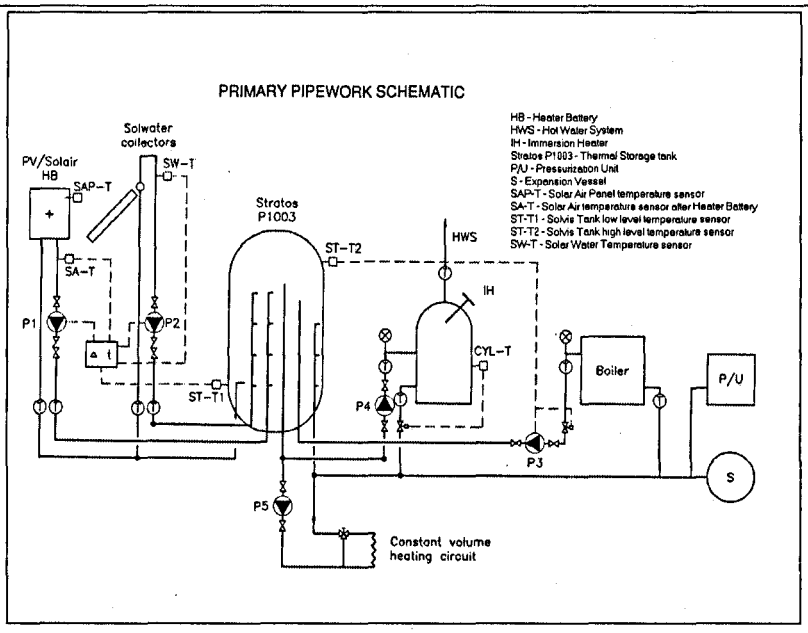

Figure 4.12 -Schematic Diagram of Water Heating System

Figure 4.12 shows a schematic diagram of the main hot water heating and thermal storage system, which is central to all space heating and hot water provision within the building. During winter operation, space heating and ventilation is provided by the same volume of air, which is ducted around the building and released through low level displacement units. Fresh air is pre-heated by the VPV-SAS and exhaust heat recovery before being brought up to supply temperature within the main heater battery in the Air Handling Unit (AHU). This heater battery is supplied directly from the Stratos Central Heat Store which is in turn supplied by input from the solar hot water collectors, the dual fuel boiler and return heat from the AHU heater battery. During summer, space heating is not required; however the Central Heat Store accepts input from the solar hot water collectors and VPV-SAS System, when available, to supply the building's hot water requirements.

The plant associated with this system is spread across two plantrooms. Plantroom 1 (see Figure 4.13) is located in an unheated out-building to the west of the main building and houses the central heat store, hot water cylinder and dual fuel boiler (along with water filtration and sterilisation systems, electrical switchgear and controls). Plantroom 2 is

located in the roofspace below the VPV/SA collectors (see Figure 4.14) where the air heating and distribution plant is located.

Figure 4.13 – Plant Room 1

Figure 4.14 – Plantroom 2

4.3.1.1 Central Heat Store

The storage tank specified for the BHEC has been specially constructed for the particular requirements of the system, with inputs from the various systems at different levels within the tank (Figure 4.15). This enables stratification within its volume so that inputs of heat at a lower temperature than the maximum within the tank does not dilute the higher temperature water.

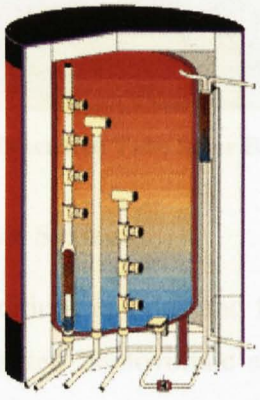

Figure 4.15 – Diagram of a Stratified Thermal Storage Tank

Hot water is supplied to the tank from four main sources via three input pipes which possess nozzles at various heights within the tank to enable the stratification (see Figure 4.13). As water enters the tank it discharges at the appropriate level corresponding to its temperature. The four inputs are the Ventilated Photovoltaic / Solar Air (VPV/SA) collector, the evacuated tube solar hot water array, the dual fuel boiler and the return from the air handling unit (AHU) which provides the active space heating

4.3.1.2 Solar Hot Water System

An array of 120 Thermomax evacuated tube solar hot water collectors (see Figure 4.16) are provided on the upper roof adjacent to the clerestory windows of the Exhibition Hall. When available, heated hot water is supplied directly to the Central Heat Store.

Due to technical problems this system was not operational during the course of this research.

Figure 4.16 – The Evacuated Tube Solar Hot Water Collectors

4.3.1.3 Ventilated Photovoltaic System

Depending on environmental conditions and demand for space and water heating within the building, the combined Ventilated Photovoltaic and Solar Air Systems (VPVSAS) can be scheduled by the BEMS to run under four modes of operation. Figure 4.17 shows

the installed collectors. The VPVSAS system and damper settings which control the modes of operation are illustrated in Figure 4.18 and Table 4.6.

Figure 4.17 – The Combined PV/Thermal and Solar Air Collectors

Mode 1 – Pre-heat for ventilation:

This is the main mode of operation during winter months or periods of cold weather. Its main objective is to pre-heat fresh, incoming ventilation air prior to entering the AHU, where it is heated to the correct temperature before being circulated to the building. Air temperature is boosted in the AHU via heat recovery from extract air and via a heater battery supplied by the central heat store. If the building return air is at a temperature lower than that which is being provided by the VPV/SA collectors, the AHU may be by-passed to ensure that solar heated air is not cooled before being boosted to supply temperature within the heater battery.

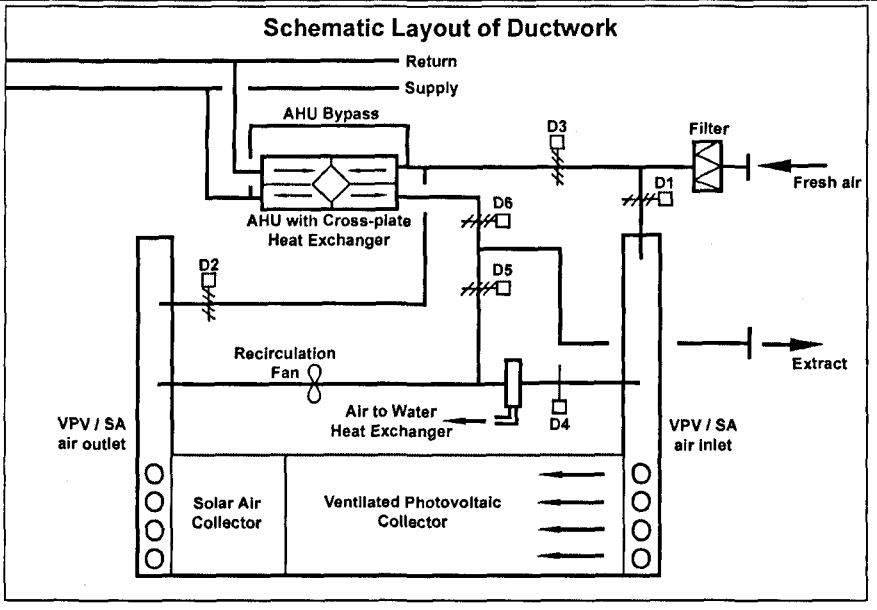

Figure 4.18 – Schematic Diagram of the Air Heating System

Mode of Operation	Dampers Open	Dampers Closed
1. VPV/SA to AHU	D1, D2, D6	D3, D4, D5
2. VPV/SA by-pass	D3, D6	D1, D2, D5
3. Surplus heat vented	D1, D5	D2, D4, D6, D3
4. VPV/SA to heater battery	D4	D1, D2, D5

Table 4.6 – Operation of Dampers to Control VPV-SAS Modes of Operation

Mode 2 – VPV/SA Collector By-pass

This mode of operation is used when heat provided by the VPVSAS is not needed for space heating requirements within the building. During these periods, fresh ambient air may by-pass the solar collectors and feed directly to the AHU.

Mode 3 – VPV/SA Re-circulation for Hot Water Provision

Under this mode of operation air is actively re-circulated through the collectors to achieve higher temperatures than may be obtained during a single pass. After exiting the collectors, the heated air re-enters the plantroom where it passes through a re-circulation

fan and an air-to-water heat exchanger from where heat can be transferred to the central heat store.

This Mode of operation can be run in conjunction with Mode 2.

Figure 19 – Re-circulation Fan used during VPV-SAS Mode 2

Mode 4 – Surplus Heat Vented

When there is no call for space heating and the central storage tank is at capacity, surplus heat from the collectors can be vented to the atmosphere to avoid overheating the PV modules, thereby maintaining cell efficiency.

4.3.1.4 Dual Fuel Boiler

The main boiler has a rated output of 19kW. The dual fuel capability means that fuel may be harvested from trees around the Millennium Park when mature. Until then, gas oil will be the back up fuel used for space heating and hot water provision.

4.3.1.5 System Controls

The system is regulated by the temperature of the central storage tank, the availability of energy from the solar collectors and from the backup boiler. Heat is supplied by the boiler when sensor ST-T2 (see Figure 4.12) at high level in the central heat store indicates a temperature lower than 65°C.

Pumps supplying hot water from the solar collectors are operated on a temperature differential with sensor ST-T1 located at low level in the Central Heat Store. When there is no call from space heating and sensor SA-T within the VPV/SA collectors indicates that useful heat can be made available to the Central Heat Store, the re-circulation fan is switched on and pump P1 operated to supply heated water from the air-to-water heat exchanger to the Central Heat Store. When the tank cannot take any more hot water the pump to the tank is shut down and VPV-SAS Mode 4 operated.

The solar water system is initiated when the water temperature sensor SW-T in the manifold of the collector is 10°C greater than that of the central store. When no more heat is required the pump (P2) for this collector is shut down and the evacuated tubes are left to regulate their own temperature by means of an integral high temperature cut-off within each tube.

All thermal systems within the building are controlled by the Trend Building Energy Management System (BEMS), which is located in Plantroom 1.

4.3.2 Ventilation

The building operates a mixed mode ventilation strategy depending on time of year. During winter when heat needs to be retained within the building, a mechanical system is used in combination with space heating requirements. The BEMS uses CO_2 sensors used to assess occupancy and regulate ventilation requirements.

During summer, mechanical ventilation is switched off and the building converts to a full natural ventilation with night-time cooling of the mass. Air enters through openable doors provided with louvers to maintain security. Air exits via high level opening clerestory windows in the exhibition hall.

4.3.3 Electrical Systems

The electrical system of the BHEC has been designed to minimize the electrical load of the building and to provide for these requirements by on-site generation where possible.

The two main sources of power are the wind turbine and the PV array with a backup connection to the electricity grid when energy is not available from wind or solar sources. Due to the dynamic nature of the system, metering is provided for all components to assess the energy flow and contributions made to the load by the wind turbine, PV array and the grid.

To keep the electrical load to a minimum, systems and appliances have been carefully selected throughout the building. This selection process has removed appliances deemed unnecessary to the building's normal operation and specification of equipment, which show low energy consumption under the European Union Energy Consumption Code.

4.3.3.1 Wind Turbine

As one of the main aims of the development is to demonstrate technologies that promote sustainable development to the community, the main wind turbine is the focus of on-site power generation. The project also provides a rare opportunity to demonstrate a medium sized wind turbine in a semi-urban environment and for a specific building rather than feeding power into the grid as its main purpose.

The wind turbine is to provide the main source of electricity for the building. It is situated at the southern end of the parkland (see Figure 4.1) where it will benefit from the highest elevation in the park and maintains the maximum possible distance from residential areas to the east and west. A Jacobs 25kWp turbine was installed in June 2002 (Figure 4.21), unfortunately however, this machine has since been destroyed in high winds. It has been estimated that when operational this wind turbine will produce approximately 30MWh/pa (subject to wind conditions).

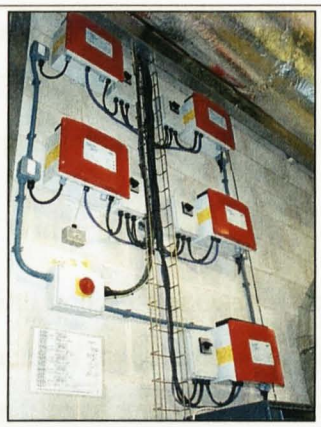

Figure 4.20 – PV Invertors

Figure 4.21 – Main Wind Turbine (similar model originally installed)

4.3.3.2 Photovoltaic System

It is clear that there is a massive potential for the utilization of PV in buildings, however, for this vast physical potential of the solar resource to materialize in cost effective applications, it is crucial that large enough markets emerge to cut down the price per watt of PV (Sick, 1996). The system installed in the MPVC is therefore a working exhibit that demonstrates the viability of PV systems in the UK.

The PV system is situated on the lower 35° roof where it can maximize efficiency during the summer months when less power is being generated from the main wind turbine. The array covers an area of 33.7m^2 and has a rated output of 4kWp. Seimens monocrystalline silicon cells (12% efficiency) make up modules mounted into the Grammer Solar Air Collectors. Estimates suggest that this array will provide 4MWh of electricity for use within the building.

Power is provided to the buildings three-phase system via five Sunny Boy Invertors (Figure 4.20).

4.3.3.3 Grid Connection

Being a public amenity building, grid connection is required as backup during periods when wind and solar generation are not available. The connection installed by the REC (Powergen) provides a two-way meter that enables surplus power generated on-site to be

supplied into the national grid. Under present arrangements, this electricity is supplied free of charge, however, the metering does provide data on the buildings level of electrical autonomy throughout the year.

4.3.4 Water Services

The building has been designed to be autonomous in water supply. Rainwater is collected from the roof and stored in a 20 000 litre tank buried to the north of the building. This water is filtered and treated with UV sterilization before being used within the building. The water use is minimized by the application of a composting toilet in the unisex disabled washroom, low-flush toilets throughout, the provision of waterless urinals and spray taps.

4.3.5 Monitoring System

Three sources of data acquisition are used. The main Building Energy Management System provides data on building services and control of the building. Additional and more detailed performance data is recorded on data loggers which have been used to record performance of the combined PV/Thermal and Solar Air collector system. Finally, the onsite weather station takes continuous readings on ambient temperature, global horizontal radiation, wind speed, relative humidity and rainfall.

4.4 Review of systems after installation

All systems were installed successfully as described in the previous sections. Even though this particular environmental control strategy had never been applied in other buildings, few complaints were made by the building users and the system maintained thermally comfortable internal conditions.

Unfortunately, a number of technical problems were encountered and the following have been listed here as they had a direct impact on this research:

- Vandalism of the PV/Thermal collectors soon after installation. Thermal integrity maintained but not electrically commissioned until 2002. No electrical output or data is available before this time.
- Re-circulation fan installed in the wrong direction. Not corrected until 2002 so the system did not operate properly prior to correction.
- Solar hot water system became inoperable soon after installation due to the evacuated tube heat exchangers expanding and splitting the manifold. System is still inoperable at time of writing.
- General problems with BEMS during first year of operation due to poor commissioning procedures.
- General problems with data loggers during first year of operation resulting in holes in data sets.

4.5 Conclusions

This Chapter has introduced the environmental design and services strategy of the Brockshill Environment Centre. This demonstration and research building employs many well documented approaches and systems to further the ambition of being autonomous in energy and water supply. The unique aspect for this particular building is the combination of these approaches into a system, which services a particular public utility building.

As with many low energy buildings that respond to external environments, problems have been encountered when in operation. It is therefore important that the building design and services are assessed and results disseminated to the construction industry so future designs may be refined.

Chapter 5

Combined Photovoltaic Thermal Systems – Theory and Application

5.1 Introduction

Within the remaining chapters of this thesis, the main research activities are presented and discussed in relation to context provided within Chapters 1 to 4.

This Chapter introduces the main research field associated with PV/Thermal (PV/T) theory, mathematical modelling and application. From this basis, the mathematical theory of the VPVSAS method is presented and discussed in relation to past work.

A series of formulae is presented, which are used by two new subroutines to represent a PV/T collector and a Solar Air (SA) collector. These subroutines have been installed within TRNSYS and ESP-r simulation programmes (see Chapter 6). The Chapter concludes with the presentation of combined PV/T and SA collector performance with the validity of this method discussed.

Further to solar thermal concepts presented in Chapter 3, this Chapter builds a historical context to PV/T theoretical development.

5.2 Solar thermal collectors: theoretical development and mathematical modelling

A model for the thermal analysis of conventional flat plate collectors was originally proposed (Hottel & Woertz, 1942) to provide a relatively simplistic method of accurately calculating the performance of specific collectors. It was further developed and refined (Whillier, 1967; Hottel & Whillier, 1955; Bliss, 1959) and widely disseminated (Duffie & Beckman, 1991) to become a well-used method of calculation within the solar energy field. The result of these developments is the following equation for the useful energy gain that can be provided:

$$Q_u = A_c F_R [S - U_L (T_{in} - T_a)] \qquad [5.1]$$

where Q_u = Useful gain (W)
A_c = Area of collector (m^2)
F_R = Collector heat removal factor
S = Solar radiation per unit area (W/m^2)
U_L = Collector overall heat loss coefficient (W/m^2C)
T_{in} = Inlet temperature (C)
T_a = Ambient temperature (C)

This equation is central to thermal calculations undertaken by the VPVSAS.

5.3 Recent research activities using these approaches

Dating back to the late 1970s, research into PV/T systems has focused on the integration of PV cells into the absorber plate of standard solar thermal collectors (see Chapter 3). Many different configurations of building integrated PV/T collectors have been considered, however, all use the common concept that waste heat from the PV cells is directly transferred into air, water or phase changing liquids and made available for use within the applied building.

Through the application of PV cells to the absorber plate of a standard solar thermal collector, approximately 10% less incident solar radiation is made available for heat transfer to the fluid medium. This is due to lower optical absorption by the PV material compared to a standard black absorber plate (Sandnes & Rekstad, 2002).

Depending on system requirements, the design of a PV/T application may be adapted to favour a particular output. For example, the addition of an extra layer of glazing in front of the PV material will give up to 30% higher thermal efficiencies to the detriment of PV cell efficiency, which may reduce by 16% due to optical losses (Tripanagostopoulos *et al*, 2002). The cost of PV modules and the worth of electrical power generated from a PV/T system generally results in PV output being optimised at the expense of thermal generation.

5.3.1 PV/T for water heating

The widespread application and understanding of flat-plate solar hot water collector systems has helped further research into PV/T water heating collectors, with a number of small-scale demonstration schemes now in place. With regard to thermal output, theoretical efficiencies of between 60-80% have been calculated (Bergene & Løvvik, 1995). From this basis, various collector configurations / designs have been constructed and tested. Numerical models developed at Eindhoven University of Technology, calculated in steady state 1D, 2D, 3D and dynamic 3D have all followed an experimental result of 56% efficiency ± 5% (Zondag *et al*, 2002). However, thermal efficiencies have been found to vary considerably when a typical load profile is applied, ranging from 12 and 41% depending on water tank temperature, ambient temperature and incident solar radiation (Huang *et al*, 1999 & 2001).

Studies of this technology in Saudi Arabia have identified a significant annual variation in collector performance. High summer temperatures mean that thermal yields and efficiencies are high, as would be expected, at the expense of PV cell efficiency, which decreases by 30% from a maximum (Al Harbi *et al*, 1998). Winter conditions are shown to be preferential for PV/T water heating in this geographic location.

5.3.2 PV/T for air heating

Theoretical thermal efficiencies of between 17-51% have been calculated for PV/T air collectors (Prakash, 1994). Comparative studies of these collectors have considered passing air above or behind the PV material, both sides of the absorbing surface or a double pass arrangement. Conclusions were made that the best overall performance (related to PV efficiency, thermal output and fan power required) is found by taking air across the front and rear of the PV material concurrently (Hegazy, 2000). However, the standard configuration remains a single air pass behind the absorbing surface. Optimisation of this format has focused on increasing solar absorptance and reducing the infrared emittance. Following research conducted at the Massachusetts Institute of Technology, it has been recommended that infrared emissivity from the collector is kept below 0.25, solar transmissivity is maintained above 0.85, a non-selective secondary absorber is provided along with a high-transmissivity / low-emissivity cover above the PV cells (Cox & Raghuraman, 1985).

Research concerned primarily with façade PV/T air heating systems has focused on air gap variation and flow regimes to optimise natural buoyancy forces and temperature rise (Moshfegh & Sandberg, 1998; Sandberg & Moshfegh, 2002; Brinkworth *et al*, 2000). Under standard test conditions, air-flow within hybrid PV/T façade elements has been measured to be approximately 0.04 m/s^{-1} (Crick *et al*, 1997). When compared to an optimum flow rate of 2.0 m/s^{-1} the limited air flow presents implications to PV cell efficiencies, although there is potential for significant rises in temperature. Provided mechanically, this higher velocity will reduce operating cell temperatures by 18°K and provide an 8% increase in electrical power output in comparison to conventional PV façades (Krauter *et al*, 1999).

5.4 Application and demonstration of PV/T systems

To further innovation and application of PV/T systems in the built environment, an IEA sponsored PV/T workshop in 1999 developed five main driving issues that should be addressed:

- The satisfaction of architectural design
- The satisfaction of building energy requirements
- Client satisfaction
- The satisfaction of the end user or building occupants
- The creation of a useful and delightful space to inhabit

(Leenders and Van der Ree, 1999)

These criteria were proposed at a time when a number of key built examples were in place with design lessons considered. These built examples cover a range of PV/T configurations, building uses and climatic conditions.

5.4.1 Multi-functional façade systems

The public library at Mataró (see Figure 5.1), near Barcelona, is provided with arrays of opaque and semi-transparent hybrid PV/T modules to give a rated PV output of 53kWp (Lloret *et al*, 1997). The main façade of this landmark project supplies electricity and heating to the building, while maintaining daylight penetration with reduced risk of summertime overheating. The provision of a ventilated chamber within each hybrid façade element enables warm air to be generated via natural convection from PV surfaces. This pre-heated air is taken to a conventional gas heating system, where it is brought up to supply temperature. During warm seasons, surplus heated air within the façade may be vented to the exterior, thereby maintaining PV cell efficiencies. A number of research studies have been undertaken with regard to parametric estimation for numerical modelling (Infield *et al*, 2000 and Mei *et al*, 2002), performance assessment (Eicker *at al*, 1998 & 1999) and validated simulation investigations (see 7.3).

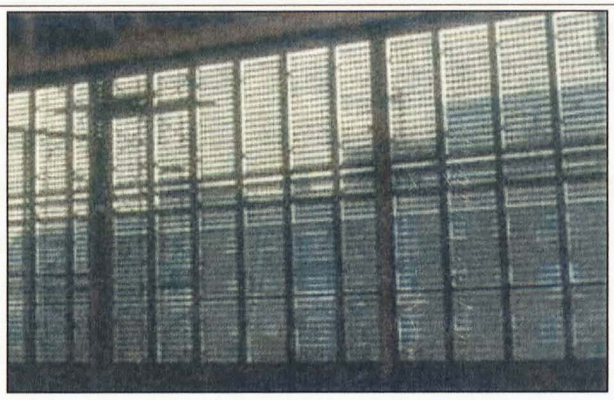

Figure 5.1 – Multifunctional façade of the Mataró public library

The ELSA (European Laboratory of Structural Assessment) building (see Figure 5.2) located in Ispra, northern Italy, provides a 505m^2 array on its south facing façade. This PV array is made up of amorphous PV modules and is rated at 21 kWp (Bazillian *et al*, 2001). An air gap is provided behind these modules to form solar chimneys, which are linked into the main building ventilation system. This building and incorporated PV/T system, have been modelled as part of the PV-HYBRID-PAS study (see 7.2) and assessed under a number of hypothetical system configurations (Clarke *et al*, 1998).

Figure 5.2 – The Elsa building

SOLARWALL is an innovative solar thermal cladding system developed by Conserval Engineering Inc. of Toronto, Canada. In its basic form, SOLARWALL (see Figures 5.3 & 5.4) uses corrugated metal cladding that is perforated with holes to let air permeate into a plenum between the cladding and building envelope. Heated air may then be used to

pre-heat ventilation air during the winter or induce fresh ventilation air to the building when the façade is operated as a solar chimney. A hybrid SOLARWALL system has been developed to incorporate PV modules in front of the corrugated metal cladding. Test results indicate an efficiency at 900W/m^2 and 100 m^3/h.m^2 of 51.8% (Hollick, 1998). This study concluded that a combined PV/SOLARWALL panel will improve the efficiency of the PV panel and that the overall total efficiency will be greater than the standard thermal efficiency of the SOLARWALL system.

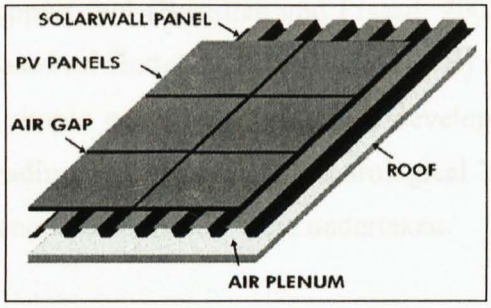

Figure 5.3 – The SOLARWALL concept (courtesy of Conserval Inc.)

Figure 5.4 – A SOLARWALL installation (courtesy of Conserval Inc.)

The Doxford Solar Office (see Figures 5.5 & 5.6) utilises waste heat from a 73 kWp façade mounted array to pre-heat ventilation air. Surplus heat may be vented at the top of the façade, where specially placed fins and a gully improve air movement and efficiency of the PV system.

Figure 5.5 – Doxford Solar Office (courtesy of whitbybird)

Figure 5.6 – Doxford Multifunctional Façade (courtesy of Studio E Architects)

5.4.2 Modular PV/T heat recovery systems for residential buildings

With particular emphasis on residential scale application, research undertaken at the University of New South Wales (UNSW), Sydney, has involved numerical model development (Bazillian *et al*, 2001a) and experimental testing (Bazillian *et al*, 2001b) of a modular co-generation system.

The main objective of this work focused on the development of a validated decision support tool (Bazillian and Prasad, 2002) for use in the design of solar home systems. Based on Hottel-Whillier-Bliss (HWB) related formulae (see 5.2 and 5.7) and coded into a simple equation solver (EES developed by the University of Wisconsin) capable of reading TMY (Typical Meteorological Year) weather files, transient simulations of a co-generation collector were undertaken.

This algorithm was validated using data collected from a test installation in Sydney that consisted of 20 PV modules (740Wp roof array) mounted above an insulated duct 150mm in depth. The duct could be mechanically or naturally ventilated with heated air provided directly into the building.

Published work shows good agreement between theoretical calculations and monitored data. The exercise also indicates a good level of parametric analysis, particularly in the assessment of various Nusselt heat transfer equations (see 5.6). It is unclear from published work as to the thermal and electrical loads to which the co-generation collector is subject. There are also concerns regarding the air flow regime within the duct due to module connection flanges and the adaptability of the design tool when considering collector geometry and constructions different from that tested.

5.5 PV/T transient simulation activities

A distinction is required between transient simulation activities of component PV/T collectors and building integrated PV/T simulation where output from the collector

provides energy to a specific modelled load. A particular benefit of the VPVSAS method is that performance analysis of PV/T systems can be undertaken for both scenarios.

Building integrated PV/T simulation is covered in detail in Chapter 7, where the VPVSAS method is related to two major research projects in this area. These projects focused on the multi-functional façade applied to the Pompeu Fabre library at Mataró (see 7.4.1) and the JOULE III funded PV-HYBRID-PAS project and associated research (Clarke *et al*, 1997).

At component level, the main body of work has been conducted by Garg & Adhikari (1997, 1998 & 1999), who have focused on the assessment of system efficiencies for various collector configurations using HWB based theory for calculation.

For reference purposes only, it should be noted that specific TRNSYS PV/T water heating (see 5.3.1) components have been developed (Rockendorf *et al*, 1999; Kalogirou, 2001).

5.5.1 Standard TRNSYS components

The HWB method has been used for calculating the transient performance of solar collectors using TRNSYS (SEL, 2000), initially incorporated into the Type 73 subroutine for theoretical flat plate solar collectors. Using this Type, the efficiency and performance of the collector can be calculated using the properties of the collector construction and materials. The majority of solar collector subroutines (Type 1 collectors) within TRNSYS now request efficiency information calculated during standard test conditions (SRCC, 1995). Due to information being unavailable for the Brockshill Environment Centre PV/T collector and the fact that a more extensive range of variables cannot be included for calculation, these standard TRNSYS Types are not suitable for use in the VPVSAS study.

A subroutine has also been released within the standard TRNSYS library that describes a PV/Thermal collector where the thermal and electrical output can be calculated. Called Type 50, this is based on the standard Type 73 (HWB) subroutine. It uses updated

formulas based on work by Florshuetz (1976), which extends the HWB model using the assumption that the local PV cell conversion efficiency is a linear decreasing function of the local cell temperature over the operation range of the combined collector. For monocrystalline silicon, this temperature coefficient can be taken as -0.4%/°C above STC (Twidell & Weir, 1986) and for amorphous silicon, -0.13/°C (Affolter *et al*, 1997). As with Type 73 this subroutine requests an overall collector efficiency factor (F') (see 5.7.3) to be stated as a parameter rather than be calculated in a transient manner. When F' is calculated in this detailed way the resulting F_R provides a more dynamic representation of the heat removal capabilities of the collector.

5.6 PV/T performance and parametric assessment

Studies into parameter estimation have been conducted for ventilated PV facades (Infield *et al*, 2000) and PV/T air collectors (Sopian *et al*, 1996; Sandberg & Moshfegh, 1998).

Under the VPVSAS study, empirical validation has been undertaken to assess the relative importance of parametric input. Similar to investigations into analytical and empirical validation techniques for dynamic thermal models for buildings (Lomas, 1991), statistical assessments have been made for the main input variables (see Chapter 8). Results are discussed in relation to previous work in this area.

5.7 VPVSAS new subroutines: mathematical basis

5.7.1 Objectives of VPVSAS new subroutine formulation

- To be able to fully describe and calculate the collector efficiency factor for the PV/T and Solar Air collectors.
- To provide accurate geometry and structure of the collectors, including fin dimensions within the solar air collector.
- To be able to fully describe and calculate the back and edge losses from the collectors.

- To obtain outputs from individual collectors mounted in series and parallel, along with overall calculations.

Due to the fact that the collector in question is a combined PV/Thermal and Solar Air collector, the air collector section is described slightly differently from that of the PV (see 5.7.8). This is due to the variations in top losses from the collector and heat transfer characteristics within the air stream due to finned surfaces.

The following sections provide and describe the underlying formulae coded into algorithms and used within the new subroutines developed under the VPVSAS investigation.

In the first instance these subroutines have been developed and tested within the TRNSYS simulation environment. The subroutine that describes the PV/T collector has been called Type 150 while the solar air collector takes the name Type 151.

5.7.2 Collector Overall Heat Losses

Top Loss Coefficient (U_t)

The following equation was developed by Klein (1975) as a method of calculating the convective and radiative losses from top of a collector in a form that would be useful for hand and computer calculations. In its original format, the radiative losses are calculated to ambient temperature as standard flat-plate solar water and air collectors provide an insulating glass cover. As PV/T collectors provide PV material at the outer surface, radiative losses are calculated using the sky temperature (T_s). This equation has been validated against experimental data and found to give results within ±0.3 W/m^{2}C between ambient temperature and 200°C (Duffie & Beckman, 1991).

$$U_t = \left\{ \frac{N}{\frac{C}{T_{in}}\left[\frac{(T_{in}-T_a)}{(N+f)}\right]^{0.33}} + \frac{1}{h_w} \right\}^{-1} + \frac{\sigma(T_{in}+T_s)(T_{in}^{\,2}+T_s^{\,2})}{(\varepsilon_p + 0.0005Nh_w)^{-1} + \left(\frac{2N+f-1}{\varepsilon_g}\right) - N} \quad [5.2]$$

where $f = (1.0 - 0.04 \times h_w) + (5 \times 10^{-04} \times h_w^{\ 2}) + (1.0 + 0.091 \times N)$

$C = 365.9 \times [1.0 - 0.00883 \times \beta + 0.0001298(\beta^2)]$

β = Slope of the collector

N = Number of covers

ε_p = Emittance of Plate

ε_g = Emittance of glass (0.88)

h_w = Wind heat transfer coefficient (W/m^{2}C)

σ = Stefan-Boltzmann constant

Back & Edge Loss Coefficients (U_b, U_e):

Dimensional parametric input along with specification of insulation thickness and thermal conductivity facilitates the calculation of losses from the back and edges of the collector.

$$U_b = \frac{k_i}{L_b} \qquad [5.3]$$

where k_i = Thermal conductivity of insulation (W/mC)

L_b = Thickness of insulation

To be in-line with top and back loss coefficients, the edge loss coefficient is calculated as a proportion of collector area.

$$U_e = \frac{\left(\frac{k_i}{L_e}\right) \times A_{edge}}{A_c} \qquad [5.4]$$

where A_{edge} = Area of edge (perimeter x depth of collector)

A_c = Area of collector

L_e = Thickness of the edge insulation

The overall heat loss coefficient (U_L) is then sum of top, back and edge loss coefficients:

$$U_L = U_t + U_b + U_e \qquad [5.5]$$

Florschuetz Extension to U_L:

The overall loss coefficient is recalculated under the Florschuetz extension to the HWB model to account for the variation in transmittance of the cover system due to the change in solar cell efficiency with temperature.

$$\tilde{\eta} = \eta \times Pf[1.0 - \beta r(T_a - T_r)] \qquad [5.6]$$

where η = Solar cell efficiency at reference temperature
Pf = Cell packing factor
βr = Temperature coefficient of PV cell efficiency
T_r = Reference temperature for cell reference efficiency

The cell packing factor is a ratio of the PV coverage to collector area. For thin film technologies, 100% coverage of the collector surface may be achieved, compared with octagonal monocrystalline cells, which will leave areas of the collector uncovered. The overall heat loss coefficient is renovated to consider the presence and performance of the PV material:

$$\tilde{U}_L = U_L - \tau\alpha \times S \times \tilde{\eta} \times \beta r \qquad [5.7]$$

where $\tau\alpha$ = Transmittance absorptance product

5.7.3 Collector Heat Removal Factor

The second variable required by Equation 5.1, is the heat removal factor (F_R). In order to calculate this variable, radiative and convective heat transfer coefficients must be identified along with a dimensionless mass flow rate.

In order to calculate the radiative heat transfer coefficient (h_r) an initial plate temperature of 10°C above the collector inlet temperature is used. At a later stage in the algorithm an updated plate temperature is established and a process of iteration instigated to identify a plate temperature with higher validity.

$$h_r = \frac{4\sigma \overline{T}_p^{\,3}}{(1/\varepsilon_{pv}) + (1/\varepsilon_b) - 1} \qquad [5.8]$$

where $\overline{T}_p$ = T_{in} + 10°C on first iteration
ε_{pv} = Emissivity of PV plate
ε_b = Emissivity of back plate

Calculation of the convective heat transfer coefficient (h) requires the assessment of dimensionless fluid flow within the collector. An estimated Reynolds number is required in the first instance.

As the VPVSAS study is not looking at the variation in temperature across the ducted air stream, the temperature and therefore the thermal conductivity of the air will be assumed to be constant within the duct. For this reason, the convective heat transfer coefficients for both duct walls will be considered equal.

$$\mathrm{Re} = \frac{\dot{m} D_h}{Af\mu} \qquad [5.9]$$

where $\dot{m}$ = mass flow rate (kg/s)
D_h = Hydraulic diameter
Af = Cross dimensional area of fluid flow
μ = Dynamic fluid viscosity (kg $m^{-1}s^{-1}$)

For flat plate collectors, the Hydraulic diameter is taken as twice the plate spacing (Duffie & Beckman, 1991). As with the calculation for radiative heat transfer, the dynamic fluid viscosity is calculated using an initial temperature 10°C above inlet temperature on the first iteration.

It is expected that the Reynolds number will be higher than 2100 for flat plate collectors, indicating that the flow will be turbulent. For this reason, the Nusselt number is calculated using the Kays & Crawford (1980) formula for fully developed turbulent flows with one side heated and the other side insulated:

$$Nu = 0.0158(\mathrm{Re})^{0.8} \qquad [5.10]$$

The convective heat transfer coefficient can then be calculated for a specific air temperature:

$$h = \frac{Nu \times k_a}{D_h} \qquad [5.11]$$

where k_a = Thermal conductivity of air at specific temperature (W/mC)

The radiative and convective heat transfer coefficients can then be used to calculate the collector efficiency factor (F').

Through analysing thermal networks of various types of solar air collector configuration, Duffie & Beckman (1991) have presented equations for collector efficiency factor based on energy balances on the collector cover, plate and fluid yield. The following equation describes a standard collector where ducted airflow removes heat from behind the absorbing plate and in front of an insulated rear panel. This configuration is shown in Figure 5.7.

$$F' = \left\{1 + \frac{U_L}{h_1 + \left[(1/h_2) + (1/h_r)\right]}\right\}^{-1} \qquad [5.12]$$

where h_1 & h_2 convective heat transfer coefficients are set equal

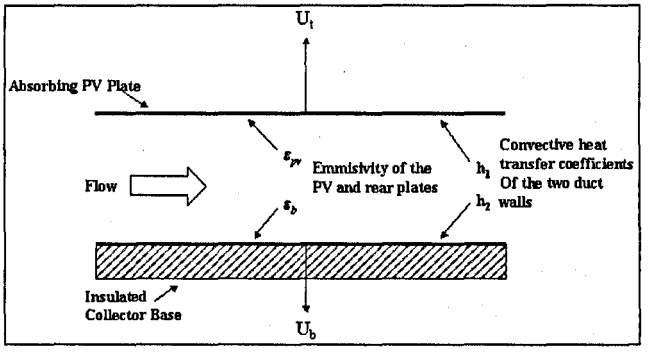

Figure 5.7 – PV/Thermal collector configuration

Once the collector efficiency factor is available, a dimensionless collector mass flow rate ($Dṁ$) can be calculated, which can then be used to identify the collector flow factor (F''):

$$Dṁ = \frac{ṁC_p}{A_c U_L F'} \qquad [5.13]$$

where C_p = Specific heat of fluid (kJ/kgC)

$$F'' = Dṁ\left[1 - e^{-1/Dṁ}\right] \qquad [5.14]$$

With this flow factor available, the main collector heat removal factor (F_R) can be calculated, as required within equation 5.1.

$$F_R = F' \times F'' \qquad [5.15]$$

Within TRNSYS Types 50 and 73, Equations 5.13 – 5.15 are presented in the following manner:

$$F_R = \frac{ṁC_p\left[1 - \exp\left(\frac{-F' \times U_L \times A_c}{ṁC_p}\right)\right]}{A_c \times U_L} \qquad [5.16]$$

Using this method F' is provided as a parameter and therefore not calculated transiently. If calculated separately (as is done under the VPVSAS process), F'' can be used later in the algorithm to obtain updated fluid and plate temperatures for reiteration and recalculation of initially assumed values.

5.7.4 Useful thermal gain from the collector

When considering the thermal potential of a PV/T collector, energy converted by PV material needs to be removed from the incident radiation. Florschuetz proposed the

following solar radiation adaptation that considers the presence and performance of PV material PV as described in Equation 6.

$$\widetilde{S} = S\left(1 - \frac{\widetilde{\eta}}{\alpha}\right) \qquad [5.17]$$

where α = Absorptance of the collector plate

The useful thermal gain from the PV/T collector can now be calculated:

$$Q_u = F_R \times A_c\left[\widetilde{S} \times \tau\alpha - U_L(T_{in} - T_a)\right] \qquad [5.18]$$

where $\tau\alpha$ = Transmittance absorptance product

5.7.5 Electrical Output of the Collector

As presented by Florschuetz and used by TRNSYS Type 50, the following equation is also used under the VPVSAS study:

$$Q_e = S \times \widetilde{\eta} \times \tau\alpha\left\{1 - \frac{\eta_r \times P_f \times \beta_r}{\widetilde{\eta}}\left[F_R \times (T_{in} - T_a) + \left(\frac{S \times \tau\alpha}{U_L}\right) \times (1.0 - F_R)\right]\right\} \qquad [5.19]$$

5.7.6 Fluid and plate temperatures

All variables are now available for the calculation of mean plate (T_{pm}) and fluid (T_{fm}) temperatures.

The following equation provides input to Equation 5.8 if reiteration is required, replacing the assumed plate temperature:

$$T_{pm} = T_{in} + \frac{(Q_u / A_c)}{(U_L \times F_R)}(1 - F_R) \qquad [5.20]$$

Similarly, the following equation provides input to Equations 5.9 & 5.11 (updating the dynamic fluid viscosity and the thermal conductivity of air respectively), if required.

$$T_{fm} = T_{in} + \frac{(Q_u / A_c)}{(U_L \times F_R)}(1 - F'') \quad [5.21]$$

5.7.7 Type 150 & Type 151 Output

Once T_{pm} has converged to within a predefined tolerance, iterations cease and the main variables calculated through the algorithm are provided as performance metrics for evaluation. As TRNSYS uses a modular structure, the output from one Type component provides the input to the next. The connection of collectors in series therefore requires the provision of outlet temperature for each collector, not just the overall array. This outlet temperature (T_o) is calculated using the following equation:

$$T_o = T_{in} + \frac{Q_u}{\dot{m} C_p} \quad [5.22]$$

Efficiencies are provided as output variables using the following simple formulas:

Heat Removal Efficiency (η_h)

$$\eta_h = \frac{Q_u}{A_c \times S} \quad [5.23]$$

Electrical Efficiency (η_e)

$$\eta_e = \frac{Q_e}{A_c \times S} \quad [5.24]$$

5.7.8 Adapted formulas for specific solar air collector

The standard Klein formula, which calculates top losses (Equation 2) is required as solar air collectors are usually provided with a glazed cover. Radiative losses are therefore calculated to ambient temperature for this type of collector.

The collector efficiency factor needs to be updated from that of the PV/Thermal section to account for the finned surfaces. This involves the input of fin dimensions and

calculation of the Fin Efficiency (F_F) and Fin Efficiency of Plate (F_P) as reported by ASHRAE (1999). The required dimensions are shown in Figure 5.8.

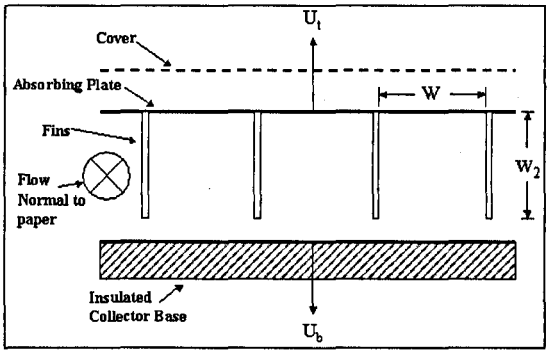

Figure 5.8 – Dimension of fins in the solar air collector

Fin Efficiency (F_F):

$$m' = \sqrt{h / k \times Y_f} \qquad [5.25]$$

where Y_f = Thickness of the fin

$$F_F = \frac{\tanh\ W_2 \times m'}{W_2 \times m'} \qquad [5.26]$$

Fin Efficiency of Plate (F_P):

$$m'' = \sqrt{h / k \times Y_p} \qquad [5.27]$$

where Y_p = Thickness of plate

$$F_P = \frac{\tanh \times m'' \times (W - Y_f / 2)}{m'' \times (W - Y_f / 2)} \qquad [5.28]$$

These fin and plate efficiencies are incorporated in an updated collector efficiency factor (F'_o):

$$F'_o = F'\left[1+\frac{1-F'}{\frac{F'}{F_P}+\frac{W\times h}{2\times W_2\times h\times F_F}}\right] \quad [5.29]$$

When calculating the radiative heat transfer coefficient for the solar air collector, the emissivity of the absorbing plate is specified rather than the PV backing material that is in contact with the air stream.

$$h_r = \frac{4\sigma\overline{T}_p^{\,3}}{(1/\varepsilon_p)+(1/\varepsilon_b)-1} \quad [5.30]$$

where ε_p = Emissivity of the plate

Lastly, standard solar radiation data is used in this calculation of Q_u (Equation 18), as no alteration is necessary for PV energy conversion.

$$Q_u = F_R \times A_C(S\times\tau\alpha - U_L(T_{in}-T_a)) \quad [5.31]$$

5.7.9 Calculation of combined PV/T and solar air collector

Before the above formulae were written into algorithms that could be installed within simulation programs, they were tested under standard conditions to see if calculated output were acceptable for this type of solar collector arrangement. Using these formulae, the calculated performance of the combined collector installed at Brockshill Environment Centre is presented in Figure 5.9.

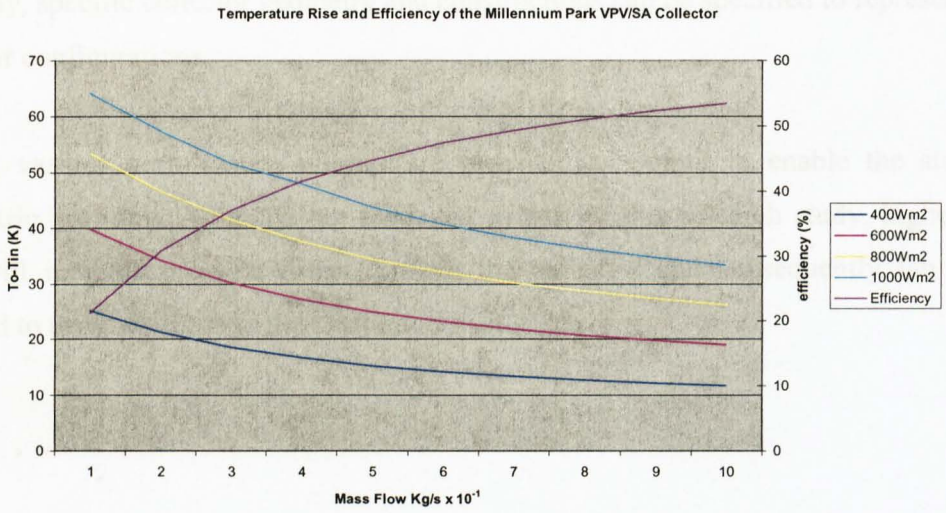

Figure 5.9 – VPVSAS Algorithm output

This shows collector outlet temperature and efficiency when the collector is subject to varying intensities of incident radiation and flow regime within the air channel. As expected, the slower mass flow rates will provide increased outlet temperatures at a lower thermal energy conversion efficiency. Conversely, higher flow rates will transfer more heat but at a lower outlet temperature. Increased levels of radiation show increased outlet temperature under all flow regimes.

5.8 Conclusions

This Chapter has described the theoretical basis of the VPVSAS method in relation to main field of PV/T research and application. Using HWB concepts the standard TRNSYS component, Type 50, utilises a similar approach to the PV/T section of the VPVSAS method. Through the use of the new Type 150 subroutine, three fundamental improvements can be identified.

Firstly, the collector efficiency factor can be calculated under prevailing conditions compared with the static parametric input under Type 50. This enables more representative convective and radiative heat transfer coefficients to be calculated.

Secondly, specific collector geometry and constructions can be specified to represent new collector configurations.

Finally, various performance metrics are provided as output to enable the study of parametric profiling. Although not modelled as part of this research study, higher flow rates will increase pressure drops through the collector and subsequently fan power required to drive air through the system.

Chapter 6

Building Energy Simulation

6.1 Introduction

Building energy simulation as a discipline is now practised widely within the construction industry in the design of energy efficient, thermally comfortable and economically viable buildings. Within the field of "Building Physics", simulation tools of varying levels of complexity have been developed which cater for research activities through to standard design processes. This Chapter introduces the current application of building energy simulation within the design process, followed by detailed descriptions of simulation development tools used within this research. The Chapter concludes with a discussion on the transferability of the VPVSAS Method for use within the design process.

6.1.1 Role of building energy simulation in the design process

The use of engineering guides, such as those published by CIBSE or ASHRAE, in combination with fairly straightforward hand calculations, is the standard method of designing building services and maintaining thermal comfort throughout the year. The guides themselves are comprehensive pieces of literature, based upon empirical data, however, simplifications have been made in the procedures to reduce errors associated

with a large number of variables. The fact that the simplified procedures in the guides are applied very generally, means that they have been formulated to be conservative to ensure that the designs that result from their use do not fail.

There are a number of factors that are forcing a change in this approach to design. Newer and more cost-effective construction techniques mean that the building form is departing more frequently from the stacked rectangular box, preferred by engineers due to its simplicity. The data that these published guides are based upon are therefore, less applicable to these new building forms and the spaces within them.

The move towards engineering simulation tools is also being driven by the ongoing revision to UK Building Regulations and the environmental credentials to which some developers aspire. This necessitates design teams to collaborate in a fashion only previously seen in very specific design projects.

The resulting innovation and need for early assessment of design strategies, has helped drive a steady development of commercial software products over the last 20 years. An additional factor that will further increase the demand for building performance simulation will be the forthcoming implementation of a new European Directive on the energy performance of buildings. This will enforce minimum energy standards and certification of most buildings at construction, major refurbishment, sale or change in lease.

A further common use of Building Energy and Environmental Modelling (BEEM) tools is in addressing life cycle costing issues. With appropriate use, initial capital outlay on building services can be minimised through optimisation of the form and fabric of the building. Running and maintenance costs are then also minimised through the building's operational life.

6.1.2 Research application of building energy simulation

Research requirements dictate a level of adaptability, which is usually not needed when building energy simulation is undertaken within the commercial sector. For this reason, it is standard practice to code small, bespoke programs, which respond exactly to the researchers needs. Alternatively, there are a small number of simulation environments that provide users with a platform for the development of new subroutines. These subroutines or modules can then make use of numerous utilities that are provided under a standard simulation environment. The main benefit that researchers take from this method of simulation is the duel approach that can look at component performance in isolation or as part of a wider system. This also facilitates validation exercises and comparison with previous research activities in field.

A number of different simulation environments and approaches were reviewed at a preliminary stage in this research to ascertain the most adaptable platform on which to develop simulation methods and associated validation activities. For reasons of interoperability and an excellent track record of research support, ESP-r (ESRU, 2000) and TRNSYS (SEL, 2000) were chosen.

6.1.3 Building energy and environmental modelling – an integrated approach

The most commonly used BEEM tools are Dynamic Thermal Modelling (DTM) packages, which are based on a 'zonal' approach to energy and mass flow calculations. Industry standard packages such as TAS and IES (formerly known as Facet) have developed significantly in popularity over the last five years. The clear advantage of these methods is that they are transient, allowing the buildings to be simulated through time in a relatively short amount of computing time, to gain understanding on annual performance. It should be noted that simplification is also inherent in this approach, in that each zone, no matter what its shape or size, is reduced to a point (termed a 'node') that represents a volumetric space. This node is then linked to other nodes that may

represent construction materials or other air volumes (zones) with which it exchanges thermal energy, mass air-flow resulting from pressure differences, and other properties. As a design tool, DTM generates comprehensive data sets, which can quickly inform the design process and suggest optimisation to the building design through any number of iterations. The behaviour of zones can also be considered under the influence of building management control algorithms built into the software.

Commercial zonal modelling software has now developed to the point where an integrated design approach can be supported within a single modelling environment. Most software packages now provide highly developed supplementary modules that can calculate annual solar regime, appropriate HVAC sizing, day-lighting and luminare performance, detailed mass flow, building energy management systems / controls, assessments on Building Regulations compliance and in some instances a limited CFD capability.

As stated earlier in this thesis, it is an intention of this research that the VPVSAS method will be made available for use by design teams interested in the viability of PV/T or SA collectors. At present, the most widely used simulation packages, such as TAS or IES, are released as executable programs that cannot be adapted in isolation from the main software developer. For this reason, development for VPVSAS has been undertaken in ESP-r and TRNSYS so that it may be made available in the future. Under TRNSYS, it is also possible to formulate bespoke programs that focus on a specific type of simulation. This means that the user does not need to train on the full simulation environment. An example of this approach is the output from the IEA Solar Heating and Cooling Programme, Task 19, (Hastings, 2000), which produced a program that simulates solar air heating systems, called TRNSAIR (Transsolar, 1998) (6.3.2).

6.2 ESP-r

ESP-r (Environmental Systems Performance; r for "research") is a transient energy simulation program, which is capable of modelling the energy and fluid flows within combined building and plant systems under specified control regimes. The program originates from PhD research carried by Professor Joe Clarke (Clarke, 1977) and has been under constant development at the University of Strathclyde since that time. ESP-r is coded in Fortran 77 and C, and has historically been operated on a UNIX platform. The program has recently been adapted to run on LINUX workstations and been made available under an 'Open Source' licence. These changes have resulted in a more widespread utilisation of the program, which had originally seen limited use outside of a small number of specialist research institutions.

ESP-r is made up of a number of interrelated program modules that perform duties of project management and geometric input, simulation, results analysis, database management, report writing and data export. Further to these main utilities, ESP-r provides specialist modules such as 2D computational fluid dynamics (CFD), daylight analysis using Radiance and 'Special Materials', which can calculate Photovoltaic systems performance (see 7.2.2) along with other metrics.

The standard convention of DTM is to specify volumes (or "Zones") which are defined in terms of geometry, construction material composites and operational profiles. Within ESP-r, this is done using the Project Manager module (shown in Figure 7.1). Material properties are held on a database from which specific wall, floor, roof and window configurations can be built and applied to each Zone. This process is repeated to build multi-zone representations of the building in question. Once the required number of Zones are described, mass air-flow connections can be specified both for internal air flow and points external to the building. This completes the information required to undertake simulation using appropriate climate data for the location, however, building control profiles are usually described so as to calculate the transient thermal load of the building

and assess thermal comfort criteria. One of the main benefits of ESP-r over other DTM programs is the ability to adapt and read input files that have been generated by the Project Manager and other input modules. This is essential for research purposes as non-standard operations can be undertaken and errors corrected.

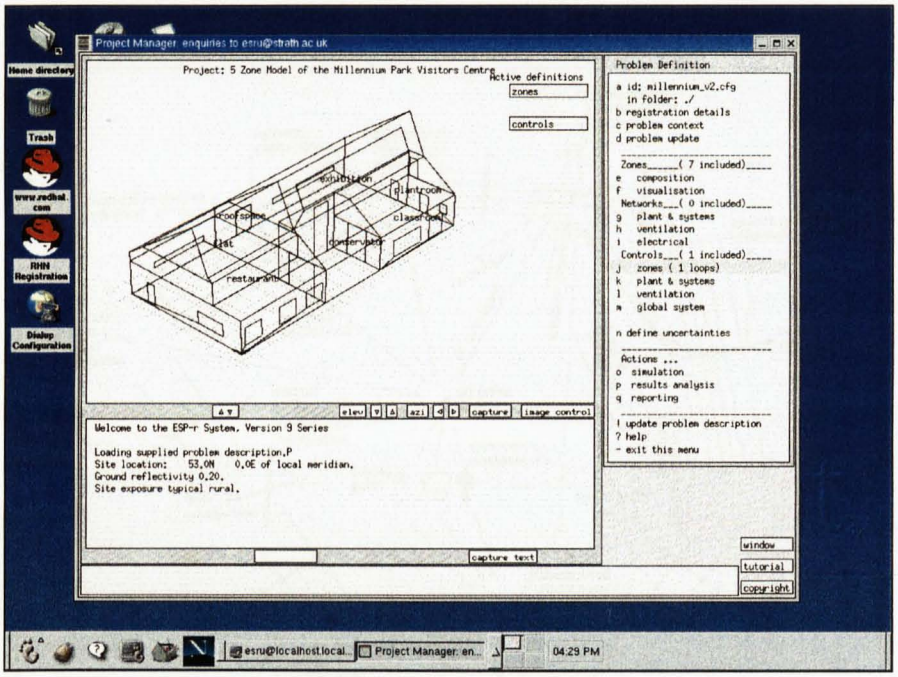

Figure 6.1 – ESP-r Graphical User Interface showing Project Manager Module

6.2.1 Calculation of heat and mass flow dynamics

The main ESP-r simulation routines are based on large matrices that calculate all thermodynamic processes occurring within the building at each time step (often over 8760 hours to represent 1 year) when exposed to varying climatic conditions, read from a climate file. Figure 6.2 shows the large number of contributing variables that need to be calculated for each zonal volume (represented by a 'node'). When this number of calculations is undertaken for large multi-zone building models and for a simulation run for a full year of operation, the computational time required can be extensive. For this reason modelling activities often consider representative spaces or focus on areas of the

building that are of particular interest in a design context. From this basis, a technique of 'discretisation' is used which termed a 'control volume flux-balance' approach (Kelly, 1998), which uses control volumes (or zones) and a series of controlled networks that represent energy subsystems. By doing so, the energy balances associated with plant components can be applied to the overall building model matrices.

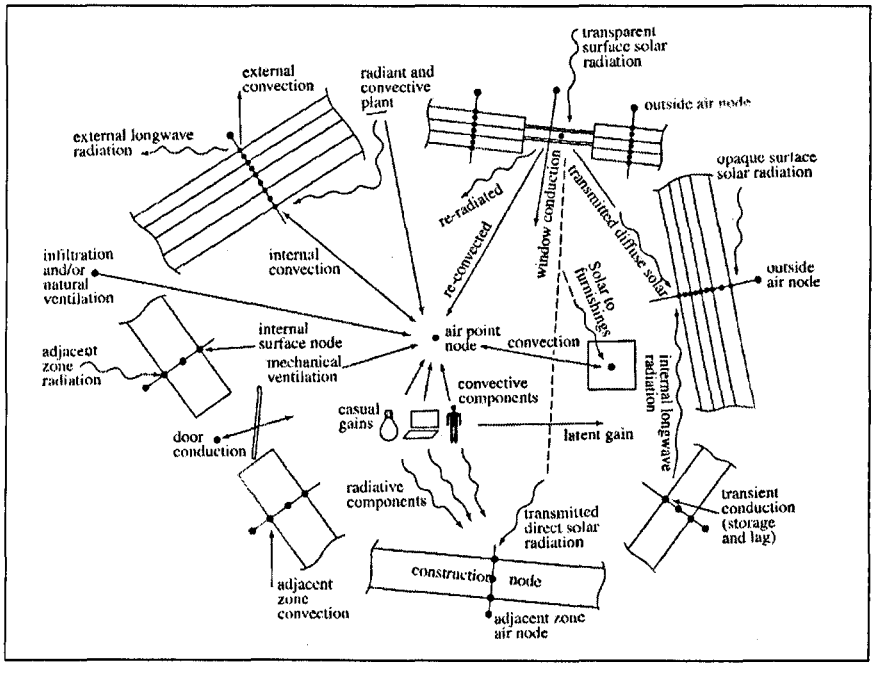

Figure 6.2 – Building energy flow paths (reproduced from: Clarke, 2001)

6.2.2 Plant simulation

The thermal controls for an ESP-r model can be set to give an overall amount of energy to a space to attain a set point temperature or a plant network can be specified to service the heating and cooling of a space. Through using the plant simulation approach, more detailed information can be calculated on system performance and the whole system may be considered to be more representational as the building environmental control system will operate the plant on space temperature actuation.

The development of VPVSAS Method required the installation of PV/Thermal and Solar Air collector components within ESP-r. For this software package, this procedure can be considered as non-standard for developers outside ESRU, University of Strathclyde. The process of installation involves the placement of a new subroutine within a shell that can be read by the main ESP-r program. As calculations proceed through the main matrices, redirection to the new subroutine is made at the required stage with outputs placed into the appropriate form and supplied back to the main matrix for calculations to proceed.

Limited information on the installation process in published (Aasem, 1993) in a PhD Thesis, however, ESRU should be contacted for guidance.

6.3 TRNSYS

TRNSYS has been under continuous development by the Solar Energy Laboratory (University of Wisconsin, Madison) since 1975 and has been commercially available since that date. From an early stage in development, TRNSYS was designed to simulate the transient performance of thermal energy systems. A modular approach is used to solve large systems of equations described by Fortran subroutines. Each Fortran subroutine contains a model for a system component. By creating an input file, the user directs TRNSYS to connect the various subroutines to form a system. The TRNSYS engine calls the system components based on the input file and iterates at each time step until the system of equations is solved. The alternative to this method is for the researcher to write a single, monolithic program that models only the system at hand. Subsequent changes to the system configuration are more difficult with monolithic programs than they are with modular programs such as TRNSYS.

Unlike many other programs, TRNSYS allows users to completely describe and monitor all interactions between system components. For example, the user determines the connections between the output of the pump and other system components. The modularity of the program allows the user to have as many pumps, chillers, cooling coils and solar panels as necessary, in any desired configuration. Because the components are

written in Fortran, a user can easily generate a TRNSYS component to model any new technology that is created. Historically, TRNSYS has been used for simulating solar thermal systems, modern renewable energy systems including PV and wind power, more general HVAC systems, and buildings.

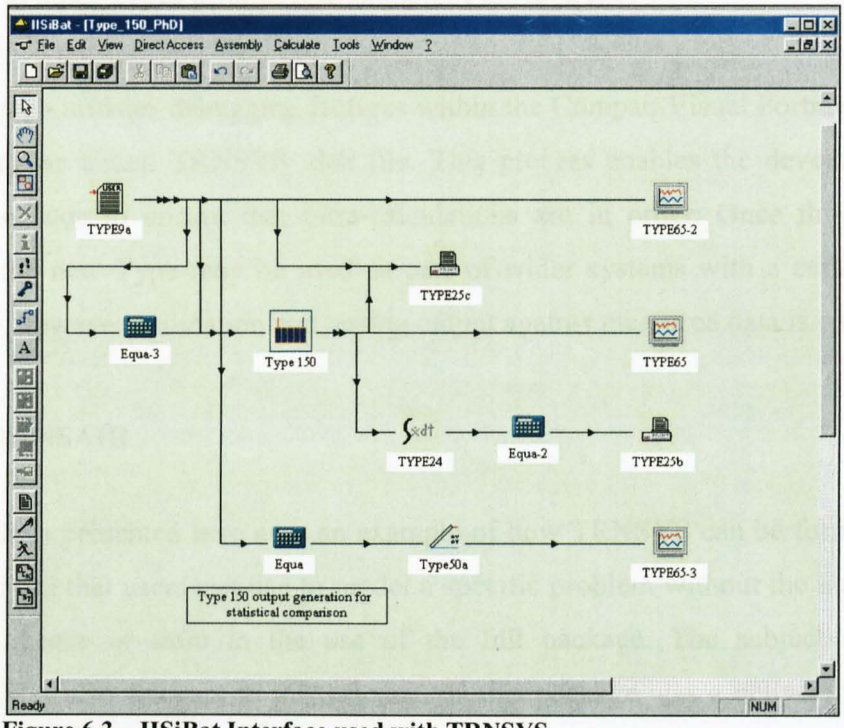

Figure 6.3 – IISiBat Interface used with TRNSYS

6.3.1 'Type' formulation and testing

New TRNSYS 'Types' or subroutines are implemented using a multi-stage approach. Firstly the algorithm is written in Fortran, ideally using the Compaq Visual Fortran Developer Studio. Within this algorithm, a standard TRNSYS format is used, that firstly describes interactions with the main TRNSYS simulation facilities and identifies the number of input, parameters and outputs.

The second stage is a re-compilation of the main TRNSYS Dynamic Link Library (trnlib.dll). This is facilitated within the Compaq Visual Fortran Developer Studio along with conversion of new Type Fortran files into an intermediate format required by

TRNSYS (TypeX.obj). The new trnlib.dll and intermediate files need to replace any existing files within the C:/trnsys15 file structure.

Stage 3 involves describing the new Type within IISiBat, so that it may be implemented and linked to other Types prior to formulation of the .dck file.

The final stage initiates debugging features within the Compaq Visual Fortran Developer Studio using an actual TRNSYS .dck file. This process enables the developer to step through the code to ensure that intra-calculations are in order. Once this process is complete, the new Type may be used as part of wider systems with a certain level of confidence, however, validation and testing output against measured data is encouraged.

6.3.2 TRANSAIR

TRANSAIR is presented here as it an example of how TRNSYS can be formulated into small packages that users can use to model a specific problem without the need to buy a TRNSYS licence or train in the use of the full package. The subject covered by TRANSAIR is also relevant to this research as this package was a deliverable supplied through the IEA Task 19 Study into Solar Air Systems (Hastings, 2000). Six different solar air system configurations can be assessed (as shown in Figure 6.4) with the user specifying a simple building load scenario.

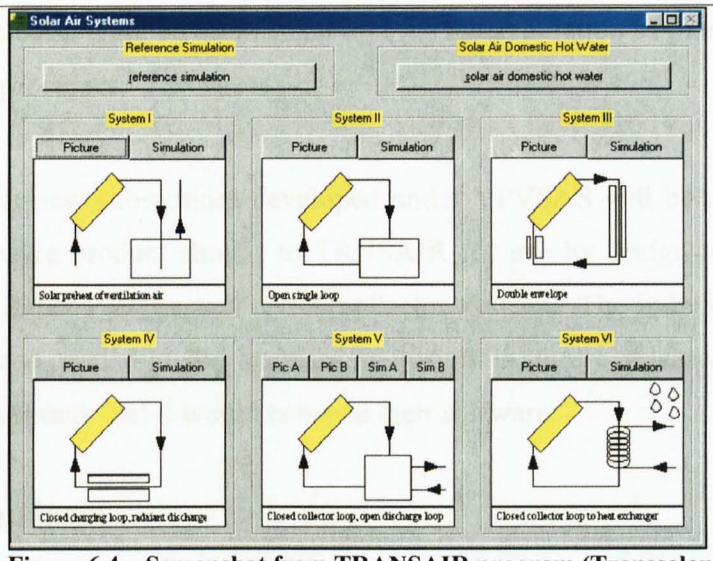

Figure 6.4 – Screenshot from TRANSAIR program (Transsolar, 1998)

When considering the appropriate development of the VPVSAS Method, TRANSAIR was not suitable of incorporation or development as this software package is commercially licensed and released as an executable program so there was no access to the code.

6.4 Interoperability

The standard development of software and especially simulation environments does not lend naturally itself towards interoperability. The user is therefore commonly in a situation where a decision is required at the start of a problem solving exercise to chose an appropriate tool that will be used during the course of the investigation. The relative needs of research against standard, quick reference uses preferred by commercial organisations help drive duel approaches to what are commonly similar problems.

In the VPVSAS method, interoperability has been addressed through the use of similar subroutines within different simulation platforms. It could be said that both of these packages have strong bases within the research community, however, ESP-r being under Open Source License is expected to gain in popularity in the next few years while

TRNSYS can be considered an established tool for the simulation of plant networks with associated solar processes.

It is intended that new subroutines developed under VPVSAS will be developed into a stand-alone software product similar to TRNSAIR for use by design teams during the development of either PV/Thermal or SA collector systems. The individual subroutines will also be made available for standard inclusion in future releases of ESP-r and TRNSYS if the vendors feel it would enhance their software.

6.5 Conclusions

Building energy modelling tools and the field of building physics in general is constantly evolving. Whether used within a design context or for research purposes, the selection of the right tool or methodology is vital if valid and helpful conclusions are to be drawn.

With regard to the development of the VPVSAS Method, TRNSYS and ESP-r were chosen as they both provide adaptable environments under which models can be developed and results analysed.

Chapter 7

Simulation of Combined PV/Thermal Systems

7.1 Introduction

Considerable research has been conducted on theoretical and numerical modelling of PV/T collector performance (see Chapter 5), however, activities involving full simulation of building integrated PV/T systems are limited in comparison. At component level, simulation studies have focused on performance analysis (Garg & Adhikari, 1997), studies into the fluid flow behind PV arrays, using both CFD and other methods of numerical analysis (Moshfegh & Sandberg, 1998) and the use of water as the heat transfer media (Kalogirou, 2001). When considering contribution from PV/T collectors to the heating load of an associated building, two investigations stand out as providing innovative simulation methodologies that aid in the assessment of potential applications. These studies were PV-HYBRID-PAS and investigations related to the Mataró library in Barcelona.

Once these studies have been outlined, the Ventilated Photovoltaic and Solar Air Simulations (VPV-SAS) method will be described in relation to this earlier work. This VPV-SAS method is central to the research aims stated at the beginning of this thesis and has been developed in association with the applied PV/T system installed at the Brockshill Environment Centre. As the collectors installed at the Brockshill Environment

Centre are bespoke and fabricated especially for this installation, standard performance data was not available. The VPV-SAS method therefore starts from a theoretical basis and compares calculated with measured performance.

7.2 PV-HYBRID-PAS

Funded in part by the European Commission's Non Nuclear Energy Programme - JOULE III, and carried out by a consortium of organisations co-ordinated by the European Economic Interest Grouping PASLINK and JRC Institute for Advanced Materials, the key objective of this project was to develop a standard scheme for the performance evaluation of hybrid PV building components. The main emphasis was placed on the development of procedures for assessing the thermal and electrical performance of components, with attention also given to maintenance and durability, air and water tightness, ventilation and daylighting aspects.

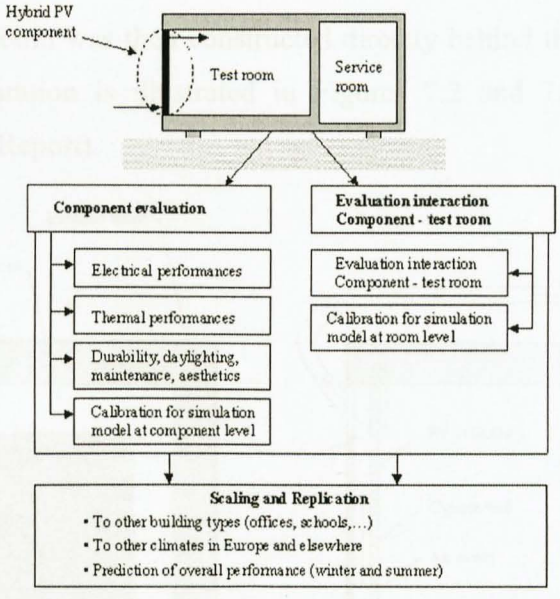

Figure 7.1 – PV-HYBRID-PAS evaluation scheme (re-drawn from PV-HYBRID-PAS Final Report)

The study was carried out over a two-year period from 1997 with two main phases to the investigation. Firstly, reference hybrid PV components were developed and tested at several PASLINK (the European grouping of out door test centres) test centres, using

standardised test procedures. These test results then served as calibration for simulation procedures developed using ESP-r (ESRU, 2000). A concept of 'scaling and replication' was then used to extrapolate the results obtained at a component level, from the PASLINK test sites, to real buildings and to different climatic conditions (Vandaele *et al*, 1998). This process is illustrated in Figure 7.1.

7.2.1 Component and Test Room Evaluation

Experimental work focused on the construction and evaluation of a reference wall and small test room. This reference wall included two poly-crystalline PV modules mounted centrally within an insulated frame, providing a 22.9% PV aperture within the wall. A 50mm air cavity was provided behind these modules and in front of a removable opaque wall. This wall could then be inter-changed with glazed or vented elements depending on test configuration. The air gap behind the PV modules could be mechanically ventilated with inlet through louvers at the base of the wall and ducted extract at the top of the cavity. A small test room was then constructed directly behind this reference wall. This experimental configuration is illustrated in Figures 7.2 and 7.3 (redrawn from PV-HYBRID-PAS Final Report).

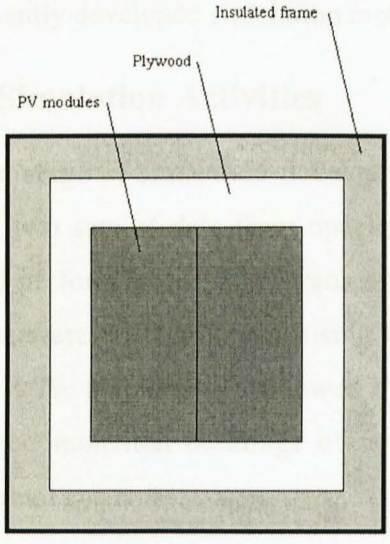

Figure 7.2 – Front view from Outside the test cell

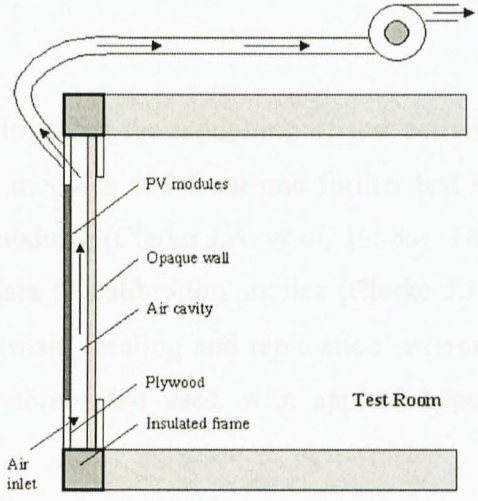

Figure 7.3 – Cross-section of reference component mounted in the test cell

Instrumentation included temperature sensors on PV modules, air inlet, air outlet and at various points within the test room. A detailed on-site weather station monitored the following variables for use during calibration:

- Incident solar radiation - total horizontal (W/m^2)
- Incident solar radiation - diffuse horizontal (W/m^2)
- Incident solar radiation - total vertical (W/m^2)
- Ambient temperature - dry bulb (^oC)
- Relative humidity - external (*%*)
- Wind speed - external (*m/s*)
- Wind direction, external (*angle*)

Additional data was collected for assessment of radiation on the vertical plane:

- Incident solar radiation - diffuse vertical (W/m^2)
- Reflecting solar radiation from the PV on the vertical (W/m^2)
- IR (thermal) radiation on the vertical (W/m^2)

Data was then collected for various reference wall configurations, ventilation flow rates and at the various PASLINK locations for performance evaluation and calibration of subsequently developed simulation methodologies (Vandaele *et al*, 1997).

7.2.2 Simulation Activities

The first stage of simulation development involved the modelling of test activities that covered two sets of data from opaque PV modules and from one further test site that assessed performance of semi-transparent modules (Clarke J.A. *et al*, 1998a). These test activities were then calibrated using test data (3 calibration studies [Clarke J.A. *et al*, 1998b, 1998c and 1998d]) followed by the main 'scaling and replication' exercises that considered modelled buildings of various forms and uses, with applied hypothetical PV/Thermal systems.

7.2.2.1 ESP-r Simulation Methodology for PV-HYBRID-PAS

A representative cross section of building types and applied systems was formulated to assess a varied range of application issues. These application issues are outlined in Table 7.1.

Building / System / Operational Variables	Application Issue
PV Module Type	Hybrid building integrated PV Non-hybrid building integrated PV Roof-mounted Facade-mounted
PV cell type	Amorphous silicon Mono- or poly-crystalline silicon
Utilisation strategies for heat	Pre-heat of ventilation air Space heating / storage Ventilation cooling Heat sinks (swimming pool / process heat / domestic hot water)
Utilisation strategies for electricity	Autonomous use for lighting Grid connection Local storage DC or AC use (requirement for inverter)
Building type	High heat loss / low direct solar gain Low heat loss / low direct solar gain Low heat loss / high direct solar gain
Occupancy factors	Daytime use only (e.g. school, office) 24 hour use (e.g. hospital)
Climate	Effect on utilisation
Ventilation strategy	Natural ventilation Forced ventilation
Comparison with other technologies	Solar water heating Ventilation heat recovery Transparent insulation Daylighting facade features

Table 7.1 Application Issues specified for PV-HYBRID-PAS Simulation Studies (Wouters and Vandaele, 1998)

For suitable description of PV/Thermal systems within ESP-r that did not require the call on a specific PV/T component from the plant component database, a 'special materials' facility was added to the program. Using this facility, standard constructional elements could be assigned attributes that correspond to PV cells or advanced glazings. Detailed

irradiance calculations could then be undertaken for the particular surface and an intra-constructional solar algorithm invoked to calculate the layer energy absorption as a function of the prevailing solar incidence angle and the radiation flux retransmission back to the external environment.

A specific PV algorithm could then be used to calculate the electrical energy generated using the following input variables:

- Open circuit voltage (V)
- Short circuit current (I)
- Reference insolation (W)
- Reference temperature (K)
- Number of series connected cells (-)
- Number of parallel connected branches (-)
- Number of panels in surface (-)

This PV modelling facility has been developed into a standard procedure within the ESP-r program (Clarke J.A. *et al*, 1998e).

The surplus solar energy is then passed back to the construction node energy balance equation, which results in nodal temperature rise for the particular material. From this point the power and heat data is passed on to separate networks within the simulation (as described in Chapter 6). The usual format for model formulation within the PV-HYBRID-PAS simulation exercises, provided PV/T collectors as very thin thermal zones with 'special materials' provided on the collector surface, with frame and collector back surfaces specified as conventional multi-layer constructions. An air-flow-network could then be specified, that feeds ambient or re-circulated air to the collector. A further plant network is then required to take the final collector (thin thermal zone) node temperature as the inlet temperature for the required heating system. In this way, useful gain from the collector(s) can then be used for purposes within the building as required by the control strategy.

7.2.3 PV-HYBRID-PAS Conclusions

In relation to work described within this thesis, three main conclusions can be taken from the modelling section of PV-HYBRID-PAS:

1. From the various scenarios investigated, no obvious application paradigm for hybrid PV systems was identified.

2. Hybrid PV systems could deliver significant heating energy savings, but are most effective for applications where pre-heating of ventilation air is important and in sunny, cold climates.

3. That the employed methodology would have benefited if additional information on solar absorption, reflection and transmission had been provided by the PV manufacturers.

As to the overall conclusions from PV-HYBRID-PAS, attention was drawn to possible errors in identification of thermal efficiencies at component level, as significant variation was noticed as a function of boundary conditions. Recommendations then followed that either performance assessment should be carried out under very well described conditions or that the majority of the component efficiencies be determined through calculation. Clearly, the costs associated with the performance assessment procedures undertaken by PV-HYBRID-PAS were significant, and that for future investigations the alternative of performance determination through calculation would result in substantial cost reductions.

A distinction was made between thermal efficiencies of hybrid PV systems at component / façade level and building level. As has been demonstrated (Chapter 5), thermal efficiencies of >50% can be achieved at component level through optimal levels of insulation, appropriate choice of air gap and air velocity. However, at building level, results indicated that a large part of the collected heat is not usable under many building types due to periodic supply and demand differences and risks associated with overheating.

It was concluded that three main niche markets could be identified:

1. Buildings with a rather long heating season combined with limited solar gains.
2. A large need for direct heat gains; for example swimming pools.
3. Poorly insulated buildings with limited glazed surface.

'As only niche applications can be identified...it is evident that this substantially reduces the potential market for hybrid PV systems in buildings' (Wouters and Vandaele, 1998).

7.3 Mataró Library Related Research

Collaborative research into thermal modelling of building integrated, ventilated PV facades was carried by CREST (Loughborough University) and the Department of Building Physics at the Hochschule für Technik, Stuttgart. This investigation was carried out as part of ongoing research into the performance of the installed ventilated PV façade at the Mataró library, near Barcelona (see Chapter 5).

With an overall aim to assess the potential of ventilated PV facades and solar air collectors integrated into buildings, the investigation developed a modelling methodology capable of direct comparison with monitored data from the Mataró library. This data was then used to validate the developed thermal model so that performance of such a system could be assessed for different European locations.

The method used to simulate the installed system at Mataró, consisted of three main components: the ventilated PV façade; the flat plate solar air collectors; and a single zone building model (Mei *et al*, 2001 & 2003), which reflects the applied configuration. Published work to date has described the simulation of ventilation pre-heat within the façade to off-set winter heating loads (Infield *et al*, 1999). During summer months the heated air is vented to the atmosphere, however, the cooling potential of this heated air is currently being investigated. The high performance solar air collectors are located at the top of the façade to boost temperature and therefore increase buoyancy driven flows.

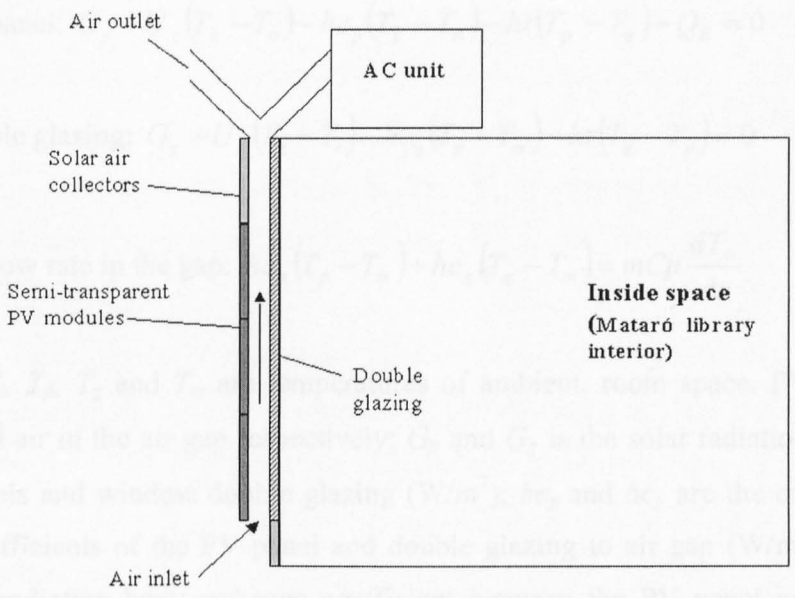

Figure 7.4 – Simplified schematic of the Mataró PV façade
As applied under modelling exercises (re-drawn from Mei *et al*, 2001)

This passive flow may be used in warmer periods to induce ventilation to the building; alternatively, forced convection can be used to improve heat transfer within the collectors and to reduce the PV cell operating temperature. The configuration of the Mataró façade and thermal model is shown in Figure 7.4.

The thermal model required for this specific façade system differs from standard PV/Thermal collectors in that the rear of the collector is glazed and that the PV cells are arranged for semi-transparency. This façade arrangement was originally modelled, by this collaboration, using Hottel-Whillier-Bliss (HWB) concepts. A simplified PV façade thermal representation method was also developed as a tool for architects and engineers that reduced the complexity of the required HWB calculations (Infield *et al*, 1999). From this mathematical basis, a transient one-dimensional thermal sub-model was developed that could be used to simulate the thermal performance of the façade with or without forced convection. This subroutine was implemented in the programming language Delphi and compiled as a DLL for use within TRNSYS (SEL, 2000). The steady state energy balances for the PV façade are stated as:

- for PV panel: $G_p - U_p(T_p - T_a) - hc_p(T_p - T_m) - hr(T_p - T_g) - Q_E = 0$ [7.1]

- for double glazing: $G_g - U_g(T_g - T_i) - hc_g(T_g - T_m) - hr(T_g - T_p) = 0$ [7.2]

- for air flow rate in the gap: $hc_p(T_p - T_m) + hc_g(T_g - T_m) = mCp\frac{dT_m}{dx}$ [7.3]

where: T_a, T_i, T_p, T_g and T_m are temperatures of ambient, room space, PV panel, glass window and air in the air gap respectively; G_p and G_g is the solar radiation observed by the PV panels and window double glazing (W/m^2); hc_p and hc_g are the convective heat transfer coefficients of the PV panel and double glazing to air gap (W/m^{2}K); hr is the long wave radiation heat exchange coefficient between the PV panel and the double glazed window (W/m^{2}K); U_p and U_g are the thermal transmittance between the PV panel to ambient and the double glazing to room space (W/m^{2}K); Q_E is the electrical power generated by the PV panels (W/m^2); m is mass flow rate (kg/s); Cp is the specific heat capacity of the fluid (kj/kg K), and temperature gradient of the air gap is referred to the gap height, x (Mei *et al*, 2001).

The solar air collectors were modelled in a more conventional manner, as described by Duffie and Beckman (Duffie & Beckman, 1991), and as used within TRNSYS Type 1 flat plate solar collector and Type 50 PV/T collector (see Chapter 5). These collector subroutines used the following formulas for efficiency (η) and outlet temperature ($T_{o,c}$):

$$\eta = \frac{Q_u}{G_T A_c} = F_R(\tau\alpha) - \frac{F_R U_L(T_{i,c} - T_a)}{G_T} \quad [7.4]$$

$$T_{o,c} = \frac{Q_u}{mCp} + T_{i,c} \quad [7.5]$$

(standard nomenclature as stated earlier in this thesis)

As with TRNSYS Types 1 and 50, this method makes use of collector test results when presented as a linear plot of η versus $(T_{i,c} - T_a)/G_T$ with an intercept $= F_R(\tau\alpha)$ and slope $= F_R U_L$. For modelling of the Mataró system, the heat gain for the solar air collector was assumed to be directly transferred to the building during the winter heating season, while during the summer is was vented directly to the atmosphere (Mei *et al*, 2001).

During the development of numerical models to assess the potential contribution to heating and cooling strategies (see Chapter 5), the building was modelled using PREBID and applied to the TRNSYS multi-zone building load generator, Type 56. This method of building thermal modelling was later superseded by a model based on the ASHRAE transfer function method (ASHRAE, 1993), which was coded for installation within TRNSYS. The complete system of ventilated PV façade, solar air collectors and building could then be modelled within TRNSYS and results validated against monitored data from the Mataró library. This monitored data was taken during unoccupied periods with HVAC plant switched off to avoid unaccountable thermal gains and also included on-site weather data for standardisation between measured data and simulated results.

Once an acceptable comparison was obtained, the model was used to assess heating and cooling loads for the building with applied occupancy and appropriate control profiles (daily and seasonal). As a complete weather set was not available from the Mataró site, METEONORM software (Meteotest, 1999) was used to generate annual weather files for Barcelona, along with Stuttgart and Loughborough, UK, so that the performance of the Mataró library and it's applied systems could be assessed under varying European climates.

For direct comparison between locations, the Barcelona model was used for the other locations even though in reality, slight variations in design would occur to account for the different climatic conditions. The model was also adapted to provide a conventional masonry and glazed (15%) façade for comparison with the multi-functional PV façade under investigation.

Findings from annual simulations of the three locations using the two façade types, indicated that only the Barcelona location would benefit from a reduction in annual heating and cooling load (9.3 MWh) due to the losses associated with the glazed facades in the colder climates. When considering the ventilation pre-heat in isolation from the annual heating and cooling loads, up to 12% of heating energy could be saved at the Barcelona location, with 2% saved under the Stuttgart and Loughborough conditions (Mei *et al*, 2001).

7.4 VPVSAS Method

The Ventilated Photovoltaic and Solar Air Simulation (VPVSAS) method is central to the research described in this thesis. Building on elements of the PV-HYBRID-PAS and Mataro investigations, this method was designed with a number of key objectives:

- To facilitate detailed parametric specification and description of PV/T and SA collector subroutines for use by transient building energy and plant simulation programs.
- To enable performance assessment of these collectors and their contribution to specific building loads, under various system configurations, control strategies and building operational profiles.
- To provide direct comparison with monitored data from the installed system at the Brockshill Environment Centre for validation purposes.
- To form the basis of a method that may be used by design professionals under varying levels of complexity, system configuration and location.

7.4.1 VPVSAS Method in Relation to Previous Work

In relation to work carried out under the PV-HYBRID-PAS program, the VPV-SAS method differs in that PV/T and SA collectors are modelled as plant components instead of thin geometrically modelled zones. In the development of the VPV-SAS method there was no intention to supersede this important study, however, the process of module

testing, model calibration and the 'scaling and replication', under PV-HYBRID-PAS, necessitated an alternative method of modelling the specific collectors applied at the Brockshill Environment Centre.

Due to the available resources of the PV-HYBRID-PAS investigation, the performance of specific modules could be analysed to provide parametric input to the modelling exercises. In particular, the 'special materials' facility within ESP-r requires a convective heat transfer coefficient to be specified for calculation of energy flows between nodal representations of the PV material and working fluid. For this method to be used for modelling the collectors at Brockshill Environment Centre, an assumption would therefore have to made concerning this very important coefficient.

A further limiting factor concerned the applicability of PASLINK testing methodology in relation to the Brockshill collectors, as testing involved specific air flow rates considered appropriate for the hypothetical simulation exercises to follow. As described earlier in this thesis (4.3), the air flow through the Brockshill collectors varies depending on the mode of operation and ventilation requirements within the building, resulting in changes to the convective heat transfer coefficient. Simulation development leading to the VPV-SAS method, therefore required the transient calculation of such coefficients.

There are clear parallels between the Mataró related investigations and the objectives of stated under the development of the VPV-SAS method, and modelling activities aligned to the installed Brockshill VPV system. The main challenge in modelling the Mataró system concerned the accurate calculation of thermodynamic processes within the façade element. This being complicated by the direct and indirect thermal interactions between the façade and the space behind, along with contribution to solar gains within the building, due to the semi-transparent nature of the façade element. At Brockshill, the collectors have no direct thermal interaction with the building as they are supported on fixings above a heavily insulated roof. This simplifies the configuration of the modelling procedure in that the PV/T collectors can be modelled as separate subroutines as done with the SA collectors in Mataró related work. However, the incorporation of ventilation heat recovery at Brockshill, means that the modelling of the building and plant network

needs to be carried out concurrently. This is of particular importance during ventilation pre-heat mode, when heated air from the collectors is passed through a cross-plate heat exchanger before being boosted to supply temperature. The space heating load can then be accurately calculated, as collector outlet temperature and ventilation extract temperature are also calculated for each time step. A clear difference between the two investigations is the emphasis, carried by the VPV-SAS method, on interaction between the collectors (under various modes of operation) and the dynamic nature of the associated building. This is achieved through transient simulation of both plant and a multi-zone thermal model of the building with applied operational and occupancy profiles.

Conclusions from PV-HYBRID-PAS identified the need for good manufacturer's data regarding thermodynamic processes and external influences. As this data is often of limited availability, it was concluded that calibration studies for VPV-SAS needed to include parametric evaluations in order to assess potential sources of error during PV/T component model set up.

After considering previous investigations in relation to the modelling requirements of the Brockshill system along with a prerequisite of this research to undertake sensitivity analysis on parametric settings, the new VPV-SAS methodology needed to incorporate:

- Interaction between building and plant energy modelling.
- Transient calculation of the collector efficiency factor (F'), incorporating the convective heat transfer coefficient between plate (PV) and collecting fluid.
- Detailed geometric input for each type of collector.
- Facilities to enable parametric studies.
- Output data sets directly comparable with monitored findings.

7.4.2 VPV-SAS Method Development

7.4.2.1 Component Development

In line with formulas described earlier in this thesis (see Chapter 5) that calculate thermodynamic and electrical performance, algorithms were developed into subroutines that represent separate PV/T and SA collectors. These subroutines were written using Fortran so could be made available to both TRNSYS and ESP-r. Due to the good component development facilities provided by TRNSYS, along with the presence of the rudimentary PV/T collector subroutine, Type 50 (standard TRNSYS library), components were developed, debugged and tested using this software package. As required by TRNSYS protocol, the new PV/T component was designated as Type 150, while the new SA component became Type 151.

TRNSYS, being of modular format, requires that subroutines present information that allows for interaction with the main simulation processes, along with input, parameter and output variable designation (see Appendix A for variables used by Types 150 and 151). Appropriate units need to be coded into the subroutine for all input and output variables, so that assured interaction can be maintained when Type subroutines are linked together to create the system under investigation. In order to update TRNSYS to incorporate new routines, the whole program needs to be recompiled into a new executable DLL file. The final process involved description of new subroutines within IISiBat so that the TRNSYS .dck file could be generated automatically using this graphical front-end interface.

Type 150 was initially developed using the code structure of Type 50. This algorithm was developed to incorporate required formulae given in Chapter 5, and adapted to represent the SA collector subroutine Type 151.

7.4.2.2 Stage 1 Modelling – Linking TRNSYS / ESP-r Output for New Components

Once output from the new subroutines was considered to be within an acceptable range of expected performance (Shankland *et al*, 2000), a methodology was developed to estimate the contribution that the Brockshill collectors could make to space and water heating

through the year. Monitored data was not yet available during this stage of development. This involved the detailed modelling the Brockshill Environment Centre within ESP-r (incorporating appropriate geometry, materials, heating and ventilation regime, and occupancy profiles), to simulate the annual space heating and ventilation load of the building. An output file was then generated containing hourly load data for a full years operation. Figure 7.5 shows the wire-frame representation of the Brockshill Environment Centre, as generated by ESP-r.

A new TRNSYS Type was developed to read this ESP-r output file and assess what contribution the combined collectors could make to heating load at each time step. When heated air is available from the collectors during periods of no space heating and ventilation load, this energy can be made available for water heating via the air-to-water heat exchanger. In this instance, the performance (effectiveness) of the air-to-water heat exchanger is expressed as a parameter. Simulations carried out under TRNSYS and ESP-r used the same weather file (CIBSE reference year, Kew 1967). This methodology is described in Figure 7.6.

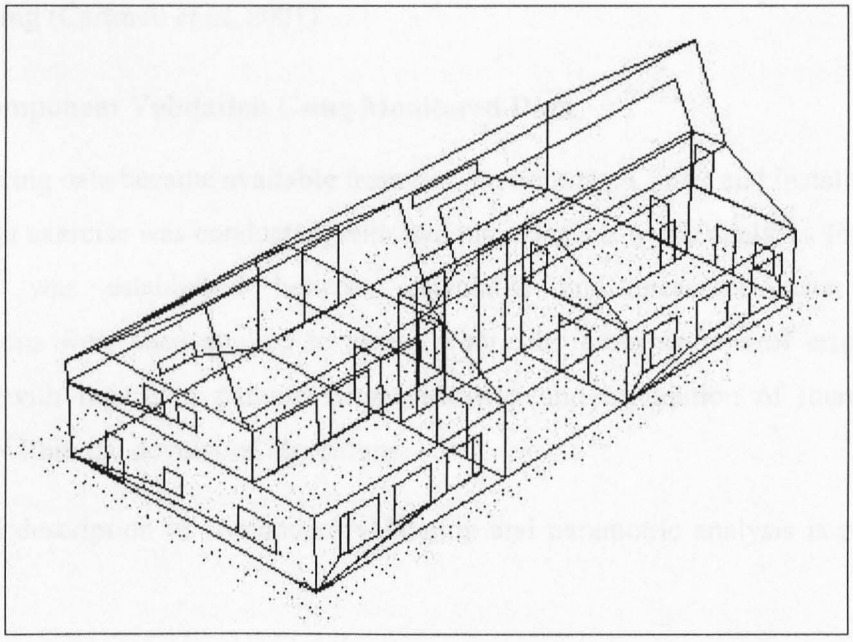

Figure 7.5 – Wire-frame image of the Brockshill Environment Centre modelled within ESP-r

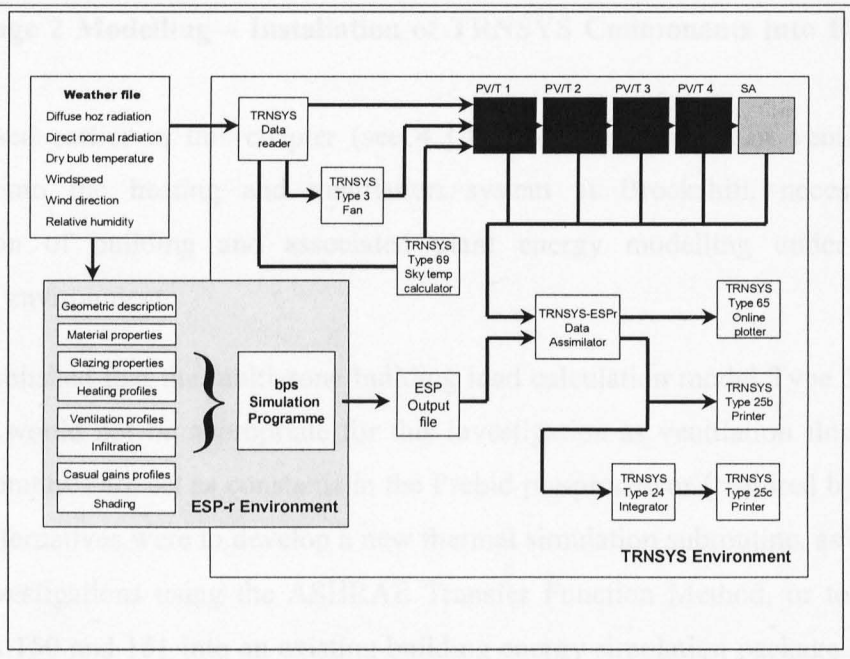

Figure 7.6 – Information flow diagram through the combined simulation process

Output from this investigation indicated that 1715kWh would be contributed towards space heating from the VPV/SA collectors, while 9618kWh would be made available to water heating (Cartmell *et al*, 2001).

7.4.2.3 Component Validation Using Monitored Data

As monitoring data became available from the Environment Centre and installed systems, a validation exercise was conducted, with two main aspects to the analysis. Firstly, broad agreement was established between calculated and measured data. Statistical investigations were then applied to assess where the main sources of error could be expected, with regard to parametric specification and calculation of thermodynamic processes within the developed algorithms.

A detailed description of component validation and parametric analysis is presented in Chapter 8.

7.4.2.4 Stage 2 Modelling – Installation of TRNSYS Components into ESP-r Plant Database

As discussed earlier in this chapter (see 4.3.1), the incorporation of ventilation heat recovery into the heating and ventilation system at Brockshill, necessitated the combination of building and associated plant energy modelling under the same simulation environment.

It was established that the multi-zone building load calculation model Type 56, used by TRNSYS, would not be appropriate for this investigation as ventilation flow rates and inlet temperatures are set as constants in the Prebid pre-processor (required by Type 56). The two alternatives were to develop a new thermal simulation subroutine, as done under Mataró investigations using the ASHRAE Transfer Function Method, or to install the new Types 150 and 151 into an existing building energy simulation package. ESP-r was therefore seen as the ideal package to use, as its plant modelling capabilities were well documented and output from the plant network could be split to supply different zones within a model (as applied at Brockshill).

This line of application is problematic in that TRNSYS and ESP-r use fundamentally different methods of calculation. As described earlier (Chapter 6), ESP-r uses extensive matrices to calculate plant related energy and mass flow balance equations, which are solved simultaneously with matrices related to the building performance. In order to install TRNSYS components into the ESP-r plant component database, the main algorithm needs to be encapsulated into a standard coding structure, which is called at the appropriate point within the matrix. This structure is known as the generic matrix coefficient generator. A further file known as a static template is also required, where component parameters and related information is stated (both of these files are coded in Fortran). Once these files are installed, ESP-r needs to be re-compiled so that the new subroutines become part of the main executable program. Finally, the plant component database being used needs to be updated so that the new components can be accessed and incorporated into plant networks.

Elements of this process and general rules for installing new plant components into the ESP-r plant database have been documented (Aasem, 1993), however, the validation undertaken for the new TRNSYS components needed to be extended to ensure that calculated performance remained concurrent between the two simulation environments.

7.4.2.5 Investigations into Whole System Performance under the Various Modes of Operation

In line with the above modelling methodology, two out of the four modes of operation applied at Brockshill were considered under research described in this thesis. This covered Ventilation Pre-heat and Re-circulation modes, however, VPV Bypass and Vented PV modes were considered beyond the scope of this investigation. If these modes were to be considered then performance of the evacuated tube solar hot water system and stratified tank would have to be considered when actuating PV vent mode, and controls for natural ventilation strategies would need to have been considered for VPV By-pass mode.

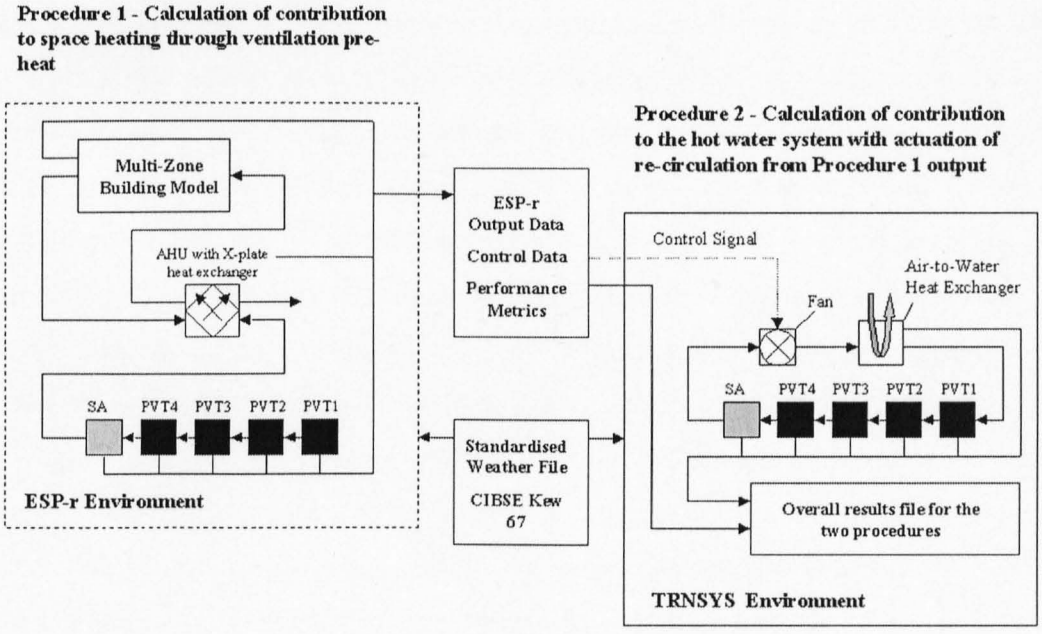

Figure 7.7 – The two-stage simulation approach used by the VPVSAS Method

A detailed description of simulation exercises undertaken is presented in Chapter 8, along with main findings for each mode considered. The main processes involved in simulating the two modes of operation are outlined in Figure 7.7.

7.5 Conclusions

This Chapter has provided background to the field of building integrated PV/T system simulation as context for the new VPV-SAS methodology. This new method of combining building and plant energy modelling has facilitated parametric analysis and removed reliance on test cell data required by the two main preceding studies on the subject. The method also benefits from the specification and analysis of highly detailed plant and building energy models, which may be simulated in isolation or as part of an integrated system approach.

Chapter 8

VPVSAS Method: Simulation, Performance Evaluation and Discussion

8.1 Introduction

This Chapter presents the main research findings. As stated in Chapter 1, the two main objectives in the development of a new methodology for the simulation of a combined PV/Thermal and Solar Air collector system involved analysis of parametric and input data as part of initial validation, and overall performance assessment of the system installed at the Brockshill Environment Centre. The VPVSAS Methodology has been developed with an intention to provide an adaptable set of simulation components that can be used to describe specific and new collector configurations. This provides researchers and designers of such systems with a means of gaining initial performance data without the need for testing a specific collector under standard test conditions. Due to the adaptable nature of the VPVSAS Method, this Chapter will follow the development process that has been undertaken. Individual sections of the methodology may then be taken or disregarded as appropriate if used by others subsequently.

The Chapter starts by describing the processes used to assess the quality of simulation output. As discussed in Chapter 7, the two main investigations concerned with simulation of PV/Thermal collectors (multi-functional, semi-transparent facades [Mei *et al*, 2000] and scaling and replication using standard test conditions [Clarke *et al*, 1998]) were deemed inappropriate due to limited capabilities in specific description and data analysis. For this reason, it was decided that Type 50 (the standard TRNSYS PV/Thermal subroutine) would be developed in line with the aims of research described in Chapter 1.

Further development of Type 50 has been undertaken to produce Type 150, which is the VPVSAS Method representation of a PV/Thermal collector. This new subroutine differs from the standard TRNSYS component in two fundamental ways. Firstly, the collector geometry, construction and description of material thermodynamic properties can be described in fine detail compared with Type 50, which simply states an area of solar collection. This level of description means that internal thermal processes can be calculated in a transient manner instead of being stated as a parameter. This is therefore the second enhancement provided by the VPVSAS subroutine, with continual calculation of the collector efficiency factor (5.7.3) and the overall collector heat loss coefficient (5.7.2). Through simulation of Type 50 under a range of F' and U_L settings and comparison with monitored data the relative importance of these static parameters as opposed to transiently calculated variables are assessed.

Focusing on the new Type 150 subroutine, sensitivity analysis is performed on parameters and input variables that effect F' and U_L. This provides valuable information that designers of subsequent systems may use in collector description.

Once an acceptable level of comparability has been achieved, the subroutine is linked into a larger model (firstly described within TRNSYS) that is used to calculate overall system performance throughout the year. As described in Chapter 6, specific plant modelling software packages generally have limited capabilities for detailed load analysis. Under the VPVSAS Methodology there are two approaches that may be taken. Both of these use hourly building heating load data generated by ESP-r. Combined

Approach 1 (CA1) takes output data from an ESP-r building simulation and provides hourly data into a TRNSYS model. Contribution to the building load can then be calculated on an hourly basis with surplus energy provided to solar hot water (as operated by the Brockshill system). The second approach, Combined Approach 2 (CA2), is more complex in model development, however has the potential for greater use in the design process. This approach provides the Type 150 subroutine for use directly within the ESP-r modelling environment. Using this approach the overall plant network can be described, including heat recovery, solar contribution to specific zones and detailed control regimes.

8.2 Validation exercises and parametric assessments

As described in Chapter 4, one series of the combined collector has been monitored to provide data for air and surface temperatures. This data has been used for comparison with simulated output where input weather files generated from the onsite weather station to provide a standardised testing environment. Air is only passed through the collectors when energy is available and there is a call for either space heating or hot water load within the building. To give an accurate comparison between collector operation and simulation, data is taken from the BEMS, which indicates when specific dampers are open to enable air to pass through the collector series.

8.2.1 TRNSYS project development

Prior to the building opening in April 2001, the author assisted Dr Neil Shankland in the design, procurement, installation and testing of the monitoring system (including the on-site weather station, sensor installation, data logger set-up and interface with the BEMS). Due to commissioning of the monitoring and data logging systems, good quality data sets became available for ventilation preheat from November 2001. Prior to this date, there was also very little call on space heating due to passive solar design of the building and high levels of insulation. From November the BEMS switched to ventilation preheat for large sections of the day, which provided the first prolonged sections of data for analysis.

Due to the extensive amount of time required to transfer weather and other input data into a usable form (due to very slight time differences in data collected from the VPVSAS loggers, BEMS and weather station), it was decided that validation and analysis of simulation output would focus on one representative week. A week of suitable data was found between the dates, 8th and 14th November 2001 from data set covering the first six months of operation. This section was chosen as monitored data sets were commonly incomplete due to problems with either the BEMS, data loggers or weather station readings. Due to the short heating season of the building, there was also limited sections of time where a call was made for ventilation pre-heat by the BEMS. The main weather data for this period is presented in Figures 8.1 to 8.3. Figure 8.1 shows incident radiation on the plane of the collector. Data for ambient dry bulb temperature (Figure 8.2) and wind speed (Figure 8.3) were taken from the main weather station. For this period of time wind direction varied between north-west and south, however south-south-west could be noted as the prevailing wind direction during this seven day period. As we will see, air-flow rate through the collector has a major impact on collector performance. For this reason, the mass flow rate of air passing through the collectors was monitored and provided as input to the Type subroutines under investigation. Measured mass flow rates through the week are presented in Figure 8.4. This represents a volume being provided to the building regardless of whether it is channelled through the collector or not.

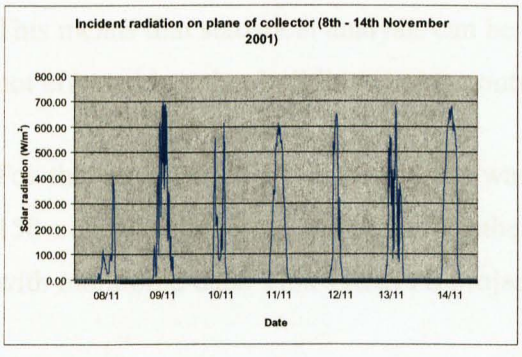

Figure 8.1 – Incident radiation

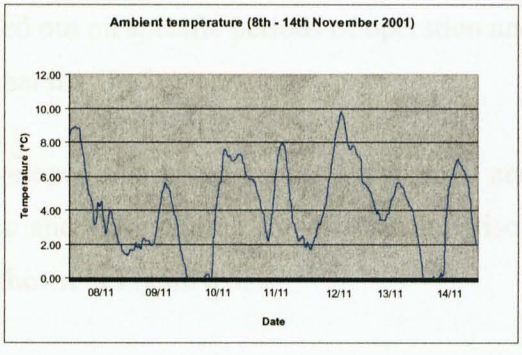

Figure 8.2 – Ambient temperature

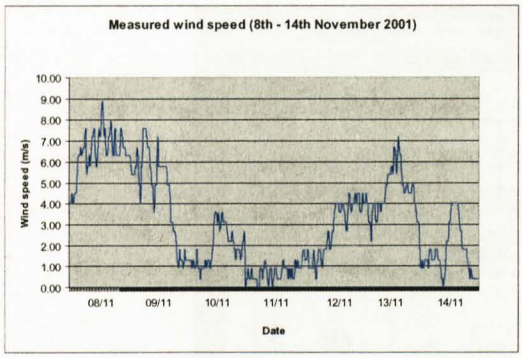

Figure 8.3 –Wind Speed

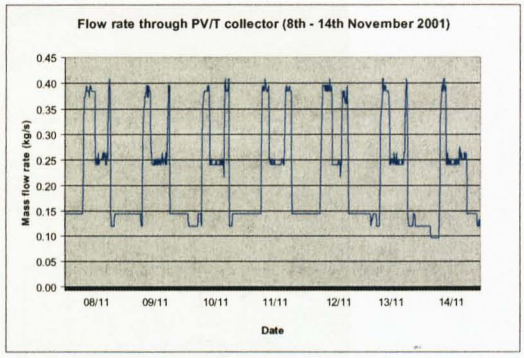

Figure 8.4 – Measured mass flow rate through the collector

Figure 8.4 shows the mass flow rate through the collector as controlled by the BEMS in relation to particular heating and ventilation requirements in the building. This clearly shows that a certain call was given to supply and extract fans throughout the night time. The reason for this is not understood, however, numerous faults were reported during the first year of operation (and indeed to date). For this reason, TRNSYS simulations were controlled on damper positions as set by the BEMS so only periods of airflow through the collector are simulated. This can be clearly seen in Figure 8.6.

In order that analysis of collector performance is only carried out for periods when the collector is in operation, damper readings are provided as input to another new, bespoke TRNSYS subroutine that sets all outputs to zero when the collector is not being used. This means that statistical analysis can be carried out on specific periods of operation and not effected by other building energy controls that may be in operation.

For this exercise, a TRNSYS project was developed that could simulate Types 50 and 150 concurrently using the same weather data and flow regime for direct comparison with monitored data. This TRNSYS project is shown in Figure 8.5.

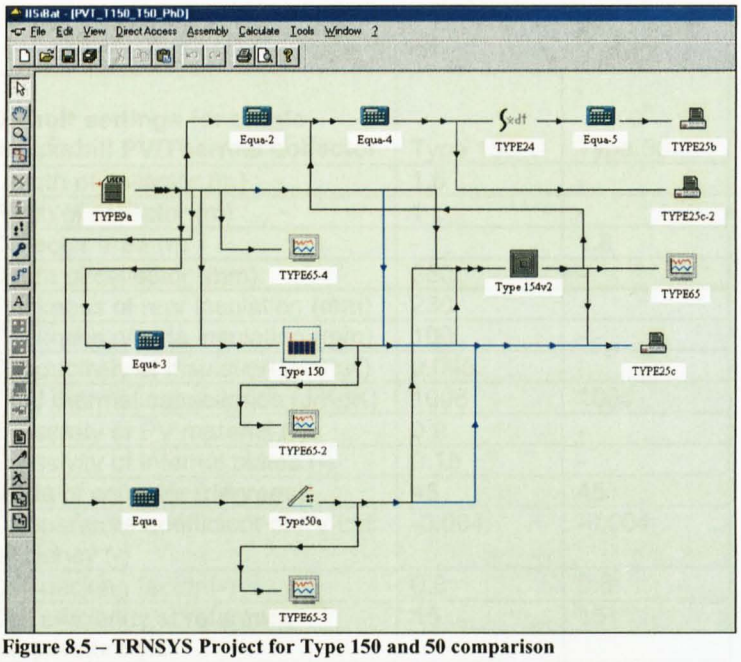

Figure 8.5 – TRNSYS Project for Type 150 and 50 comparison

To give a brief description of this particular project setup, weather and input data is taken from a .ascii file and read by the Type 9a Data Reader subroutine. A single collector is specified to represent the first PV/Thermal collector of a single series. As the full collector at Brockshill is made up of five parallel collector series, the measured mass flow rate is divided by five prior to Type 50 and 150 input (this is specified within Equa and Equa-3 TRNSYS Types as seen in Figure 8.5). Simulation of the two Types under investigation takes place using time steps of 10 minute intervals, with a total simulation of 1008 steps that cover 1 week of operation. Output data from the collectors are then taken to a new Type 154 subroutine, which reads damper settings at each time step to assess whether the monitored system is in operation. If dampers are set to take air through the Brockshill collector, then Type 50 and 150 output is taken to the main output sections of the TRNSYS project. Collector air temperatures are recorded for direct comparison with monitored data along with a rate of thermal energy conversion to give an overall thermal performance for the collector during the simulation run.

Default settings for single Brockshill PV/Thermal collector	Type 150	Type 50
Length of collector (m)	1.8	-
Width of collector (m)	1	-
Collector area (m^2)	-	1.8
Depth of collector (mm)	250	-
Thickness of rear insulation (mm)	230	-
Thickness of side insulation (mm)	100	-
Conductivity of insulation (W/mK)	0.045	-
Fluid thermal capacitance (J/KgK)	1006	1006
Emissivity of PV material (-)	0.9	-
Emissivity of internal plates (-)	0.15	-
Slope of collector (degrees)	45	45
Temperature coefficient of PV cell efficiency (-)	-0.004	-0.004
Cell packing factor (-)	0.8	0.8
Cell efficiency at reference temperature (%)	15	15
Temperature of cell reference efficiency (°C)	25	25
Transmittance of cover system (-)	0.9	0.9
Collector plate absorptance (-)	0.9	0.9
F' – collector efficiency factor (-)	-	0.7
U_L – Collector loss coefficient (Wm^2K)	-	6

Table 8.1 – Default setting for VPVSAS Type 150 and TRNSYS Type 50

The two collector Types were set up to describe as accurately as possible the first PV/Thermal collector in series at Brockshill. When then same parameter was required, this was standardised for each Type set up. Table 8.1 shows the default settings for the two Types being examined.

The main difference between the parameters required for each Type is the detailed collector description required by Type 150, with overall F' and U_L specified for Type 50. Initial settings for F' and U_L were kept at defaults provided under the TRNSYS standard component library (TRNSYS version 15.3).

8.2.2 PV/Thermal Type 150 testing

Results of outlet temperature were taken at each time step and compared with measured data. This output is presented in Figure 8.6 to show the general agreement between calculated temperatures and those recorded at Brockshill.

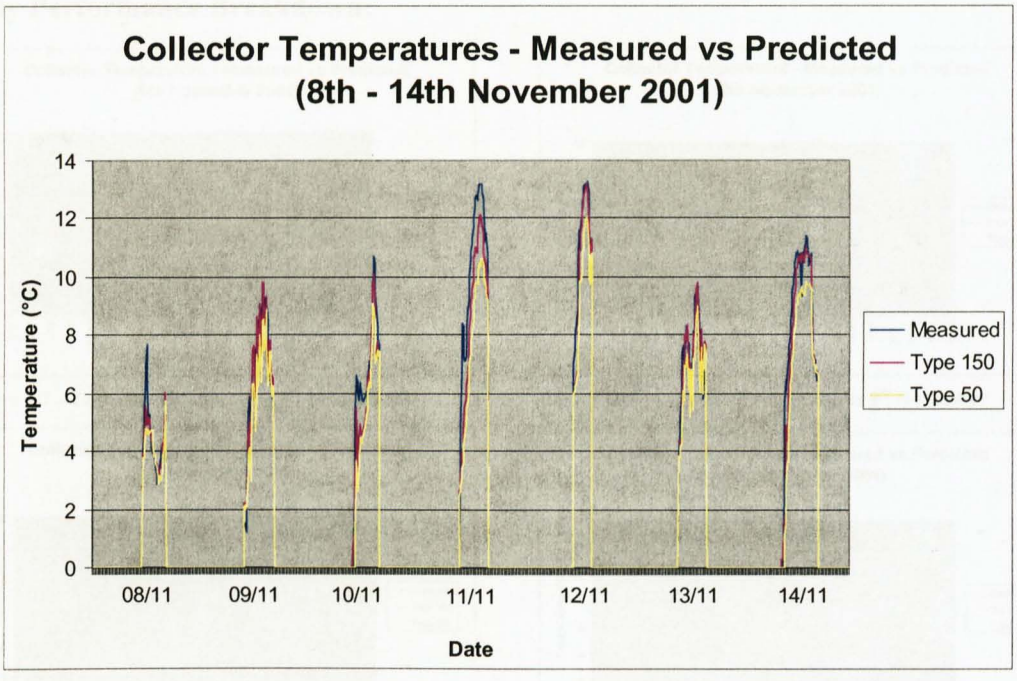

Figure 8.6 – Collector temperatures for test week: measured vs Type 150 and Type 50

Analysis of these results was undertaken to assess the quality of calculated temperatures both for overall performance and at each point during the simulation run. This considered temperature differences from monitored data at each time step to provide overall Mean Temperature Difference (MTD) and Root Mean Square (RMS) statistics for Types 50 and 150 over the study period. The RMS was taken as a suitable metric for comparison of data sets following research carried out on empirical validation of dynamic thermal modelling software packages (Lomas, 1991). Table 8.2 gives overall results and performance metrics using default settings given in Table 8.1.

Data source	Mean Temperature Difference (°C)	RMS Temperature Difference (°C)	Solar Thermal Energy Conversion (kWh)
Brockshill data collection	-	-	7.514
Type 150	0.5	1.25	7.453
Type 50	1.24	1.73	5.158

Table 8.2 – Overall collector performance

Daily Performance Breakdown:

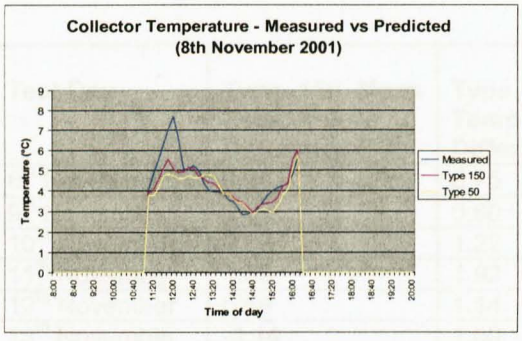

Figure 8.7 – Collector Temperature 8th November

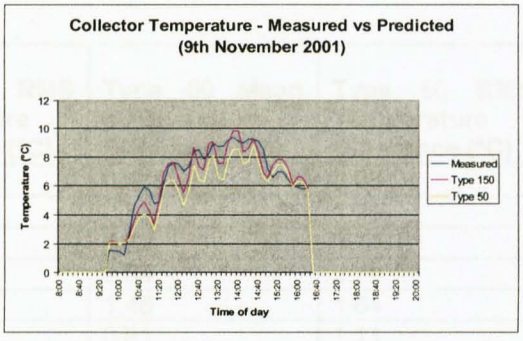

Figure 8.8 – Collector Temperatures 9th November

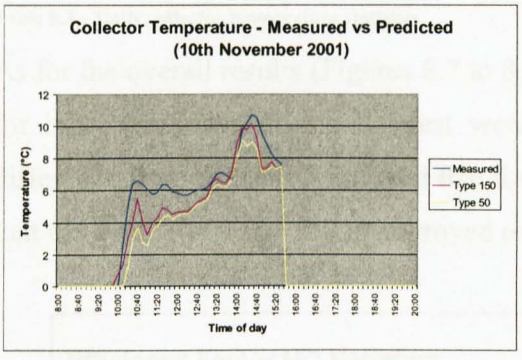

Figure 8.9 – Collector Temperatures 10th November

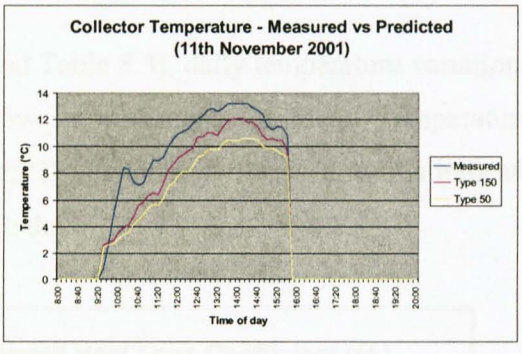

Figure 8.10 – Collector Temperatures 11th November

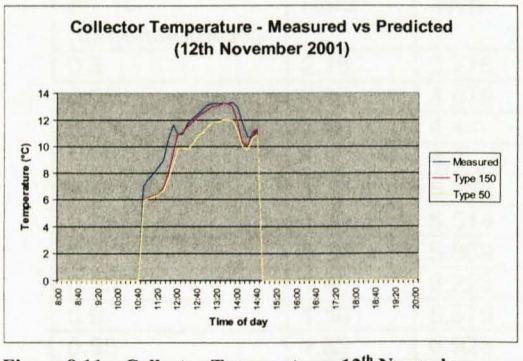

Figure 8.11 – Collector Temperatures 12th November

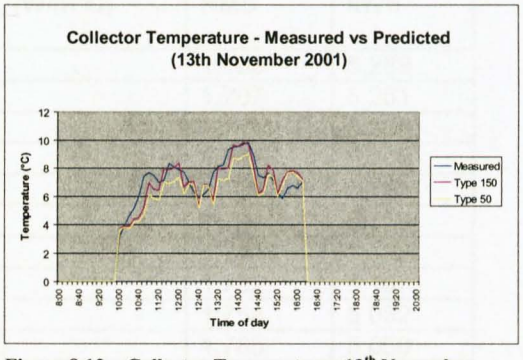

Figure 8.12 – Collector Temperatures 13th November

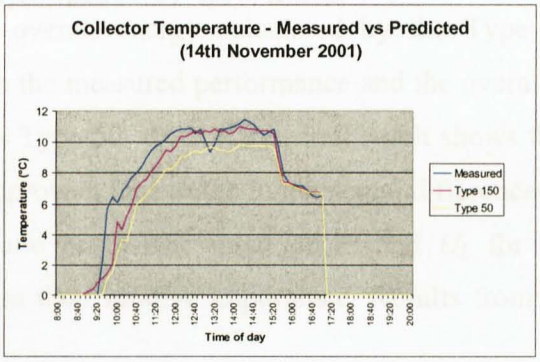

Figure 8.13 – Collector Temperatures 14th November

Test Day	Type 150 Mean Temperature Difference (°C)	Type 150 RMS Temperature Difference (°C)	Type 50 Mean Temperature Difference (°C)	Type 50 RMS Temperature Difference (°C)
8th November	0.24	0.75	0.41	0.95
9th November	0.00	0.80	0.81	1.25
10th November	0.85	1.22	1.33	1.74
11th November	1.58	1.92	2.54	2.79
12th November	0.59	1.14	1.48	1.64
13th November	-0.14	1.00	0.61	1.11
14th November	0.46	1.30	1.43	1.87

Table 8.3 – Daily collector temperature statistics

As for the overall results (Figures 8.7 to 8.13 and Table 8.3), daily temperature variations for individual days during the test week show improvements in Mean Temperature difference from measured data and that the RMS Temperature Difference results indicate that the quality of Type 150 is improved on each day.

Efficiency Factor (*F'*) Variation			Overall Heat Loss Coefficient (U_L) Variation		
F' (dimensionless)	RMS	kWh	U_L (W/m^{2}C)	RMS	kWh
0.5	2.18	3.716	1	1.169	5.289
0.55	2.07	4.079	2	1.707	5.261
0.6	1.95	4.44	3	1.714	5.235
0.65	1.84	4.8	4	1.721	5.209
0.7	1.73	5.158	5	1.728	5.183
0.75	1.63	5.514	6	1.734	5.158
0.8	1.54	5.869	7	1.744	5.133
0.85	1.46	6.223	8	1.752	5.107
0.9	1.38	6.575	9	1.758	5.082
0.95	1.32	6.925	10	1.765	5.058
Δ *F'* for range	**0.86**	**3.209**	**Δ U_L for range**	**0.066**	**0.231**

Table 8.4 – Type 50 performance with F' and U_L variation

Even though the overall energy calculated by the Type 150 collector shows good comparability with the measured performance and the overall MTD demonstrates a clear improvement from Type 50, the RMS overall result shows that the quality of calculated output could be improved. Due to the fundamental differences between Types 150 and 50 with regard to static parametric input of F' and U_L for Type 50, range tests were performed to assess their relative importance. Results from these tests are presented in Table 8.4.

It is clear from these results that F' and to a lesser extent U_L collector performance is significantly effected by settings chosen. As Type 150 calculates these at each time step, sensitivity analysis was undertaken to deduce importance of settings and input variables.

8.2.3 Type 150 performance and parametric sensitivity analysis

As stated previously, Type 150 was developed with performance evaluation being given a high priority. Not only do the numerous outputs enable parametric assessment but also show any major failings within the algorithm during simulation and problems of interaction with other subroutines. Following on from analysis of Type 50, Type 150 can now show transient variation in F' and U_L. This variation can be clearly seen in Figure 8.14 and Figure 8.15.

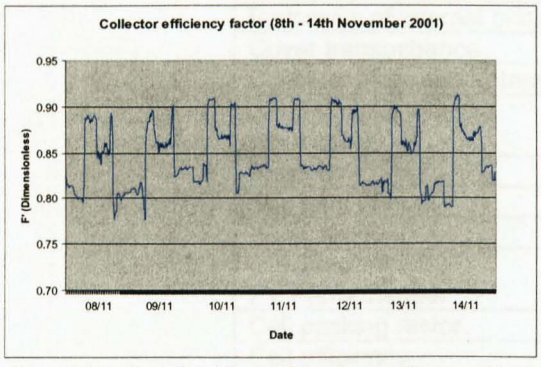

Figure 8.14 – Calculated Type 150 collector efficiency factor

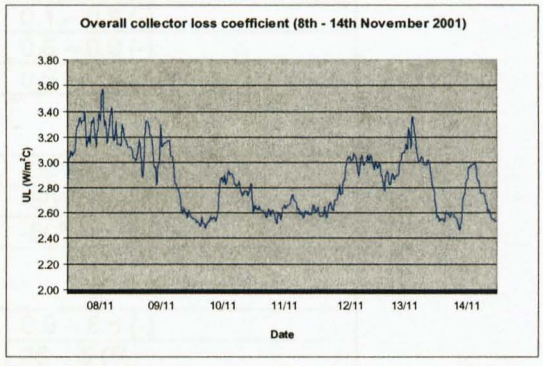

Figure 8.15 – Calculated Type 150 collector loss coefficient

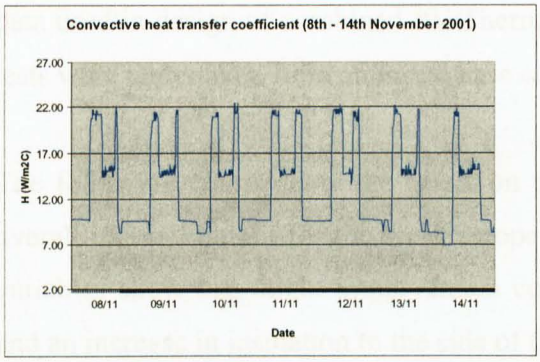

Figure 8.16 – Calculated Type 150 convective HTC (heat transfer between plate & fluid)

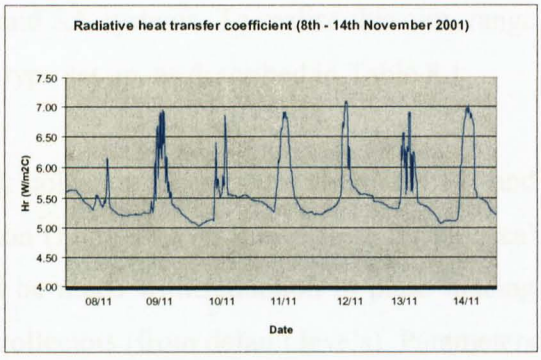

Figure 8.17 – Calculated Type 150 radiative HTC (heat transfer between plate & fluid)

The form of the collector efficiency factor plot is dominated by the collector mass flow rate, while the calculated U_L shows a clear replication in form of the wind speed regime for this time period. As would be expected the convective HTC is directly related to the flow rate and the radiative HTC linked to the amount of incident solar radiation.

Variable	Range tested
Physical properties:	
Plate spacing	50 – 5 (mm)
Back insulation (thickness)	10 – 250 (mm)
Side insulation (thickness)	10 – 250 (mm)
Conductivity of insulation	0.1 – 0.01 (W/mK)
Thermophysical properties:	
Emissivity of PV material	0.7 – 0.9 (-)
Emissivity of internal plates	0.1 – 0.9 (-)
Cover transmittance	0.6 – 0.9 (-)
Collector plate absorptance	0.6 – 0.9 (-)
Input data:	
Mass flow rate	-30% to +30%
Sky temperature	-50% to + 50%
Wind speed	-50% to +50%
PV Performance:	
Cell packing factor	0.9 – 0.5 (-)
Cell efficiency	25 – 5 (%)

Table 8.5 – Parameter and input variables ranges tested

These plots give a general indication as to the inputs effecting the main thermodynamic processes occurring within the collector. In response to one of the main aims stated in

Chapter 1, this research is interested in the relative importance of input and parametric data used in design of combined PV/Thermal and SA systems. To realise this aim, range tests were undertaken from an initial base case type set up, as described in Table 8.1

The following charts show the effect on peak collector temperature (Figure 8.18) and overall thermal output for the week in operation (Figure 8.19). Range tests for physical variables show that slight improvement could be made with reduction in plate spacing and an increase in insulation to the side of the collectors (from default levels). Parameters that have the main impact across the range are cover transmittance and plate absorptance with internal plate emissivity indicating that a possible improvement through change of plate specification. Of the input parameters, flow rate dominates which highlights the importance of the control and systems setting. Wind speed also shows a significant impact on collector performance with its effect on U_L. Finally PV material used dictates

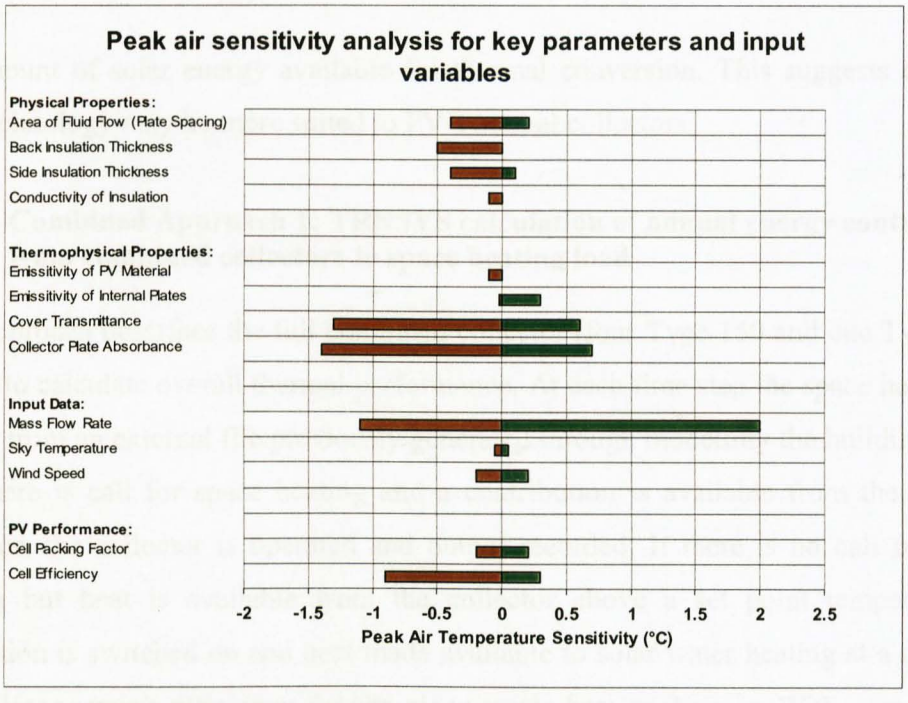

Figure 8.18 – Sensitivity analysis considering peak air temperatures

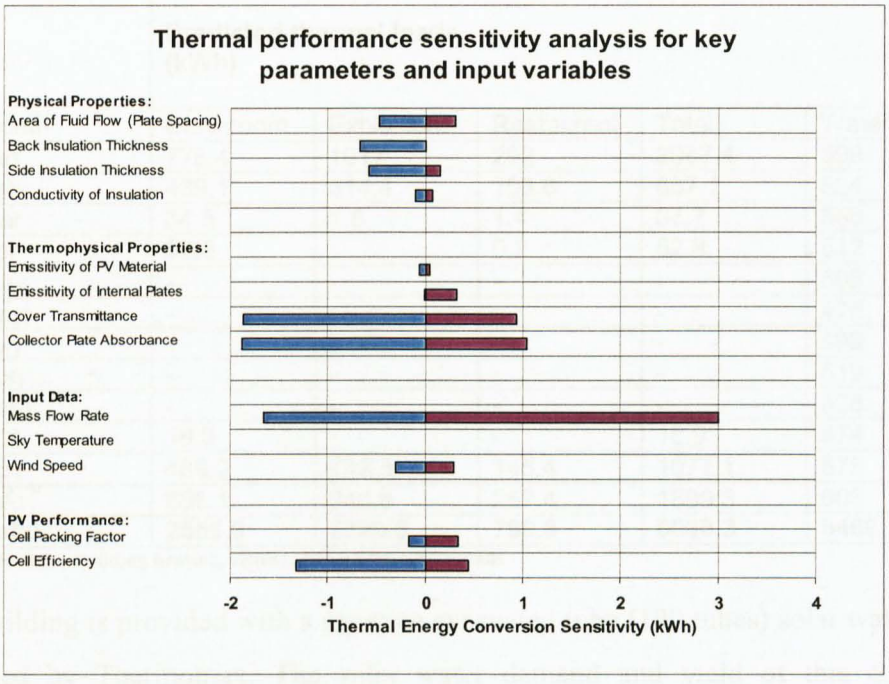

Figure 8.19 – Sensitivity analysis for overall energy conversion

the amount of solar energy available for thermal conversion. This suggests that a thin film technology may be more suited to PV/Thermal collectors.

8.2.4 Combined Approach 1: TRNSYS calculation of annual energy contribution from combined collectors to space heating load

This approach describes the full combined collector (four Type 150 and one Type 151 in series) to calculate overall thermal performance. At each time step the space heating load is read from an external file previously generated through modelling the building in ESP-r. If there is call for space heating and a contribution is available from the combined collector, the collector is operated and output recorded. If there is no call from space heating but heat is available from the collector above a set point temperature, re-circulation is switched on and heat made available to solar water heating at a designated thermal conversion efficiency for the air-to-water heat exchanger. With comparison to predicted thermal loads (Table 8.6), detailed results from CA1 are given in Table 8.7 and Table 8.8

Month	Predicted thermal loads (kWh)				
	Classroom	Exhibition	Restaurant	Total	Water
Jan	778.4	1017	292	2087.4	598
Feb	439.1	314.4	103.6	857.1	524
Mar	84.5	1.8	1.4	87.7	556
Apr	52.6	-	0.2	52.8	512
May	-	-	-	-	506
June	-	-	-	-	475
July	-	-	-	-	499
Aug	-	-	-	-	519
Sept	-	-	-	-	528
Oct	18.9	-	-	18.9	574
Nov	488.2	443.5	145.4	1077.1	575
Dec	695.1	946.8	257.4	1899.3	603
Total	**2556.8**	**2723.5**	**799.8**	**6080.3**	**6469**

Table 8.6 – Building heating, ventilation and hot water loads

The building is provided with a separate evacuated tube (120 tubes) solar water collector, provided by Thermomax. The solar water demand and yield of this collector was calculated using Thermomax SolarMaster software.

Month	Predicted thermal yields (kWh)				PV Yield (kWh)
	VPV/SA space heating	VPV/SA thermal store	Solar water	Dual fuel boiler	
Jan	420	35.8	366	1863.6	64.4
Feb	446.3	204.7	504	226.1	122
Mar	71.99	907.3	771	-	299.9
Apr	46.29	835.6	800	-	270.9
May	-	1554.4	962	-	494.4
June	-	1702	1009	-	535.4
July	-	1697	1004	-	530.5
Aug	-	1374	958	-	429.1
Sept	-	577.2	915	-	179.2
Oct	-	575	742	-	182.5
Nov	362.7	117	505	667.4	82
Dec	368	39	345	1750.3	58.5
Total	**1715.2**	**9618.6**	**8881**	**4507.4**	**3248**

Table 8.7 – Predicted yields

Month	Contribution to thermal load		Contribution to hot water load (VPV/SA)		Contribution to hot water load (Solar Hot Water Collector)	
	Proportion of load (%)	Yield provided (kWh)	Proportion of load (%)	Yield provided (kWh)	Proportion of load (%)	Yield provided (kWh)
Jan	21.8	455.8	-	-	61.2	366
Feb	75.9	651	-	-	96.1	504
Mar	100	87.7	100	556	-	-
Apr	100	52.8	100	512	-	-
May	-	-	100	506	-	-
June	-	-	100	475	-	-
July	-	-	100	499	-	-
Aug	-	-	100	519	-	-
Sep	-	-	100	528	-	-
Oct	100	18.9	100	574	-	-
Nov	44	479.7	-	-	87.8	505
Dec	21.4	407	-	-	57.2	345
Total	-	2152.9	-	4169	-	1720
Annual Contributions						
	35%		64.4%		26.5%	

Table 8.8 – Proportion of building loads contributed by the combined VPV/SA collector

These results show that under this calculated load, the combined collector contributes a portion of space heating load (35%) with larger benefits available to the water heating load. This relegates the call on the designated solar hot water collector to winter contribution. In reality, the solar water collector would routinely take the storage tank temperature to a point where there would be no call to the combined collector re-circulation fan.

8.2.5 Combined Approach 2: VPVSAS application to ESP-r

The next approach saw the introduction of TRNSYS tested subroutines directly into the ESP-r plant database. This does introduce a greater level of complexity to the overall model, although now the combined collector can be simulated together with other components that make up the installed system and react to a more detailed control system. As discussed earlier in this thesis, one of the main limitations of isolated building and plant modelling is the interaction between internal temperatures and plant supply and extract. Under the requirements of the Brockshill system, heat recovery is of major

importance and this could not be accounted for using the TRANSAIR tool or indeed the straight space heating load analysis used under the CA1.

Combined Approach 2 (CA2) is presented in this thesis as an initial study into the potential of combined building and combined PV/Thermal Solar Air collector systems. Due to the complexity of plant component installation within ESP-r and the limited amount of work that has been carried out in this specific area, CA2 is described here as a starting point for further work. Algorithms used, installation files and processes required for implementation are provided in Appendix A.

The combined building energy and plant ESP-r model of the Brockshill Environment Centre used the plant network shown in Figure 8.20. As described in Chapter 4, this network represents Mode 1 (Pre-heat of air supplied into the building for ventilation and space heating). Ambient air is brought into the system, taken through the combined collectors, boosted through heat recovery and then brought up to supply temperature within the main heater battery. Air is then ducted to the three main spaces in proportions measured during system operation.

Connections

	Sending comp	@	Node		to	Receiving comp	@	Node	Conn Type	Mass Div
a	outside air		ambient		-->	inlet_duct		air node 1	zone/amb	1.000
b	inlet_duct		air node	1	-->	supply_fan		air node 1	to compt	1.000
c	supply_fan		air node	1	-->	PVT_1		air node 1	to compt	1.000
d	PVT_1		air node	1	-->	PVT_2		air node 1	to compt	1.000
e	PVT_2		air node	1	-->	PVT_3		air node 1	to compt	1.000
f	PVT_3		air node	1	-->	PVT_4		air node 1	to compt	1.000
g	PVT_4		air node	1	-->	Solar Air Coll		air node 1	to compt	1.000
h	Solar Air Coll		air node	1	-->	heat_exchanger		air node 1	to compt	1.000
i	heat_exchanger		air node	1	-->	heating_coil		air node 1	to compt	1.000
j	heating_coil		air node	1	-->	supply_duct_1		air node 1	to compt	0.363
k	heating_coil		air node	1	-->	supply_duct_2		air node 1	to compt	0.303
l	heating_coil		air node	1	-->	supply_duct_3		air node 1	to compt	0.333
m	exhibition		zone air		-->	convg_1		air node 1	zone/amb	1.000
n	classroom		zone air		-->	convg_1		air node 1	zone/amb	1.000
o	restaurant		zone air		-->	convg_2		air node 1	zone/amb	1.000
p	convg_1		air node	1	-->	convg_2		air node 1	to compt	1.000
q	convg_2		air node	1	-->	heat_exchanger		air node 2	to compt	1.000
r	heat_exchanger		air node	2	-->	extract_fan		air node 1	to compt	1.000
s	extract_fan		air node	1	-->	exhaust_duct		air node 1	to compt	1.000

+ add/delete/copy

? Help
- Exit

Figure 8.20 – ESP-r plant network configuration with applied VPVSAS collectors

The installation and application of the above plant network with a control set point related to dry bulb temperature within the Exhibition Hall demonstrated a clear reduction

in building space heating load to 5690 kWh. This contribution of 390 kWh from the combined collector is well short of the thermal yield predicted using CA1 (6.4% of space heating load compared to 35% under CA1). Through checks on the supplementary plant component outputs, the component was found to be performing correctly with clear increases in collector air temperature along the collector series. This should therefore provide ambient air at a higher temperature to the main heater battery, which is being called for space heating. The solution to this unexpected performance was found in the contribution of energy to space heating at specific time steps. When a call is made for space heating in the morning, the heater battery uses the required amount of energy to bring spaces (specifically the Exhibition as used for actuation) up to the set point temperature. This is done, however, during the short heating season associated with this low energy building, there is little contribution from the combined collector at this time in the day. Later, when solar heating can be provided from the collectors, the building is generally at set point temperature and under this modelling approach little contribution is observed. In the real environment, the provision of space heating is less instantaneous and solar pre-heating makes a larger contribution.

The exercise does show that the potential contribution to space heating is not only limited for low energy buildings in the UK climate, but the control regime also has a major impact on the potential contribution from this type of solar collector system.

8.3 Discussing the viability and potential of the VPVSAS Method

In the provision of new buildings that respond to the general desire for sustainable development, there is a fine balance between design and construction that provide for energy minimisation, without severe penalties in thermal comfort and economic viability. Although many of the theoretical principles of environmental design (passive solar gain, natural ventilation, use of thermal mass etc.) have been applied through history, modern requirements on buildings dictate that detailed design should be provided to reduce risk

both in terms of building functionality and cost structure. As low energy buildings present risk in both of these areas, design procedures have become more complex to help design teams undertake their various tasks. Many of these design tools, both conventional and computer based, have focused specifically on energy efficiency and energy demand reduction through design, or on maximising energy conversion within supply systems. It is then difficult to assess performance of buildings that demonstrate an integrated approach to energy. In this research and previous work in the area of building integrated PV/Thermal systems application, attempts have been made to understand and develop design tools for this specific role.

8.3.1 VPVSAS Method in relation to PV-HYBRID-PAS research

The three different research projects (PV-HYBRID-PAS, Mataró related studies and the VPVSAS Method) have used different approaches, which respond to the PV/Thermal collector configuration and the software tools available for development. PV-HYBRID-PAS has a close relationship to the VPVSAS Method due to the use of ESP-r as the dynamic thermal modelling environment used for building energy load generation. The limiting factors and main reason for the VPVSAS Method using TRNSYS based subroutines for calculations lie in the statically set convective HTC ascertained under standard test conditions. This information was not available for the collectors used at Brockshill and with an intention that the VPVSAS Method could be used in the design of new collector configurations, a more adaptable approach was deemed necessary. If the 'scaling and replication' strategy had been employed, as used under PV-HYBRID-PAS, parametric assessments would have been severely restricted to the standard outputs given in the ESP-r 'Results Analysis' module. To access the required metrics, further development of ESP-r would have been required, which given the nature and intricacy of ESP-r code and program structure would have been beyond the resources available in time and expertise at the Institute of Energy & Sustainable Development.

8.3.2 VPVSAS Method in relation to Mataró related research

The multi-functional PV/Thermal façade installed at the Mataró library differs significantly from the combined collector at Brockshill. The vertical and predominantly natural air-flow through the façade combined with the semi-transparency of the elements and fully building integrated nature of the installation take modelling activities along different lines of approach. Similarities do lie in the fact that for that both the Mataró study and VPVSAS Method use TRNSYS as the main modelling environment. Calculation of the building heating demand is also different in that Mataró related research uses the ASHRAE transfer function to provide a basic load calculation, where as the VPVSAS Method can pull load data from a detailed dynamic thermal model of the building with associated operational profiles and control regime. Mataró library and Brockshill Environment Centre do share a common goal of environmental design with applied PV/Thermal technologies, however, variation in climatic conditions between Barcelona and Leicester along with different operations requirements dictate very different technological solutions and subsequently, modelling approaches.

8.3.3 Contribution to knowledge from the VPVSAS Method

The main benefits provided by the VPVSAS Method are in detailed PV/Thermal and SA description, parametric analysis and adaptability in consideration of building energy loads to which the combined collectors are contributing. Information provided by these three main factors should be considered as the main contribution to current knowledge presented in this thesis.

Developing the TRNSYS Type 50 PV/Thermal subroutine and adapting formulas from the Hottel-Whillier-Bliss model for PV/Thermal collectors the VPVSAS Method can now calculate the collector efficiency factor and overall heat loss coefficient transiently. As this is done through detailed collector description, these new subroutines (Type 150 and Type 151) may be used by designers of PV/Thermal and SA collectors to provide

performance assessment before building collector prototypes and testing under standard test conditions.

The parametric study conducted as part of the work provides the designer of such collectors with initial information on the relative importance of specific parameter settings and input variables. This means that weighting can be given to certain influences within the calculation procedure and a range of performance attributed when assumptions are made during model set up.

If hybrid technologies, such as PV/Thermal or CHP systems, are to be operated as efficiently as possible, they should be designed carefully to meet building energy demands where possible throughout the day and year. These technologies are usually higher in capital cost than conventional systems, so appropriate design has a higher level of importance than standard energy conversion appliances. The VPVSAS Method can assist in this load analysis either to give an overall estimate by applying transient load data into a TRNSYS project or in greater detail as an integrated model under ESP-r. Both of these procedures will benefit from further research to establish standard modelling procedures and further detailed validation activities.

8.3.4 Discussion on error in detailed modelling activities

Through development and results analysis of the VPVSAS Method it has become apparent that with increased complexity and especially in combined building energy and plant modelling unexpected output is often provided. The effect of increased variables on the error that is carried within a calculation procedure was discussed in Chapter 6 and has been demonstrated in CA2 where a limited contribution from the combined collector was calculated. If results are to become more representative for integrated building energy and plant assessments, further work should be undertaken on limitation and weighting of design variables.

8.4 Conclusions

This Chapter has described the various procedures that make up the VPVSAS Methodology. Performance of the new TRNSYS Type 150 subroutine for a PV/Thermal collector has been demonstrated and compared with standard issue TRNSYS Type 50 component. The importance of transiently calculating the collector efficiency factor and overall heat loss coefficient has been shown along with the main contributing parameter settings and input variables.

The new subroutines that represent PV/Thermal and SA collectors have been used to calculate overall system performance using approaches which showcase alternative methods of calculating combined collector performance. The output from these have been presented and discussed in the context of previous research studies in the field.

Chapter 9

Conclusions

The application of a combined PV/Thermal and Solar Air collector system at Brockshill Environment Centre represents the first installation of such technology in the UK. As configured to perform in various modes of operation that aim to meet the specific energy demands of a low energy building, the author understands that this installation is also first within a global context. This point is stated to illustrate that limited experience has been gained in the development, application and simulation of combined PV/Thermal and Solar Air collector systems.

The main output of this research is the VPVSAS Method. This has been developed in order that the three broad objectives stated in Chapter 1 could be addressed and an adaptable framework set in place for subsequent research in the field. The methodology has also taken into account the needs of designers that may make use of this approach.

Chapter 2 considered current environmental design practices to give context to the various low energy design strategies and technologies applied in the development of the Brockshill Environment Centre. This Chapter indicated that through following a low energy approach to design, interactions between the building, external environment, building services and environmental control strategy may result in a higher level of complexity compared with standard buildings. This complexity has clear implications to

the validity of modelling activities, which may be used during building and system design.

Through the study of photovoltaic principles (Chapter 3), it is clear that cell temperature has a significant impact on operational performance (-0.4% in efficiency per °C above 25°C) and therefore, a deleterious effect on operational cost and economic viability of PV systems in general. There are currently relatively few PV installations in the UK compared with other European countries, Japan and the US due mainly to costs, limited subsidies and solar regime. This means that there is a clear need to maximise the potential of PV systems in the UK, and that the study of hybrid collectors that provide both heat and electricity (at optimal energy conversion efficiencies) for use within specific buildings can be considered a worthwhile activity at this time.

The Brockshill Environment Centre now stands as an example of integrated environmental design where the building and energy systems are intrinsically coupled. The resultant complexity has been seen in operational difficulties, however, this development was always intended as a demonstration project from which lessons can be taken. The research described in this thesis forms part of these ongoing activities.

Following study of previous research in the area PV/Thermal modelling and simulation, it became clear that development of knowledge in modelling solar collectors as provided at Brockshill environment centre would be best achieved through enhancement and development of standard TRNSYS library PV/Thermal and Flat-plate solar collectors. Work carried out under the PV-HYBRID-PAS project used a method of 'scaling and replication' where a PV/Thermal collector was tested under standard test conditions, with performance for a very specific collector and operation applied as input to ESP-r. As the collectors provided at Brockshill Environment Centre had not been tested in this manner, 'scaling and replication' was not appropriate. The PV-HYBRID-PAS approach also has limitations in parametric assessment and the ability to change collector configurations. The second research investigation (related to the Mataró Library) also proved to have

limited applicability to the Brockshill PV/Thermal system. This was due to major differences in collector type, it being a façade element with semitransparent PV modules and being operated under very different climatic conditions and internal building requirements. The VPVSAS Method was therefore developed to study the performance of PV/Thermal and Solar Air components in isolation (using TRNSYS) or part of a full building energy and plant simulation (using ESP-r).

Output from the new Type 150 (PV/Thermal) and Type 151 (Solar Air) collector subroutines using a transiently calculated collector efficiency factor and overall heat loss coefficient, have been tested against measured data. With particular attention given to the PV/Thermal collector the new Type 150 subroutine calculated 7.453kWh for the main test week compared with 7.514kWh measured performance at the Brockshill Environment Centre. This Type 150 output also provided an improvement on results given by the standard TRNSYS PV/Thermal collector subroutine Type 50 (5.158kWh for the same time period, operation and weather conditions). Improvements were also noticed in the quality of temperature readings at each time step between Types 150 and 50 when compared to monitored data (Type 150 giving a mean temperature difference of 0.5°C compared with 1.24°C for Type 50). Parametric settings and input variables have been tested to provide a level of weighting that may assist future researchers or designers when modelling combined PV/Thermal and Solar Air or similar systems. The results from this exercise indicate that designers and those modelling PV/Thermal collectors should pay particular attention to the collector cover transmittance, collector plate absorptance, fluid mass flow rate and PV cell efficiency in their parametric settings.

Two approaches have been developed that model combined building energy requirements with applied PV/Thermal and Solar Air collector systems. Both of these approaches show that for buildings with a very limited heating load and season, the combined collectors contribute little towards space heating load compared with the potential that may be provided towards hot water provision. When the system is simulated within a complete building energy and plant modelling environment, with stated operational profiles and

control regime, the calculated contribution to space heating is very limited (6.4% of space heating load) and would suggest that this technology may not be most suited to this particular application or environmental control strategy.

9.1 Further Work

There are two main areas where current knowledge on the application of combined collectors could be developed. As findings from this research indicated that a limited contribution could be expected for space heating purposes, it would be interesting to find out the most appropriate building type, environmental design strategy employed and climatic conditions, that are most suited to the application of this type of system.

The field of integrated building energy and plant modelling would also benefit from further research into processes that enable performance prediction for new technologies and system configurations. Research presented in this thesis has demonstrated two possible approaches that may be used, however the level of detail and development time required would limit wide scale utilisation in a commercial design environment.

As modelling tools and design processes become ever more complex, we need to reduce the error in modelling while maintaining a level validity in prediction, which aids the design process and research into new systems. Further research will hopefully deliver consensus on accepted 'rules of thumb' which will reduce the need for explicit modelling of each proposed system, thereby reducing error in design.

References

Aasem E.O. (1993): *Practical simulation of buildings and air-conditioning systems in the transient domain.* PhD Thesis. Energy Systems Research Unit. University of Strathclyde, Glasgow, UK.

Affolter P., Gay J.B. (1997): *A new generation of hybrid solar collectors.* Proceedings - 14th European Photovoltaic Solar Energy Conference, Barcelona, Spain.

Al Harbi Y., Eugenio N.N., Al Zahrani S. (1998): Photovoltaic – thermal solar energy experiment in Saudi Arabia. Renewable Energy, 15 pp 483 – 486. Elsevier Science Ltd. London, UK.

Allard F., Alvarez S., Dascalaki E., Guarracino G., Maldonado E., Scuito S., Vandaele L. (1998): *Natural Ventilation in Buildings: A Design Handbook.* James & James (Science) Publishers, London, UK.

Anink D., Boonstra C., Mak J. (1996): *Handbook of sustainable building: An Environmental Preference Method for Selection of Materials for Use in Construction and Refurbishment.* James & James (Science Publishers), London.

ASHRAE (1999): *Handbook - Fundamentals.* The American Society of Heating Refrigeration and Air-conditioning Engineers.

Athienitis A.K., Santamouris M. (2002): *Thermal Analysis and Design of Passive Solar Buildings*. James & James (Science) Publishers, London, UK.

Baker N.V. (2000): *Energy and Environment in Non-Domestic Buildings*. Cambridge Architectural Research Ltd. Cambridge, UK.

Benemann J., Chehab O., Schaar-Gabriel E. (2001): Building Integrated PV Modules. *Solar Energy Materials & Solar Cells*, vol 67, pp 345-354. Published by Elsevier Science Limited, London, UK.

Bazillian M.D., Groanhout N.K., Prasad D. (2001a): *Simplified numerical modelling and simulation of a photovoltaic heat recovery system*. Proceedings – 17th European Photovoltaic Solar Energy Conference, Munich.

Bazillian M.D., Leenders F., Van der Ree B.G.C., Prasad D. (2001b): Photovoltaic cogeneration in the built environment. *Solar Energy*, 71 (1) pp 57 – 69. Elsevier Science Ltd. London, UK.

Bazillian M.D., Prasad D. (2001c): *Thermal and electrical performance monitoring of a combined BiPV array and modular heat recovery system*. Proceedings – ISES Solar World Congress, Adelaide, Australia.

Bazillian M.D., Prasad D. (2002): Modelling of a photovoltaic heat recovery system and its role in a design decision support tool for building professionals. *Renewable Energy*, 27 pp 57 – 68. Elsevier Science Ltd. London, UK.

Bergene T., Løvvik O.M. (1995): Model calculatios on a flat-plate solar heat collector with integrated solar cells. *Solar Energy*, 55 (6) pp 453 – 462. Elsevier Science Ltd. London, UK.

Bliss R.W. (1959): The derivation of several 'plate efficiency factors' usful in the design of flat-plate solar collectors. *Solar Energy* 17, 29-37. Elsevier Science Ltd. London, UK.

Brinkworth B.J., Cross B.M., Marshall R.H., Yang H. (1997): Thermal regulation of photovoltaic cladding. *Solar Energy*, vol 61 (3) pp 169-178. Published by Elsevier Science Limited, London, UK.

Brinkworth B.J., Marshall R.H., Ibrahim Z. (2000): A validated model of naturally ventilated PV cladding. *Solar Energy*, 69 (1) pp 67 – 81. Elsevier Science Ltd. London, UK.

BRE (1994): *Thermal insulation: avoiding risks.* Building Research Estblishment. Watford, UK.

BRE (2000): *Shading Devices for Buildings.* The Building Research Establishment. Watford, UK.

Cartmell B.P., Shankland N.J., Fiala D., Hanby V. (2001): *A Multi-operational Ventilated Photovoltaic and Solar Air Collector: Application, Simulation and Initial Monitoring Feedback.* International Solar Energy Society: Solar World Congress, Adelaide, Australia.

CIBSE (1997): *Natural Ventilation in Non-Domestic Buildings: Applications Manual AM10.* The Chartered Institute of Building Services Engineers. London, UK.

CIBSE (1998): *Building energy and environmental modelling – Applications manual AM11*. The Chartered Institute of Building Services Engineers, Balham, London, UK.

CIBSE (1999): *Guide A – Environmental Design*. The Chartered Institute of Building Services Engineers. London, UK.

CIBSE (2000a): *Testing buildings for air leakage: TM23*. The Chartered Institute of Building Services Engineers. London, UK.

CIBSE (2000b): *Mixed mode Ventilation: AM13*. The Chartered Institute of Building Services Engineers. London, UK.

CIBSE (2000c): *Understanding Building Integrated Photovoltaics TM25*. The Chartered Institute of Building Services Engioneers. London, UK.

Clarke J.A. (1977): *Environmental Systems Performance*. PhD Thesis. University of Strathclyde, Glasgow, UK.

Clarke J.A. (2001): *Energy simulation in building design* (2nd Ed). Butterworth-Heinemann, Oxford, UK.

Clarke J.A., Johnstone C., Kelly N., Strachan P.A. (1997): *The simulation of photovoltaic-integrated building facades*. Proceedings – Building Simulation Conference 1997, Prague, Czech Republic.

Clarke J.A., Hand J.W., Janak M., Johnson C.M., Strachan P.A. (1998a): *Simulation Case Study: Elsa building, Ispra, Italy*. PV-HYBRID-PAS Study for PASLINK EEIG. Energy Systems Research Unit, University of Strathclyde, Glasgow, Scotland.

Clarke J.A., Hand J.W., Janak M., Johnstone C.M., Strachan P.A. (1998b): *Calibration Study – RMS95 Modules using JRC data.* Energy Systems Research Unit, University of Strathclyde.

Clarke J.A., Hand J.W., Janak M., Johnstone C.M., Strachan P.A. (1998c): *Calibration Study – RMS95 Modules using ITW data.* Energy Systems Research Unit, University of Strathclyde.

Clarke J.A., Hand J.W., Janak M., Johnstone C.M., Strachan P.A. (1998d): *Calibration Study – PST Semi-transparent Modules using TNO data.* Energy Systems Research Unit, University of Strathclyde.

Clarke J.A., Hand J.W., Janak M., Johnstone C.M., Strachan P.A. (1998e): *PV Modelling.* Energy Systems Research Unit, University of Strathclyde.

Cox C.H., Raghuraman P. (1985): Design considerations for flat-plate-photovoltaic / thermal collectors. *Solar Energy*, 33 (3) pp 227 – 241. Elsevier Science Ltd. London, UK.

Crick F.J., Wilshaw A., Pearsall N., Hynes K. Shaw M., Young G., Baker P. (1997): *Photovoltaic ventilated façade: system investigation and characterisation.* Proceedings - 14th European Photovoltaic Solar Energy Conference, Barcelona, Spain.

DETR (2000): *Energy Consumption Guide 19: Energy use in offices.* DETR, London, UK.

DOE (1994): *Introduction to Energy Efficiency in Further and Higher Education (EEB 5).* Department of the Environment. London, UK.

DTI (1997): *Photovoltaics in Buildings, A survey of design tools*. ETSU Report No S/P2/00289/REP for the Department of Trade and Industry.

DTLR (2002): *The Building Regulations 2000: Conservation of fuel and power – Approved Document L1*. The Department of Transport Local, Government and the Regions. The Stationary Office, London, UK.

DTLR (2002): *The Building Regulations 2000: Conservation of fuel and power – Approved Document L2*. The Department of Transport Local, Government and the Regions. The Stationary Office, London, UK.

Duffie J.A., Beckman W.A. (1991): *Solar Enginering of Thermal Processes*. Wiley Interscience. New York, USA.

EEBPp (2000a): *New Practice Case Study 114: The Inland Revenue Headquarters – Feedback for designers and clients*. The UK Government Energy Efficiency Best Practice Programme.

EEBPp (2000b): *New Practice Case Study 102: The Queens Building De Montfort University – Feedback for designers and clients*. The UK Government Energy Efficiency Best Practice Programme.

EEBPp (2000c): *New Practice Case Study 115: The Ionica Building, Cambridge – Feedback for designers and clients*. The UK Government Energy Efficiency Best Practice Programme.

Eicker U., Hoefker G., Seeberger, Fux V., Infield D. (1998): *Building integration of PV and solar air heaters for optimised heat and electricity production*. Proceedings – 2nd World Conference and Exhibition on Photovoltaic Solar Energy Conversion, Vienna.

Eicker U., Fux V., Infield D., Mei L., Vollmer K. (1999): *Thermal performance of building integrated ventilated PV facades*. Proceedings – ISES Solar World Congress, Vienna.

ESRU (2000): *The ESP-r system for building energy simulation: User guide version 9 series*. Energy Systems Research Unit. University of Strathclyde, Glasgow, UK.

European Parliament (2002): *Directive 2002/91/EC of The European Parliament and of The Council of 16th December 2002 on the energy performance of buildings*. Official Journal of the European Communities. The European Parliament and The Council of the European Union. Brussels, Belgium.

Florschuetz L.W. (1976): *Extension of the Hottel-Whillier-Bliss model to the analysis of combined photovoltaic / thermal flat plate collectors*. Conference Proceedings vol. 6, pp 79 - 92. 'Sharing the Sun', A joint conference of the American section of the International Solar Energy Society and the Solar Energy Society of Canada Inc., Winnipeg, USA.

Garg H.P., Adhikari R.S. (1997): Conventional hybrid photovoltaic / thermal (PV/T) air heating collectors: steady state simulation. *Renewable Energy*, 11 (3) pp 363 – 385. Elsevier Science Ltd. London, UK.

Garg H.P., Adhikari R.S. (1998): Transient simulation of conventional hybrid photovoltaic / thermal (PV/T) air heating collectors. *International Journal of Energy Research*, 22 pp 547 – 562. John Wiley & Sons Ltd, New York, USA.

Garg H.P., Adhikari R.S. (1999): System performance studies on a photovoltaic / thermal (PV/T) air heating collector. *Renewable Energy*, 16 pp 725 – 730. Elsevier Science Ltd. London, UK.

Gutschker O., Rogaβ H., Donath A., Häusler T., Maschke U., Dewitz W. (1996): *The thermal behaviour of a photovoltaic façade.* Conference Proceedings. Eurosun '96, Freiburg, Germany.

Hall K., Warm P. (1995): *Greener Building: Products and Services Directory.* Association for Environment Conscious Building, Llandysul, UK.

Hand J.W. (1998): *Removing barriers to the use of simulation in the building design professions*. PhD Thesis. Energy Systems Research Unit. University of Strathclyde, Glasgow, UK.

Hastings R.S. (2000): *Solar Air Systems: A Design Guide*. James & James (Science) Publishers, London, UK.

Hegazy A.A. (2000): Comparative study of the performances of four photovoltaic / thermal solar air collectors. *Energy Conversion & Management*, 41 pp 861 – 881. Elsevier Science Ltd. London, UK.

Hensen J.L.M. (1991): *On the thermal interaction of building structure and heating and ventilation system*. PhD Thesis. Energy Systems Research Unit.
University of Strathclyde, Glasgow, UK.

Hollick J.C. (1998): Solar cogeneration panels. Renewable Energy, 15 pp 195 – 200. Elsevier Science Ltd. London, UK.

Hottel H.C., Woertz B.B. (1942): *The performance of flat-plate solar-heat collectors.* Trans. ASME, 64, 91-104.

Hottel H.C., Whillier A. (1955): *Evaluation of flat-plate solar collector performance.* Trans. Of Conference - Use of Solar Energy, The Scientific Basis. Vol. II, Part 1, Section A, 74 – 104. University of Arizona.

Howard N., Shiers D., Sinclair M. (1998): *The Green Guide to Specification: An Environmental Profiling System for Building Materials and Components.* Building Research Establishment, Garston, UK.

Huang B.J., Lin T.H., Hung W.C., Sun F.S. (1999): *Solar photovoltaic / thermal co-generation collector.* Proceedings – ISES Solar World Congress, Jerusalem.

Huang B.J., Lin T.H., Hung W.C., Sun F.S. (2001): Performance evaluation of solar photovoltaic thermal systems. *Solar Energy*, 70 (5) pp 443 – 448. Elsevier Science Ltd. London, UK.

IEA (2001): *Trends in photovoltaic applications in selected IEA countries between 1992 and 2000.* Report IEA – PVPS T1 – 10:2001. International Energy Agency, Photovoltaic Power Systems Programme.

Infield D., Mei L., Eicker U., Fux V. (1999): *Undertanding the Potential of Ventilated PV Façades.* International Solar Energy Society: Solar World Congress, Jerusalem, Israel.

Infield D., Mei L., Eicker U., Fux V. (2000): *Parameter estimation for ventilated PV facades.* Proceedings – 16th European Photovoltaic Solar Energy Conference, Glasgow.

Jones A. D., Underwood C.P. (2001): A thermal model for photovoltaic systems. *Solar Energy*, vol 70 (4) pp 349-359. Published by Elsevier Science Limited, London, UK.

Jones D.L., Hattersley L., Ager R., Koyama A. (2000): *Photovoltaics in Buildings: BIPV Projects*. Report Number ETSU S/P2/00328/REP. Published by ETSU on behalf of the Department of Trade and Industry New & Renewable Energy Programme.

Jones D.L., Ruyssevelt P., Standeven M., Bates J. (1997): *Survey of tools for the design of photovoltaic power systems in buildings*. Report Number ETSU S/P2/00289/REP. Published by ETSU on behalf of the Department of Trade and Industry New & Renewable Energy Programme.

Kalogirou S.A. (2001): Use of TRNSYS for modelling and simulation of a hybrid pv-thermal solar system for Cyprus. *Renewable Energy*, 23 pp 247 – 260. Elsevier Science Ltd. London, UK.

Kays W.M., Crawford M.E. (1980): *Convective Heat and Mass Transfer*. 2nd Edition. McGraw-Hill. New York

Kazmerski L.L. (1997): Photovoltaics: A review of cell and module technologies. *Renewable and Sustainable Energy Reviews* vol 1(1/2) pp71–170. Published by Elsevier Science Limited, London, UK.

Kelly N.J. (1998): *Towards a design environment for building integrated energy systems: The integration of electrical power flow modelling with building simulation*. PhD Thesis. Energy Systems Research Unit. University of Strathclyde, Glasgow, UK.

Klein S.A. (1975): Calculation of flat-plate loss coefficients. *Solar Energy*, 17. Elsevier Science Ltd. London, UK.

Krauter S., Araujo R.G., Schroer S., Hanitsch R., Salmi M., Triebel C., Lemoine R. (1999): Combined photovoltaic and solar thermal systems for façade integration and building insulation. *Solar Energy*, 67 (4-6) pp 239 – 248. Elsevier Science Ltd. London, UK.

Lasnier L., Ang T.G. (1990): *Photovoltaic Engineering Handbook.* Asian Institute of Technology, Bangkok, Thailand. Published by Adam Hilger, Bristol, UK.

Leenders F., Van der Ree (1999): *Photovoltaic / Thermal systems: Workshop on PV/T systems.* Amersfoot, The Netherlands

Lloret A., Aceves O., Andreu J., Merten J., Puigdollers. Chantant M., Eicker U., Sabata L. (1997): *Lessons learned in the electrical system design, installation and operation of the Mataró public library.* Proceedings – 14th European Photovoltaic Solar Energy Conference, Barcelona, Spain.

Lomas K.J. (1991): Dynamic thermal simulation models: new method for empirical validation. Building Services Engineering Research and Technology, 12 (1) pp 25 – 37. The Chartered Institute of Building Services Engineers, Balham, London, UK.

Lorenzo E. (Ed.) (1994): *Solar Electricity – Engineering of Photovoltaic Systems.* Universidad Politecnica, Madrid, Spain. Published by Progensa, Seville, Spain.

Mazria E. (1979): *The Passive Solar Energy Book.* Rodale Press, Emmaus, USA.

Mei L., Infield D., Eicker U., Fux V. (2001): *Thermal Modelling for Building Integrated Ventilated PV Façade.* CIBSE National Conference, London.

Mei L., Infield D., Eicker U., Fux V. (2002): Parameter estimation for ventilated photovoltaic façades. *Building Services Engineering Research & Technology* **23**(2) 81-96. Published by Arnold on behalf of the Chartered Institute of Building Services Engineers, Balham, UK.

Mei L., Infield D., Eicker U., Fux V. (2003): Thermal modelling of a building with an integrated ventilated PV façade. *Energy and Buildings* **35**(6) 605-617. Elsevier Science Ltd. London, UK.

Meteotest (1999): *METEONORM Weather file generation software.* Meteotest, Bern, Switzerland.

Moshfegh B., Sandberg M. (1998): Flow and heat transfer in the air gap behind photovoltaic panels. *Renewable and Sustainable Energy Reviews*, 2 pp 287 – 301. Elsevier Science Ltd. London, UK.

Munro D., Ruyssevelt P., Bates J. (1998): *Testing, Commissioning and Monitoring Guide for Photovoltaic Power Systems in Buildings.* Report Number ETSU S/P2/00290/REP. Published by ETSU on behalf of the Department of Trade and Industry New & Renewable Energy Programme.

Oliver M., Jackson T. (2001): Energy and economic evaluation of building-integrated photovoltaics. *Energy*, vol 26, pp 431-439. Published by Elsevier Science Limited, London, UK.

Parkinson H., Wilczek J. (1999): *The DTI Solar Energy Programme and the role of solar PV in buildings.* Conference Proceedings. CIBSE National Conference. The Chartered Institute of Building Services Engineers, Balham, London, UK.

Peuser F.A., Remmers K.H., Schnauss M. (2002): *Solar thermal systems: successful planning and construction.* James & James (Science Publishers) Ltd., London, UK.

Prakash J. (1994): Transient analysis of a photovoltaic – thermal solar collector for co-generation of electricity and hot air / water. *Energy Conversion Management*, 35 (11) pp 967 – 972. Elsevier Science Ltd. London, UK.

Rawlings R.H.D. (1999): *Photovoltaics in Buildings – What do building services engineers need to know?*. Conference Proceedings. CIBSE National Conference. The Chartered Institute of Building Services Engineers, Balham, London, UK.

Roaf S., Fuentes M, Thomas S (2001): *Ecohouse: A design guide.* Architectural Press, Oxford, UK.

Rockendorf G., Sillmann R., Podlowski L., Litzenburger B. (1999): PV-Hybrid and thermoelectric collectors. *Solar Energy*, 67 (4-6) pp 227 – 237. Elsevier Science Ltd. London, UK.

Sandberg M., Moshfegh B. (1998): Ventilated solar roof air flow and heat transfer investigation. *Renewable Energy*, 15 pp 287 – 292. Elsevier Science Ltd. London, UK.

Sandberg M., Moshfegh B. (2002): Buoyancy-induced air flow in photovoltaic facades – effect of geometry of the air gap and location of solar cell modules. *Building and Environment*, 37 pp 211 – 218. Elsevier Science Ltd. London, UK.

Sandnes B., Rekstad J. (2002): A photovoltaic / thermal (PV/T) collector with a polymer absorber plate – experimental study and analytical model. *Solar Energy*, 72 (1) pp 63 – 73. Elsevier Science Ltd. London, UK.

Santamouris M., Asimakopoulis D. (1996): *Passive Cooling of Buildings*. James & James (Science Publishers) Ltd. London, UK.

SEL (2000): *TRNSYS – A Transient System Simulation Program*. Solar Energy Laboratory. University of Wisconsin – Madison.

Shankland N.J., Lomas K.J., Eppel H., Cartmell B.P. (2000): *Renewable energy technologies for a low-energy public building*. Eurosolar, Bonn. Conference proceedings.

Simmons A. (1996): *The electrical system and its interaction with the utility grid.* Conference Proceedings – UK ISES Conference C68 on Building Integrated Photovoltaic Systems, University of Northumbria, Newcastle, UK.

Smith B.J., Phillips G.M., Sweeney M. (1982): *Environmental Science*. Longman Scientific & Technical. Harlow, UK.

Sopian K., Yigit K.S., Liu T.H., Kakac S., Veziroglu T.N. (1996): Performance analysis of photovoltaic thermal air heaters. *Energy Conversion Management*, 37 (11), pp 1657 – 1670. Elsevier Science Ltd. London, UK.

SRCC (1995): *Solar Certification – Method for determining the thermal performance rating for solar collectors*. Solar Rating and Certification Corporation. Cocoa, Florida.

Thomas (Ed.) (2001): *Photovoltaics and Architecture*. Spon Press, London, UK.

Thomas R., Grainger T. (1999): *Photovoltaics in Buildings: A design Guide*. Report Number ETSU S/P2/00282/REP. Published by ETSU on behalf of the Department of Trade and Industry New & Renewable Energy Programme.

Transsolar (1998): *TRNSAIR Manual – An easy to use program to simulate solar air heating systems*. Energietechnik GmbH, Stuttgart, Germany.

Tripanagnostopoulos Y., Nousia T.H., Souliotis M., Yianoulis P. (2001): Hybrid photovoltaic / thermal solar systems. *Solar Energy*, 72 (3) pp 217 - 234. Elsevier Science Ltd. London, UK.

Twidell J.W., Weir A.D. (1986): *Renewable Energy Resources*. E & FN Spon, London, UK.

Vale B., Vale R. (2000): *The new autonomous house*. Thames & Hudson Ltd. London, UK.

Vandaele L., Wouters P., Bloem H. (1997): *Hybrid photovoltaic building components: Overall performance assessment by testing and simulation*. 14th European Photovoltaic Solar Energy Conference, Barcelona, Spain.

Vandaele L., Wouters P., Bloem H., Zaaiman W.J. (1998): *Combined heat and power from hybrid photovoltaic building integrated components – Results from overall performance assessment*. 2nd World Conference and Exhibition on Photovoltaic Solar Energy Conversion, Vienna, Austria.

Wenham S.R., Green M.A., Watt, M.E. (1994): *Applied Photovoltaics*. Published by Key Centre for Photovoltaic Engineering. University of New South Wales, Sydney, Australia.

Whillier A. (1967): Design factors influencing solar collector performance. Low temperature engineering application of solar energy, chapter III, 27-40. ASHRAE, New York.

Wilshaw A.R., Crick F.J., Pearsall N.M. (1997): *The effects of operating temperature on the performance of PV cladding systems.* Conference Proceedings. 14th European Photovoltaic Solar Energy Conference, Barcelona, Spain.

Wouters P., Vandaele L. (1998): *PV-HYBRID-PAS – Development of Procedures for Overall Performance Evaluation of Hybrid Photovoltaic Building Components – Final Report.* Belgian Building Research Institute, Brussels.

Yannas S. (1994): *Solar Energy and Housing Design – Volume 1: Principles, Objectives, Guidelines.* Architectural Association Publications. London, UK.

Zondag H.A., De Vries D.W., Van Helden W.G.J., Van Zolingen R.J.C., Van Steenhoven A.A. (2002): The thermal and electrical yield of a PV-Thermal collector. *Solar Energy*, 72 (2) pp 113 – 128. Elsevier Science Ltd. London, UK.

PAGE NUMBERING AS ORIGINAL

Appendix A - Component Description

A.1 TRNSYS Type Subroutines

A.1.1 Type 150 – PV/Thermal Solar Collector

A.1.2 Type 15 – Solar Air Collector

A.2 ESP-r Plant component input

A.2.1 PV/Thermal Solar Collector

A.1 TRNSYS Type Subroutines

A.1.1 Type 150 – PV/Thermal Solar Collector

```
SUBROUTINE TYPE150(TIME,XIN,OUT,T,DTDT,PAR,INFO,ICNTRL,*)

C       ************************************************************************
C       *
C       *       THIS COMPONENT SIMULATES THE THERMAL AND ELECTRICAL PERFORMANCE OF
C       *       A PV/THERMAL COLLECTOR. THE TYPE HAS BEEN DEVELOPED TO EXTEND THE
C       *       CAPABILITIES OF THE TYPE 50 PV/THERMAL SUBROUTINE, IN THAT THE
C       *       COLLECTOR CAN BE DECRIBED IN MORE PHYSICAL DETAIL, OUTPUTS CAN BE
C       *       CALCULATED TO COLLECTORS MOUNTED IN SERIES, LOSSES CAN BE CALCULATED
C       *       IN MORE DETAIL AND COLLECTOR EFFICIENCY FACTOR CAN BE CALCULATED IN
C       *       A TRANSIENT MANNER AS OPPOSED TO BEING STATED AS A PARAMETER IN
C       *       TYPE 50.
C       *
C       *       VERSION 1.0 BY B.CARTMELL
C       *       29TH OCTOBER 2001
C       *
C       ************************************************************************

C  STANDARD TRNSYS DECLARATIONS


        DOUBLE PRECISION XIN,OUT
        INTEGER*4 INFO
        DIMENSION XIN(6),OUT(18),PAR(17),INFO(15)

        CHARACTER*1 TRNEDT,PERCOM,HEADER,PRTLAB,LNKCHK,PRUNIT,IOCHEK,
  +                       PRWRN
        CHARACTER*3 YCHECK(6),OCHECK(18)

        DATA EG/0.88/,SB/5.678E-08/

        REAL FR,AC,TAUALF,UL,FLWRT,CP,IR,TIN,TA,QU,TOUT,LCPV,WCPV,DCPV,
  +     BIPV,SIPV,KI,EPV,EB,BR,TR,PF,NR,NCSPV,TS,WIND,NC,F,C,HWIND,AEW,
  +     AEE,AEM,ETAA,ETAR,TINC,TAC,TSC,STF1,STF2,UT,UB,UE,ITER,TPM,TFM,
  +     HR,DV,RE,NU,KA,H,FP1,DM,FP2,FIR,QE,NH,NE


   COMMON /LUNITS/ LUR,LUW,IFORM,LUK
        COMMON /SIM/ TINE0,TIMEF,DELT,IWARN
        COMMON /STORE/ NSTORE,IAV
        COMMON /CONFIG/ TRNEDT,PERCOM,HEADER,PRTLAB,LNKCHK,PRUNIT,IOCHEK,
  +                             PRWRN


C  SET THE VARIABLE TYPES FOR INPUTS AND OUTPUTS PRIOR TO CHECHING BY RCHECK

        DATA YCHECK/'TE1','TE1','PW2','VE1','TE1','MF2'/
        DATA OCHECK/'PW2','TE1','PW2','PC1','PC1','TE1','MF2','DM1','DM1',
  +                 'DM1','DM1','DM1','DM1','TE1','TE1','PW2','VE1','DM1'/

C  FIRST CALL OF SIMULATION

        IF (INFO(7).EQ.-1) THEN
                INFO(6)=18
                INFO(9)=0
                NUMIN=6
                NP=17
```

```
            CALL TYPECK(1,INFO,NUMIN,NP,0)
            CALL RCHECK(INFO,YCHECK,OCHECK)
        END IF

C   GET PARAMETERS

        NCSPV=PAR(1)
        LCPV=PAR(2)
        WCPV=PAR(3)
        DCPV=PAR(4)
        BIPV=PAR(5)
        SIPV=PAR(6)
        KI=PAR(7)
        CP=PAR(8)
        EPV=PAR(9)
        EB=PAR(10)
        SLOPE=PAR(11)
        BR=PAR(12)
        TR=PAR(13)
        PF=PAR(14)
        NR=PAR(15)
        TAU=PAR(16)
        ALF=PAR(17)

C   CREATION OF PHYSICAL VARIABLES FROM PARAMETERS AND CONVERSION TO APPROPRIATE UNITS
C   PARS 4,5,6 CONVERTED TO METERS


        DCPV1=DCPV*1E-03
        BIPV1=BIPV*1E-03
        SIPV1=SIPV*1E-03
        AC=LCPV*WCPV
        AEW=(2*(DCPV1*LCPV))+(2*(DCPV1*WCPV))
        AEE=2*(DCPV1*LCPV)+(DCPV1*WCPV)
        AEM=2*(DCPV1*LCPV)
        AF=(WCPV-(2*SIPV1))*(DCPV1-BIPV1)
        DH=2*(DCPV1-BIPV1)
        ETAR=NR*PF
        TAUALF=TAU*ALF

C   GET INPUTS

        TIN=XIN(1)
        TA=XIN(2)
        IR=XIN(3)
        WIND=XIN(4)
        TS=XIN(5)
        FLWRT=XIN(6)

C   CONVERT T INPUTS TO DEGREES K

        TINC=TIN+273.15
        TAC=TA+273.15
        TSC=TS+273.15

C   CALCULATION OF COLLECTOR TOP LOSSES
C   F AND C FUNCTIONS REQUIRED BY THE KLEIN FORMULA. WIND CONVERTED TO A WIND HEAT
C   TRANSFER COEFFICIENT

        NC=1
        F=(1.0+0.089*HWIND-0.1166*HWIND*EPV)*(1+0.07866*NC)
        C=520*(1.0-0.000051*(SLOPE*SLOPE))
        HWIND=5.7+3.8*WIND

C   KLEIN FORMULA FOR TOP LOSSES (SUBSTITUTING TS FOR TA IN RADIATIVE SECTION)
        DELTAT=TINC-TAC
        IF (DELTAT.LT.1.0E-9) THEN
```

```
                DELTAT=1.0E-9
        END IF
        STF1=((DELTAT)/(NC+F))**0.33
        STF1=(C/TINC)*STF1
        STF1=NC/STF1+1.0/HWIND
        STF1=1.0/STF1
        STF2=EPV+0.00591*NC*HWIND
        STF2=1.0/STF2
        STF3=(2*NC+F-1+0.133*EPV)/EG
        STF3=STF2+STF3-NC
        STF4=SB*(TINC+TAC)*(TINC*TINC+TAC*TAC)
        STF4=STF4/STF3
        UT=(STF1+STF4)

C   BACK LOSSES

        UB=KI/BIPV1

C   EDGE LOSSES CALCULATED FOR A SINGLE COLLECTOR

        UE=(KI/SIPV1)*AEW/AC

C   CALCULATION OF OVERALL HEAT LOSS COEFFICIENT AND FLORSCHUTZ EXTENSION TO UL

        UL=UT+UB+UE

C   RADIATIVE HEAT TRANSFER COEFFICIENT - 5 ITERATIONS SPECIFIED FOR THE FOLLOWING FORMULAS

        ITER=1
        TPM=0
        TFM=0
10      CONTINUE

C   ON FIRST ITERATION TPM IS ASSUMED AT TIN+10 DEGREES C

        IF (ITER.EQ.1.0) THEN
                TPM=TIN+10
        END IF

        TPM1=TPM+273.15
        HR1=(1/EPV)+(1/EB)
        HR2=HR1-1
        HR=4*SB*(TPM1*TPM1*TPM1)/HR2


C   CALCULATION OF DYNAMIC VISCOSITY

        IF (ITER.EQ.1.0) THEN
          TFM=TIN+10
        END IF

C   CALCULATION OF FLUID DYNAMIC VISCOSITY AT SPECIFIC FLUID TEMPERATURE

        IF (TFM.LT.0) THEN
                DV=1.705*10E-06
        ELSE IF (TFM.GE.0.0.AND.TFM.LT.20.0) THEN
                DV=1.705*10E-06
        ELSE IF (TFM.GE.20.0.AND.TFM.LT.40.0) THEN
                DV=1.815*10E-06
        ELSE IF (TFM.GE.40.0.AND.TFM.LT.60.0) THEN
                DV=1.905*10E-06
        ELSE IF (TFM.GE.60.0.AND.TFM.LT.80.0) THEN
                DV=1.982*10E-06
        ELSE IF (TFM.GE.80.0.AND.TFM.LE.100.0) THEN
                DV=2.065*10E-06
        ELSE IF (TFM.GE.100.0.AND.TFM.LT.120.0) THEN
                DV=2.185*10E-06
```

```
        ELSE
                DV=2.320*10E-06
        END IF


C   CALCULATION OF REYNOLDS NUMBER
        DEN=(FLWRT*DH)/(AF*DV)
        DEN1=DEN**0.8
        RE1=FLWRT*DH/(AF*DV)
        RE=RE1**0.8

C   CALCULATION OF NUSSELT NUMBER

        NU=0.0158*RE

C   CALCULATION OF CONVECTIVE/FILM HEAT TRANSFER COEFFICIENT FROM THE DUCT SURFACES

        KA=TFM*7.357*10E-06+0.0242
        H=NU*KA/DH

C   REQUIRED BY THE FLORSCHUTZ EXTENSION TO THE HWB MODEL - THE FOLLOWING CALCULATES THE
C   REDUCTION IN POWER OUTPUT AS A RESULT OF INCREASE IN CELL TEMPERATURE

        ETAA=ETAR*(1.0-BR*(TR-TPM))
        ETAAA=ETAR*(1.0-BR*(TA-TR))
        ULF=UL-TAUALF*IR*ETAA*BR
        ULF1=UL-TAUALF*IR*ETAAA*BR

C   CALCULATION OF COLLECTOR EFFICIENCY FACTOR

        FP1=(1.0/H)+(1.0/HR)
        FP1=(1.0/FP1)+H
        FP1=(ULF/FP1)+1.0
        FP1=1.0/FP1

C   CALCULATION OF DIMENSIONLESS COLLECTOR MASS FLOW RATE

        DM=(FLWRT*CP)/(AC*UL*FP1)

C   CALCULATION OF COLLECTOR FLOW FACTOR

        FP2=DM*(1.0-EXP(-1.0/DM))

C   CALCULATION OF OVERALL COLLECTOR HEAT REMOVAL FACTOR

        FR1=(-ULF*FP1)/(FLWRT*CP)
        FR=(FLWRT*CP/ULF)*(1.0-EXP(FR1))


C   FLORSCHUTZ ALTERATION OF SOLAR RADIATION

        FIR=IR*(1.0-ETAA/ALF)


C   HWB EQUATION FOR USEFUL GAIN FROM COLLECTOR

        QU=AC*FR*(FIR*TAUALF-ULF*(TIN-TA))

C   ELECTRICAL OUTPUT OF THE COLLECTOR

        IR2=IR*(1-ETAAA/ALF)
        QE=1.0-((NR*PF*BR/ETAA)*((FR*(TIN-TA)+((IR2/ULF1)*(1.0-FR)))))
        QE=(AC*IR*ETAA/ALF)*QE


C   OUTPUT TEMPERATURE FROM THE COLLECTOR
```

```
      TOUT=QU/(FLWRT*CP)+TIN

C  MEAN PLATE TEMPERATURE

      TPM=((QU/AC)/(UL*FR))*(1.0-FR)+TIN

C  MEAN FLUID TEMPERATURE

      TFM=((QU/AC)/(UL*FR))*(1.0-FP2)+TIN

C  ITERATE 5 TIMES

      ITER=ITER+1.0
      IF (ITER.LT.6.0) THEN
            GO TO 10
      END IF

C  COLLECTOR EFFICIENCIES OUTPUT GENERATION
C  HEAT REMOVAL EFFICIENCY

      IF (IR.EQ.0) THEN
            IR=1
      END IF
      NH=QU/(AC*IR)


C  ELECTRICAL EFFICIENCY


      NE=QE/(AC*IR)


C  OUTPUT DESIGNATION

      OUT(1)=QU
      OUT(2)=TOUT
      OUT(3)=QE
      OUT(4)=NH
      OUT(5)=NE
      OUT(6)=TPM
      OUT(7)=FLWRT
      OUT(8)=UL
      OUT(9)=FP1
      OUT(10)=FR
      OUT(11)=H
      OUT(12)=HR
      OUT(13)=RE1
      OUT(14)=TA
      OUT(15)=TS
      OUT(16)=IR
      OUT(17)=WIND
      OUT(18)=ETAA


      RETURN 1

      END
```

A.1.2 Type 151 – Solar Air Collector

```
      SUBROUTINE TYPE151(TIME,XIN,OUT,T,DTDT,PAR,INFO,ICNTRL,*)

C     ************************************************************************
C     *
C     *       SOLAR AIR COLLECTOR
C     *
C     *       THIS COMPONENT SIMULATES THE THERMAL PERFORMANCE OF
C     *       A SOLAR AIR COLLECTOR. THE TYPE HAS BEEN DEVELOPED TO EXTEND THE
C     *       CAPABILITIES OF THE TYPE 73 SOLAR COLLECTOR SUBROUTINE, IN THAT THE
C     *       COLLECTOR CAN BE DECRIBED IN MORE PHYSICAL DETAIL, OUTPUTS CAN BE
C     *       CALCULATED TO COLLECTORS MOUNTED IN SERIES, LOSSES CAN BE CALCULATED
C     *       IN MORE DETAIL AND COLLECTOR EFFICIENCY FACTOR CAN BE CALCULATED IN
C     *       A TRANSIENT MANNER AS OPPOSED TO BEING STATED AS A PARAMETER IN
C     *       TYPE 73.
C     *
C     *       VERSION 1.0 BY B.CARTMELL
C     *       13TH NOVEMBER 2001
C     *
C     ************************************************************************

C  STANDARD TRNSYS DECLARATIONS


      DOUBLE PRECISION XIN,OUT
      INTEGER*4 INFO
      DIMENSION XIN(6),OUT(16),PAR(18),INFO(15)

      CHARACTER*1 TRNEDT,PERCOM,HEADER,PRTLAB,LNKCHK,PRUNIT,IOCHEK,
     +            PRWRN
      CHARACTER*3 YCHECK(6),OCHECK(16)

      DATA EG/0.88/,SB/5.678E-08/,EP/0.9/

      REAL FR,AC,TAUALF,UL,FLWRT,CP,IR,TIN,TA,QU,TOUT,LCPV,WCPV,DCPV,
     +     BIPV,SIPV,KI,EPV,EB,BR,TR,PF,NR,NCSPV,TS,WIND,NC,F,C,HWIND,AEW,
     +     AEE,AEM,ETAA,ETAR,TINC,TAC,TSC,STF1,STF2,UT,UB,UE,ITER,TPM,TFM,
     +     HR,DV,RE,NU,KA,H,FP1,DM,FP2,FIR,QE,NH,NE


   COMMON /LUNITS/ LUR,LUW,IFORM,LUK
      COMMON /SIM/ TINE0,TIMEF,DELT,IWARN
      COMMON /STORE/ NSTORE,IAV
      COMMON /CONFIG/ TRNEDT,PERCOM,HEADER,PRTLAB,LNKCHK,PRUNIT,IOCHEK,
     +                PRWRN


C  SET THE VARIABLE TYPES FOR INPUTS AND OUTPUTS PRIOR TO CHECHING BY RCHECK

      DATA YCHECK/'TE1','MF2','TE1','PW2','VE1','TE1'/
      DATA OCHECK/'PW2','TE1','PC1','TE1','ME2','DM1','DM1',
     +            'DM1','DM1','DM1','DM1','TE1','TE1','PW2','VE1','TE1'/

C  FIRST CALL OF SIMULATION

      IF (INFO(7).EQ.-1) THEN
            INFO(6)=16
            INFO(9)=0
            NUMIN=6
            NP=18
            CALL TYPECK(1,INFO,NUMIN,NP,0)
            CALL RCHECK(INFO,YCHECK,OCHECK)
```

```
      END IF

C  GET PARAMETERS

      POSSA=PAR(1)
      LCSA=PAR(2)
      WCSA=PAR(3)
      DCSA=PAR(4)
      BISA=PAR(5)
      SISA=PAR(6)
      KI=PAR(7)
      CP=PAR(8)
      EB=PAR(9)
      SLOPE=PAR(10)
      W2=PAR(11)
      W=PAR(12)
      YP=PAR(13)
      YF=PAR(14)
      KPF=PAR(15)
      TAU=PAR(16)
      ALF=PAR(17)
      NC=PAR(18)

C  CREATION OF PHYSICAL VARIABLES FROM PARAMETERS AND CONVERSION TO APPROPRIATE UNITS
C  PARS 4,5,6 CONVERTED TO METERS


      DCSA1=DCSA*1E-03
      BISA1=BISA*1E-03
      SISA1=SISA*1E-03
      W21=W2*1E-03
      W1=W*1E-03
      YP1=YP*1E-03
      YF1=YF*1E-03
      AC=LCSA*WCSA
      AEW=(2*(DCSA1*LCSA))+(2*(DCSA1*WCSA))
      AEE=2*(DCSA1*LCSA)+(DCSA1*WCSA)
      AEM=2*(DCSA1*LCSA)
      AF=(WCSA-(2*SISA1))*(DCSA1-BISA1)
      DH=2*(DCSA1-BISA1)
      TAUALF=TAU*ALF

C  GET INPUTS

      TIN=XIN(1)
      FLWRT=XIN(2)
      TA=XIN(3)
      IR=XIN(4)
      WIND=XIN(5)
      TS=XIN(6)

C  CONVERT T INPUTS TO DEGREES K

      TINC=TIN+273.15
      TAC=TA+273.15
      TSC=TS+273.15

C  CALCULATION OF COLLECTOR TOP LOSSES
C  F AND C FUNCTIONS REQUIRED BY THE KLEIN FORMULA. WIND CONVERTED TO A WIND HEAT
C  TRANSFER COEFFICIENT


      F=(1.0-0.04*WIND+5.0E-04*WIND*WIND)*(1.0+0.091*NC)
      C=365.9*(1.0-0.0083*SLOPE+0.0001298*SLOPE*SLOPE)
      HWIND=5.7+3.8*WIND

C  KLEIN FORMULA FOR TOP LOSSES (SUBSTITUTING TS FOR TA IN RADIATIVE SECTION)
```

```
      DELTAT=TINC-TAC
      IF (DELTAT.LT.1.0E-9) THEN
            DELTAT=1.0E-9
      END IF
      STF1=C/TINC*((DELTAT)/(NC+F))**0.33
      STF1=NC/STF1+1.0/HWIND
      STF1=1.0/STF1
      STF2=1.0/(EP+0.05*NC*(1.0-EP))+(2.0*NC+F-1.0)/EG-NC
      STF2=SB*(TINC*TINC+TSC*TSC)*(TINC+TSC)/STF2
      UT=(STF1+STF2)*3.6

C  BACK LOSSES

      UB=KI/BISA1

C  EDGE LOSSES CALCULATED FOR A SINGLE COLLECTOR

      IF (POSSA.EQ.1) THEN
            GO TO 5
      ELSE IF (POSSA.EQ.2) THEN
            GO TO 6
      END IF
      GO TO 7

5     CONTINUE
      UE=(KI/SISA1)*AEW/AC
      GO TO 8

6     CONTINUE
      UE=(KI/SISA1)*AEM/AC
      GO TO 8

7     CONTINUE
      UE=(KI/SISA1)*AEE/AC

8     CONTINUE

C  CALCULATION OF OVERALL HEAT LOSS COEFFICIENT AND FLORSCHUTZ EXTENSION TO UL

      UL=UT+UB+UE


C  RADIATIVE HEAT TRANSFER COEFFICIENT - 5 ITERATIONS SPECIFIED FOR THE FOLLOWING FORMULAS

      ITER=1
      TPM=0
      TFM=0
10    CONTINUE

C  ON FIRST ITERATION TPM IS ASSUMED AT TIN+10 DEGREES C

      IF (ITER.EQ.1.0) THEN
            TPM=TIN+10
      END IF

      TPM1=TPM+273.15
      HR=(1/EB)+(1/EB)
      HR=HR-1
      HR=4*SB*(TPM1*TPM1*TPM1)/HR

C  CALCULATION OF DYNAMIC VISCOSITY

      IF (ITER.EQ.1.0) THEN
        TFM=TIN+10
      END IF

C  CALCULATION OF FLUID DYNAMIC VISCOSITY AT SPECIFIC FLUID TEMPERATURE
```

```
      IF (TFM.LT.0) THEN
            DV=1.705*10E-06
      ELSE IF (TFM.GE.0.0.AND.TFM.LT.20.0) THEN
            DV=1.705*10E-06
      ELSE IF (TFM.GE.20.0.AND.TFM.LT.40.0) THEN
            DV=1.815*10E-06
      ELSE IF (TFM.GE.40.0.AND.TFM.LT.60.0) THEN
            DV=1.905*10E-06
      ELSE IF (TFM.GE.60.0.AND.TFM.LT.80.0) THEN
            DV=1.982*10E-06
      ELSE IF (TFM.GE.80.0.AND.TFM.LE.100.0) THEN
            DV=2.065*10E-06
      ELSE IF (TFM.GE.100.0.AND.TFM.LT.120.0) THEN
            DV=2.185*10E-06
      ELSE
            DV=2.320*10E-06
      END IF


C     CALCULATION OF REYNOLDS NUMBER
      DEN=(FLWRT*DH)/(AF*DV)
      DEN1=DEN**0.8
      RE1=FLWRT*DH/(AF*DV)
      RE=RE1**0.8

C     CALCULATION OF NUSSELT NUMBER

      NU=0.0158*RE

C     CALCULATION OF CONVECTIVE/FILM HEAT TRANSFER COEFFICIENT FROM THE DUCT SURFACES

      KA=TFM*7.357*10E-06+0.0242
      H=NU*KA/DH

C     CALCULATION OF COLLECTOR EFFICIENCY FACTOR

      FP1=(1.0/H)+(1.0/HR)
      FP1=(1.0/FP1)+H
      FP1=(UL/FP1)+1.0
      FP1=1.0/FP1

C     EXTENSION TO FP1 TO INCORPORATE FINNED SURFACES WITHIN THE AIRSTREAM
C     CALCULATION OF FIN EFFICIENCY OF FIN

      M1=SQRT(H/(KPF*YF1))

      FF=(TANH(W21*M1))/(W21*M1)

C     CALCULATION OF FIN EFFICIENCY OF PLATE

      M2=SQRT(H/(KPF*YP1))

      FP=(TANH(W1*M2))/(W1*M2)

      F10=(FP1/FP)+((W1*H)/(2*W21*H*FF))
      F10=((1-FP1)/F10)+1
      F10=FP1*F10

C     CALCULATION OF DIMENSIONLESS COLLECTOR MASS FLOW RATE

      DM=(FLWRT*CP)/(AC*UL*FP1)

C     CALCULATION OF COLLECTOR FLOW FACTOR

      FP2=DM*(1.0-EXP(-1.0/DM))
```

```
C   CALCULATION OF OVERALL COLLECTOR HEAT REMOVAL FACTOR

        FR=F10*FP2

C   HWB EQUATION FOR USEFUL GAIN FROM COLLECTOR

        QU=AC*FR*(IR*TAUALF-UL*(TIN-TA))

C   OUTPUT TEMPERATURE FROM THE COLLECTOR

        TOUT=QU/(FLWRT*CP)+TIN

C   MEAN PLATE TEMPERATURE

        TPM=((QU/AC)/(UL*FR))*(1.0-FR)+TIN

C   MEAN FLUID TEMPERATURE

        TFM=((QU/AC)/(UL*FR))*(1.0-FP2)+TIN

C   ITERATE 5 TIMES

        ITER=ITER+1.0
        IF (ITER.LT.6.0) THEN
                GO TO 10
        END IF

C   HEAT REMOVAL EFFICIENCY

        IF (IR.EQ.0) THEN
                IR=1
        END IF
        NH=QU/(AC*IR)

C       PLACE TOUT IN INFO(12) FOR RECIRCULATION PURPOSES

        INFO(12)=TOUT
        TEST=INFO(12)

C   OUTPUT DESIGNATION

        OUT(1)=QU
        OUT(2)=TOUT
        OUT(3)=NH
        OUT(4)=TPM
        OUT(5)=FLWRT
        OUT(6)=UL
        OUT(7)=F10
        OUT(8)=FR
        OUT(9)=H
        OUT(10)=HR
        OUT(11)=RE1
        OUT(12)=TA
        OUT(13)=TS
        OUT(14)=IR
        OUT(15)=WIND
        OUT(16)=TEST

        RETURN 1
        END
```

A.2 ESP-r Plant component input

To install the following components within ESP-r, the following subroutines need to be installed within the designated source code file before rebuilding ESP-r programme. The plant component database then needs to be updated with a new component that reads code 740 (this number is used for the following subroutines but may be changed as long as the new number is not used by a previously installed component).

A.2.1 PV/Thermal Solar Collector

The following subroutine needs to be installed within file /usr/esru/src/esp-r/esruplt/pcomp3.for.

```
C ******************** CMP74C ********************

C CMP74C generates for plant component IPCOMP with plant db code 740 ie.
C 1 node (ISV=21) Theoratical flat-plate PV/T solar collector
C
C Rate of heat qain is calculated using TRNSYS type150 PV/T solar collector
C developed by B.Cartmell during PhD researc. This routine calls TRNSYS Type 16
C to calculate radiation on the inclined collector surface
C
C Matrix equation coefficients COUT (in order: self-coupling, cross-
C coupling, and present-time coefficients) for energy balance (ISTATS=1),
C 1st phase mass balance (ISTATS=2), or 2nd phase mass (ISTATS=3)
C
C   ADATA: 1 Component total mass (kg)
C          2 Mass weighted average specific heat (J/kgK)
C          3 UA modulus (W/K)
C   BDATA: 1 Radiation mode (-)
C          2 Tracking mode (-)
C          3 Latitude (degrees)
C          4 Shift in solar time hour angle (degrees)
C          5 Ground reflectance (-)
C          6 Slope of surface or tracking axis (degrees)
C          7 Azimuth of surface or tracking axis (degrees)
C          8 Position of collector in series (-)
C          9 Length of PV collector (m)
C         10 Width of PV collector (m)
C         11 Depth of collector (mm)
C         12 Thickness of back insulation (mm)
C         13 Thickness of side insulation (mm)
C         14 Thermal conductivity of insulation (W/mK)
C         15 Fluid thermal capacitance (J/KgK)
C         16 Emitance of PV (-)
C         17 Emittance of back plate (-)
C         18 Temperature coefficient of cell efficiency (-)
C         19 Temperature of cell reference efficiency (C)
C         20 Cell Packing factor (-)
C         21 Local cell efficiency at reference temperature (-)
C         22 Transmittance of cover system (-)
C         23 Plate absorptance (-)
C         24 Height over sea level (m)
C         25 Flow rate correction factor (-)
C         26 Number of collectors in parallel (-)


      SUBROUTINE CMP74C(IPCOMP,COUT,ISTATS)
#include "plant.h"
#include "building.h"

      COMMON/OUTIN/IUOUT,IUIN
```

```
      COMMON/TC/ITC,ICNT
      COMMON/TRACE/ITCF,ITRACE(MTRACE),IZNTRC(MCOM),ITU

      COMMON/SIMTIM/IHRP,IHRF,IDYP,IDYF,IDWP,IDWF,NSINC,ITS
      COMMON/Pctime/TIMSEC
      COMMON/PTIME/PTIMEP,PTIMEF
      COMMON/PCTC/TC(MPCOM)

      COMMON/PCEQU/IMPEXP,RATIMP
      COMMON/PITER/MAXITP,PERREL,PERTMP,PERFLX,PERMFL,itrclp,
     &      ICSV(MPNODE,MPVAR),CSVI(MPNODE,MPVAR)

      COMMON/C9/NPCOMP,NCI(MPCOM),CDATA(MPCOM,MMISCD)
      COMMON/C10/NPCON,IPC1(MPCON),IPN1(MPCON),IPCT(MPCON),
     &      IPC2(MPCON),IPN2(MPCON),PCONDR(MPCON),PCONSD(MPCON,2)
      COMMON/C12PS/NPCDAT(MPCOM,9),IPOFS1(MCOEFG),IPOFS2(MCOEFG,MPVAR)
      COMMON/PDBDT/ADATA(MPCOM,MADATA),BDATA(MPCOM,MBDATA)
      COMMON/PCVAL/CSVF(MPNODE,MPVAR),CSVP(MPNODE,MPVAR)
      COMMON/PCVAR/PCTF(MPCON),PCRF(MPCON),PUAF(MPNODE),PCQF(MPNODE),
     &      PCNTMF(MPCOM),
     &      PCTP(MPCON),PCRP(MPCON),PUAP(MPNODE),PCQP(MPNODE),
     &      PCNTMP(MPCOM)
      COMMON/PCOND/CONVAR(MPCON,MCONVR),ICONTP(MPCON),
     &      ICONDX(MPCOM,MNODEC,MPCONC)
      COMMON/PCDAT/PCDATF(MPCOM,MPCDAT),PCDATP(MPCOM,MPCDAT)

      common/simsdy/iss,isf
      COMMON/CLIM/IDIF(MT),ITMP(MT),IDNR(MT),IVEL(MT),IDIR(MT),
     &IHUM(MT),IDIFF,ITMPF,IDNRF,IVELF,IDIRF,IHUMF
      COMMON/CLIMIP/QFPP,QFFP,TPP,TFP,QDPP,QDFP,VPP,VFP,DPP,DFP,HPP,HFP

      DIMENSION XIN(15),PAR(15),OUT(21),INFO(10),sav1(20)

      PARAMETER (SMALL=1.0E-15)
      REAL    COUT(MPCOE)
      character outs*124
      logical closea,closeb
      data time/0.0/,info1/0/,info16/0/
            DATA EG/0.88/,SB/5.678E-08/

C Trace output
      IF(ITC.GT.0.AND.NSINC.GE.ITC.AND.NSINC.LE.ITCF.AND.
     &  ITRACE(37).NE.0) WRITE(ITU,*) ' Entering subroutine CMP74C'

C Initialize pointers to inter-connection(s) ICON, and node(s) INOD
      ICON1=ICONDX(IPCOMP,1,1)
      INOD1=NPCDAT(IPCOMP,9)

C Generate coefficients for energy balance equation
      IF(ISTATS.EQ.1) THEN

C First initialize UA modulus (for calculation of containment heat loss)
        UA=ADATA(IPCOMP,3)
        call eclose(PCNTMF(IPCOMP),-99.00,0.001,closea)
        IF(closea) UA=0.

C Now calculate heat gain Q using single node model and
C TRNSYS type1 component, unless water mass flow rate is zero.

C First mark water temperature for iteration.
        ICSV(INOD1,1)=1
        CSVI(INOD1,1)=CSVF(INOD1,1)
        call eclose(CONVAR(ICON1,2),0.00,0.0001,closeb)
        IF(closeb) THEN
          Q=0.
        ELSE
```

```
C If at start of simulation, initialise array info.
      call eclose(ptimep,1.00,0.0001,closea)
      if(closea.and.idyp.eq.iss) then

C Set arbitrary unit number
        info(1)=1

C Set initialisation flag for types 1 & 16.
        info16=-1
        info1 =-1
        ptim=ptimep
        time=ptimep
        qt=0.0
      endif

C Calculate absolute simulation time.
C and time-step, hour fraction format
        delt=timsec/3600.
        call eclose(ptim,ptimep,0.0001,closeb)
        if(.NOT.closeb) time=time+delt

C Now call type16 solar radiation processor to calculate solar
C radiation components for solar collector.
C So setup interface parameters for type16 first..
        par(1)=bdata(ipcomp,1)
        par(2)=bdata(ipcomp,2)
        par(3)=iss
        par(4)=bdata(ipcomp,3)
        par(5)=SC*3600./1000.
        par(6)=bdata(ipcomp,4)
        par(7)=0.0

C Assume calculation start time =0.0
        time0=1.0

C Calculate final time
        tfinal=(float(isf)-float(iss)+1.0)*24.0


C Set up input parameters. The first input is the
C radiation on horizontal surface (KJ/hr-m^2). Not sure
C if this is how it is calculated.!! (essam).
        xin(1)=float(IDIF(ihrp)+IDNR(ihrp))*3600.0/1000.0

C Time of last radiation data reading.
        xin(2)=float(ihrp)

C Time of next radiation data reading.
        xin(3)=float(ihrf)
        xin(4)=bdata(ipcomp,5)
        xin(5)=bdata(ipcomp,6)
        xin(6)=bdata(ipcomp,7)

C Set value of INFO(7) accoringly to indicate
C whether this is first call of TRNSYS type.
        info(7)=info16

C This statement means that radiation components
C are required for one surface. (see type16).
        info(3)=8

C Call type16.
        call type16(time,xin,out,time0,tfinal,delt,par,info,iuout)

C Get Type 150 Parameters

            POSPV=bdata (ipcomp,8)
```

```
      LCPV=bdata(ipcomp,9)
      WCPV=bdata(ipcomp,10)
      DCPV=bdata(ipcomp,11)
      BIPV=bdata(ipcomp,12)
      SIPV=bdata(ipcomp,13)
      KI=bdata(ipcomp,14)
      CP=bdata(ipcomp,15)
      EPV=bdata(ipcomp,16)
      EB=bdata(ipcomp,17)
      SLOPE=bdata(ipcomp,18)
      BR=bdata(ipcomp,19)
      TR=bdata(ipcomp,20)
      PF=bdata(ipcomp,21)
      NR=bdata(ipcomp,22)
      TAU=bdata(ipcomp,23)
      ALF=bdata(ipcomp,24)
      HOSL=bdata(ipcomp,25)
      NPARA=bdata(ipcomp,26)

C Creation of physical variables from parameters and conversion to appropriate units
C Pars 4,5,6 converted to meters

      DCPV1=DCPV*1E-03
      BIPV1=BIPV*1E-03
      SIPV1=SIPV*1E-03
      AC=LCPV*WCPV
      AEW=(2*(DCPV1*LCPV))+(2*(DCPV1*WCPV))
      AEE=2*(DCPV1*LCPV)+(DCPV1*WCPV)
      AEM=2*(DCPV1*LCPV)
      AF=(WCPV-(2*SIPV1))*(DCPV1-BIPV1)
      DH=2*(DCPV1-BIPV1)
      ETAR=NR*PF
      TAUALF=TAU*ALF

C Get inputs

      TIN=CSVF(INOD1,1)
      TA=TFP
      E_DIR=OUT(7)
      E_DIF=OUT(8)
      WVEL+IVEL(IHRF)
      FLWRT=CONVAR(ICON1,2)

      FLWRT=FLWRT*FCF
      WIND=0.1*WVEL

C   CONVERT T INPUTS TO DEGREES K

      TINC=TIN+273.15
      TAC=TA+273.15


C   CALCULATION OF COLLECTOR TOP LOSSES
C   F AND C FUNCTIONS REQUIRED BY THE KLEIN FORMULA. WIND CONVERTED TO A WIND HEAT
C   TRANSFER COEFFICIENT

      NC=1
      F=(1.0+0.089*HWIND-0.1166*HWIND*EPV)*(1+0.07866*NC)
      C=520*(1.0-0.000051*(SLOPE*SLOPE))
      HWIND=5.7+3.8*WIND

C   KLEIN FORMULA FOR TOP LOSSES (SUBSTITUTING TS FOR TA IN RADIATIVE SECTION)
      DELTAT=TINC-TAC
      IF (DELTAT.LT.1.0E-9) THEN
            DELTAT=1.0E-9
      END IF
      STF1=((DELTAT)/(NC+F))**0.33
```

```
      STF1=(C/TINC)*STF1
      STF1=NC/STF1+1.0/HWIND
      STF1=1.0/STF1
      STF2=EPV+0.00591*NC*HWIND
      STF2=1.0/STF2
      STF3=(2*NC+F-1+0.133*EPV)/EG
      STF3=STF2+STF3-NC
      STF4=SB*(TINC+TAC)*(TINC*TINC+TAC*TAC)
      STF4=STF4/STF3
      UT=(STF1+STF4)

C  BACK LOSSES

      UB=KI/BIPV1

C  EDGE LOSSES CALCULATED FOR A SINGLE COLLECTOR

      UE=(KI/SIPV1)*AEW/AC

C  CALCULATION OF OVERALL HEAT LOSS COEFFICIENT AND FLORSCHUTZ EXTENSION TO UL

      UL=UT+UB+UE


C  RADIATIVE HEAT TRANSFER COEFFICIENT - 5 ITERATIONS SPECIFIED FOR THE FOLLOWING FORMULAS

      ITER=1
      TPM=0
      TFM=0
10    CONTINUE

C  ON FIRST ITERATION TPM IS ASSUMED AT TIN+10 DEGREES C

      IF (ITER.EQ.1.0) THEN
            TPM=TIN+10
      END IF

      TPM1=TPM+273.15

      HR1=2/(EPV+EB)
      HR2=HR1-1
      HR=4*SB*(TPM1*TPM1*TPM1)/HR2

C  CALCULATION OF DYNAMIC VISCOSITY

      IF (ITER.EQ.1.0) THEN
        TFM=TIN+10
      END IF

C  CALCULATION OF FLUID DYNAMIC VISCOSITY AT SPECIFIC FLUID TEMPERATURE

      IF (TFM.LT.0) THEN
            DV=1.705*10E-06
      ELSE IF (TFM.GE.0.0.AND.TFM.LT.20.0) THEN
            DV=1.705*10E-06
      ELSE IF (TFM.GE.20.0.AND.TFM.LT.40.0) THEN
            DV=1.815*10E-06
      ELSE IF (TFM.GE.40.0.AND.TFM.LT.60.0) THEN
            DV=1.905*10E-06
      ELSE IF (TFM.GE.60.0.AND.TFM.LT.80.0) THEN
            DV=1.982*10E-06
      ELSE IF (TFM.GE.80.0.AND.TFM.LE.100.0) THEN
            DV=2.065*10E-06
      ELSE IF (TFM.GE.100.0.AND.TFM.LT.120.0) THEN
            DV=2.185*10E-06
      ELSE
            DV=2.320*10E-06
```

```
      END IF

C  CALCULATION OF REYNOLDS NUMBER
      DEN=(FLWRT*DH)/(AF*DV)
      DEN1=DEN**0.8
      RE1=FLWRT*DH/(AF*DV)
      RE=RE1**0.8

C  CALCULATION OF NUSSELT NUMBER

      NU=0.0158*RE

C  CALCULATION OF CONVECTIVE/FILM HEAT TRANSFER COEFFICIENT FROM THE DUCT SURFACES

      KA=TFM*7.357*10E-06+0.0242
      H=NU*KA/DH

C  REQUIRED BY THE FLORSCHUTZ EXTENSION TO THE HWB MODEL - THE FOLLOWING CALCULATES THE
C  REDUCTION IN POWER OUTPUT AS A RESULT OF INCREASE IN CELL TEMPERATURE

      ETAA=ETAR*(1.0-BR*(TR-TPM))
      ETAAA=ETAR*(1.0-BR*(TA-TR))
      ULF=UL-TAUALF*IR*ETAA*BR
      ULF1=UL-TAUALF*IR*ETAAA*BR

C  CALCULATION OF COLLECTOR EFFICIENCY FACTOR

      FP1=(1.0/H)+(1.0/HR)
      FP1=(1.0/FP1)+H
      FP1=(ULF/FP1)+1.0
      FP1=1.0/FP1

C  CALCULATION OF DIMENSIONLESS COLLECTOR MASS FLOW RATE

      DM=(FLWRT*CP)/(AC*UL*FP1)

C  CALCULATION OF COLLECTOR FLOW FACTOR

      FP2=DM*(1.0-EXP(-1.0/DM))

C  CALCULATION OF OVERALL COLLECTOR HEAT REMOVAL FACTOR

      FR1=(-ULF*FP1)/(FLWRT*CP)
      FR=(FLWRT*CP/ULF)*(1.0-EXP(FR1))


C  FLORSCHUTZ ALTERATION OF SOLAR RADIATION

      FIR=IR*(1.0-ETAA/ALF)


C  HWB EQUATION FOR USEFUL GAIN FROM COLLECTOR

      QU=AC*FR*(FIR*TAUALF-ULF*(TIN-TA))

C  ELECTRICAL OUTPUT OF THE COLLECTOR

      IR2=IR*(1-ETAAA/ALF)
      QE=1.0-((NR*PF*BR/ETAA)*((FR*(TIN-TA)+((IR2/ULF1)*(1.0-FR)))))
      QE=(AC*IR*ETAA/ALF)*QE


C  OUTPUT TEMPERATURE FROM THE COLLECTOR

      TOUT=QU/(FLWRT*CP)+TIN
```

```
C   MEAN PLATE TEMPERATURE

          TPM=((QU/AC)/(UL*FR))*(1.0-FR)+TIN

C   MEAN FLUID TEMPERATURE

          TFM=((QU/AC)/(UL*FR))*(1.0-FP2)+TIN

C   ITERATE 5 TIMES

          ITER=ITER+1.0
          IF (ITER.LT.6.0) THEN
                GO TO 10
          END IF

C   OUTPUT DESIGNATION

          OUT(1)=TOUT
          OUT(2)=FLWRT
          OUT(3)=QU*NPARA

       do 708 ii=1,20
 708      sav1(ii)=out(ii)

C Convert Q to Watts.
       Q=out(3)
       ptim=ptimep
       info1=0
       info16=0
      endif

C Establish heat capacity of component mass CM (J/K) and
C fluid heat capacity rate(s) C (W/K), ie. SUM(mass flow * specific heat)
      CM=ADATA(IPCOMP,1)*ADATA(IPCOMP,2)
      C1=PCONDR(ICON1)*CONVAR(ICON1,2)*SHTFLD(3,CONVAR(ICON1,1))

C Calculate current component time-constant TC
      TC(IPCOMP)=CM/AMAX1(SMALL,(C1+UA))

C Set up implicit/explicit weighting factor ALPHA (1 = fully implicit)
      IF(IMPEXP.EQ.1) THEN
        ALPHA=1.
      ELSE IF(IMPEXP.EQ.2) THEN
        ALPHA=RATIMP
      ELSE IF(IMPEXP.EQ.3) THEN
        IF(TIMSEC.GT.0.63*TC(IPCOMP)) THEN
          ALPHA=1.
        ELSE
          ALPHA=RATIMP
        END IF
      ELSE IF(IMPEXP.EQ.4) THEN
        CM=0.
        ALPHA=1.
      END IF

C Establish matrix equation self- and cross-coupling coefficients
      COUT(1)=ALPHA*(-C1-UA)-CM/TIMSEC
      COUT(2)=ALPHA*C1

C and then present-time coefficient (ie. right hand side)
      COUT(3)=((1.-ALPHA)*(PCRP(ICON1)+PUAP(INOD1))
     &         -CM/TIMSEC)*CSVP(INOD1,1)
     &        +(1.-ALPHA)*(-PCRP(ICON1))*PCTP(ICON1)
     &        -ALPHA*UA*PCNTMF(IPCOMP)
     &        -(1.-ALPHA)*PUAP(INOD1)*PCNTMP(IPCOMP)
     &        -ALPHA*Q-(1.-ALPHA)*PCQP(INOD1)
```

```
C Store "environment" variables future values
      PUAF(INOD1)=UA
      PCTF(ICON1)=CONVAR(ICON1,1)
      PCRF(ICON1)=C1
      PCQF(INOD1)=Q

C 1st phase mass (ie. dry air) balance coefficients
    ELSE IF(ISTATS.EQ.2) THEN
      COUT(1)=1.
      COUT(2)=-PCONDR(ICON1)
      COUT(3)=0.

C 2nd phase mass (ie. vapour) balance coefficients
    ELSE IF(ISTATS.EQ.3) THEN
      COUT(1)=1.
      COUT(2)=0.
      COUT(3)=0.
    END IF

C Trace output
    IF(ITC.GT.0.AND.NSINC.GE.ITC.AND.NSINC.LE.ITCF.AND.
   &  ITRACE(37).NE.0) THEN
      WRITE(ITU,*) ' Component     ',IPCOMP,':'
      WRITE(ITU,*) ' 1 node solar collector (TRNSYS type150)'
      WRITE(ITU,*) ' Matrix node(s) ',INOD1
      WRITE(ITU,*) ' Connection(s)  ',ICON1
      IF(ISTATS.EQ.1) THEN
        WRITE(ITU,*) ' CM    = ',CM,' (J/K)'
        WRITE(ITU,*) ' C1    = ',C1,' (W/K)'
        WRITE(ITU,*) ' TC    = ',TC(IPCOMP),' (s)'
        WRITE(ITU,*) ' ALPHA  = ',ALPHA,' (-)'
        WRITE(ITU,*) ' UA    = ',UA,' (W/K)'
        WRITE(ITU,*) ' Q     = ',Q,' (W)'
        WRITE(ITU,*) ' PCNTMF = ',PCNTMF(IPCOMP),' (C)'
                     WRITE(ITU,*) ' TPM   = ',TPM,' (C)
      END IF
      WRITE(ITU,*) ' Matrix coefficients for ISTATS = ',ISTATS
      NITMS=3
      WRITE(ITU,*) (COUT(I),I=1,NITMS)
      IF(ITU.EQ.IUOUT) THEN
        IX1=(IPCOMP/4)*4
        IF(IX1.EQ.IPCOMP.OR.IPCOMP.EQ.NPCOMP) call epagew
      END IF
    END IF

    IF(ITC.GT.0.AND.NSINC.GE.ITC.AND.NSINC.LE.ITCF.AND.
   &  ITRACE(37).NE.0) WRITE(ITU,*) ' Leaving subroutine CMP70C'

    RETURN
    END
```

The following subroutine needs to be installed with /usr/esru/src/esp-r/esruplt/pcomps.F

```
C ******************** CMP74S ********************
C
C CMP74S establishes for a plant component with plant db code 740 ie.
C 1 node (ISV=20) Flat plate PV/T solar collector (type150).
C whether the specified number of controlled variables is OK, and also
C whether the number of connections to this component is correct
C and whether the connected nodes are of a type as expected by the
C corresponding coefficient generator routine
C
    SUBROUTINE CMP74S(IPCOMP)
#include "plant.h"
#include "building.h"
C
```

```
      COMMON/OUTIN/IUOUT,IUIN
      COMMON/TC/ITC,ICNT
      COMMON/TRACE/ITCF,ITRACE(MTRACE),IZNTRC(MCOM),ITU
C
      COMMON/C9/NPCOMP,NCI(MPCOM),CDATA(MPCOM,MMISCD)
      COMMON/PDBDT/ADATA(MPCOM,MADATA),BDATA(MPCOM,MBDATA)
      COMMON/PCOND/CONVAR(MPCON,MCONVR),ICONTP(MPCON),
     &       ICONDX(MPCOM,MNODEC,MPCONC)

C Establish static data derivable from the data read from database
      BDATA(IPCOMP,1) =ADATA(IPCOMP,4)
      BDATA(IPCOMP,2) =ADATA(IPCOMP,5)
      BDATA(IPCOMP,3) =ADATA(IPCOMP,6)
      BDATA(IPCOMP,4) =ADATA(IPCOMP,7)
      BDATA(IPCOMP,5) =ADATA(IPCOMP,8)
      BDATA(IPCOMP,6) =ADATA(IPCOMP,9)
      BDATA(IPCOMP,7) =ADATA(IPCOMP,10)
      BDATA(IPCOMP,8) =ADATA(IPCOMP,11)
      BDATA(IPCOMP,9) =ADATA(IPCOMP,12)
      BDATA(IPCOMP,10)=ADATA(IPCOMP,13)
      BDATA(IPCOMP,11)=ADATA(IPCOMP,14)
      BDATA(IPCOMP,12)=ADATA(IPCOMP,15)
      BDATA(IPCOMP,13)=ADATA(IPCOMP,16)
      BDATA(IPCOMP,14)=ADATA(IPCOMP,17)
      BDATA(IPCOMP,15)=ADATA(IPCOMP,18)
      BDATA(IPCOMP,16)=ADATA(IPCOMP,19)
      BDATA(IPCOMP,17)=ADATA(IPCOMP,20)
      BDATA(IPCOMP,18)=ADATA(IPCOMP,21)
      BDATA(IPCOMP,19)=ADATA(IPCOMP,22)
      BDATA(IPCOMP,20)=ADATA(IPCOMP,23)
      BDATA(IPCOMP,21)=ADATA(IPCOMP,24)
      BDATA(IPCOMP,22)=ADATA(IPCOMP,25)
      BDATA(IPCOMP,23)=ADATA(IPCOMP,26)
      BDATA(IPCOMP,24)=ADATA(IPCOMP,27)
      BDATA(IPCOMP,25)=ADATA(IPCOMP,28)
      BDATA(IPCOMP,26)=ADATA(IPCOMP,29)

C Trace output
      IF(ITC.GT.0.AND.ITRACE(35).NE.0) THEN
        WRITE(ITU,*) ' Component ',IPCOMP,' pre-simulation data for a:'
        WRITE(ITU,*) ' 1 node (ISV=21) Flat-plate PV/T solar collector'
        NITMS=3
        WRITE(ITU,*) ' ADATA ',(ADATA(IPCOMP,J),J=1,NITMS)
        NITMS=26
        WRITE(ITU,*) ' BDATA ',(BDATA(IPCOMP,J),J=1,NITMS)
        IF(ITU.EQ.IUOUT) THEN
          IX1=(IPCOMP/5)*5
          IF(IX1.EQ.IPCOMP.OR.IPCOMP.EQ.NPCOMP) call epagew
        END IF
      END IF
C
C Check user specified number of controlled variables
      NCITM=0
      IF(NCI(IPCOMP).NE.NCITM)
     &  WRITE(ITU,*) ' CMP74S warning: user specified wrong number',
     &           ' of controlled variables'

C Check component has 1 connections
      NCONS=1
      DO 10 IPCONC=1,MPCONC
      IPCON=ICONDX(IPCOMP,1,IPCONC)
      IF(IPCONC.LE.NCONS) THEN
        IF(IPCON.EQ.0) THEN
          GOTO 990
        END IF
      ELSE IF(IPCON.NE.0) THEN
        GOTO 990
```

```
    END IF
 10 CONTINUE
    RETURN

C Error handling
 990 WRITE(IUOUT,*) ' CMP74S: connection error for component ',IPCOMP
    WRITE(IUOUT,*) '        should be ',NCONS,' connection(s)'
    STOP ' CMP74S: unresolvable error'
    END
```

APPENDIX B

NOT DIGITISED BY REQUEST OF THE UNIVERSITY